Electrodialysis as a key operating unit in chemical processes : From lab to pilot scale of latest breakthroughs

Guillaume Hopsort, Quentin Cacciuttolo, David Pasquier

Chemical Engineering Journal 494 (2024) 153111

Contents lists available at ScienceDirect

Chemical Engineering Journal

journal homepage: www.elsevier.com/locate/cej

Review

Electrodialysis as a key operating unit in chemical processes: From lab to pilot scale of latest breakthroughs

Guillaume Hopsort *, Quentin Cacciuttolo *, David Pasquier

IFP Energies Nouvelles, Rond-point de l'échangeur de Solaize, BP 3, 69360 Solaize, France

ARTICLE INFO

Keywords:
Electrodialysis
Ion-exchange membranes
Energy efficiency
Process electrification
Process optimization
Scale-up applications

ABSTRACT

This review article comprehensively explores the significant advancements in electrodialysis (ED) technology within the field of chemical engineering, presenting a holistic overview that spans fundamental principles, membrane materials and fabrication techniques, operational parameters, and a wide array of applications. Unlike previous studies that often narrow their focus to specific aspects of ED, this work synthesizes global advances, bridging gaps between diverse research themes to offer a coherent understanding of current trends and future directions.

ED, a membrane-based separation process driven by electric potential, is pivotal for its applications in water purification, desalination, resource recovery, and beyond. This review delves into the evolution of ion-exchange membranes, highlighting innovations in materials, alongside advances in fabrication techniques that enhance membrane selectivity and efficiency. It also scrutinizes the impact of operational parameters on the performance of ED systems, addressing challenges like ion leakage, membrane fouling, and the balance between selectivity and conductivity.

Process intensification and system optimization strategies are discussed, revealing how recent developments contribute to energy efficiency, scalability, and sustainability. The review further extends to emerging applications of ED in sectors ranging from environmental management to energy and hydrometallurgy industries, underscored by case studies that demonstrate practical implementations.

Conclusively, this article underlines the multidisciplinary approach required for the advancement of ED technologies, suggesting avenues for future research that prioritize environmental impact, economic feasibility, and technological innovation. Through this global perspective, it aims to catalyze further exploration and application of ED in addressing some of the most pressing challenges.

1. Introduction

1.1. Purpose and significance of electrodialysis in modern chemical engineering

Electrodialysis (ED) is a membrane technology that employs electric current to transport ions through selective membranes, thereby separating them from a solution and facilitating concentrations of salt and acid/base production. This technology holds a place of significant importance in modern chemical engineering, primarily due to its efficiency in terms of energy [1,2], eco-friendliness [3,4] (solvent-free operation, effluent reduction and/or valorization, etc.), and versatility in separating and purifying ionic compounds [5]. The electrification of processes has attracted even more attention given the possibility of using an energy vector through the coupling of ED technology and the use of electricity from renewable sources (solar [6–8], wind [9–11], etc. [12,13]). In an era where sustainable practices are paramount, ED offers an energy-efficient alternative to conventional separation processes, such as distillation, which often require high energy inputs [14]. Its ability to operate under mild conditions helps in preserving the integrity of sensitive molecules, making it crucial in industries like pharmaceuticals [15], food processing [16], and biotechnology [17,18]. Additionally, the technology's adaptability to various scales and its capacity to be fine-tuned for specific ion separation make it a valuable tool in water treatment [19] and desalination [20]. As concerns over water scarcity and the environmental impact of industrial processes grow, ED emerges not just as a technical solution, but as a necessary step towards sustainable chemical engineering practices. The ongoing advancements in membrane technology and system optimization further amplify its

* Corresponding authors.
E-mail addresses: hopsort.guillaume@gmail.com (G. Hopsort), quentin.cacciuttolo@ifpen.fr (Q. Cacciuttolo), david.pasquier@ifpen.fr (D. Pasquier).

https://doi.org/10.1016/j.cej.2024.153111
Received 25 April 2024; Received in revised form 11 June 2024; Accepted 12 June 2024
Available online 14 June 2024

Nomenclature

Acronyms

A^-	Anionic group bonded to the membrane
AEL	Anion-Exchange Layer
AEM	Anion-Exchange Membrane
BED	Bipolar Electrodialysis
BM	Bipolar Membrane
BPPO	Bromomethylated poly(2,6-dimethyl-1,4-phenylene oxide)
BTMA	Benzyl trimethylammonium
C^+	Cationic group bonded to the membrane
CAPEX	Capital expenditure
CEL	Cation-Exchange Layer
CEM	Cation-Exchange Membrane
CFD	Computational Fluid Dynamics
COF	Covalent Organic Framework
DAC	Direct Air Capture
DABCO	1,4-diazabicyclo-[2,2,2]octane
DBL	Diffusion Boundary Layer
DMA	Dopamine methacrylamide
DMAc	Dimethylacetamide
DMF	Dimethylformamide
DVB	Divinylbenzene
EC	Electrochemical
ED	Electrodialysis
EDTA	Ethylenediaminetetraacetic acid
EDI	Electrodeionization
EIS	Electrochemical Impedance Spectroscopy
ETFE	Poly(ethene-co-tetrafluoroethene)
HDPE	High-density polyethylene
IEM	Ion-Exchange Membrane
IL	Interfacial Layer
LCA	Life Cycle Assessment
LCCA	Life-Cycle Costing Analysis
LDPE	Low-density polyethylene
LiB	Lithium-ion Battery
M−S	Maxwell-Stefan
MMTD	2-mercapto-5-methyl-1,3,4-thiadiazole
MOF	Metal-Organic Framework
MTPP-(2,4,6-Me)	Methyl tris(2,4,6-trimethylphenyl)phosphonium
N	Nitrogen
N-P	Nernst-Plank
NMC	Nickel Manganese Cobalt
NP	Nanoparticle
OPEX	Operational expenditure
PAES	Poly(arylene ether sulfone)
PAMAM	Polyamidoamine
PAN	Polyacrylonitrile
PANI	Polyaniline
PBI	Polybenzimidazole
PDDA	Poly(diallyldimethylammonium chloride)
PE	Polyethylene
PEEK	Polyether ether ketone
PEC	Photoelectrochemical
PECH	Polyepichlorohydrin
PEF	Pulsed Electric Field
PES	Poly(ether)sulfone
PFSA	Perfluorosulfonic acid
PI	Polyimide
PMA	Phosphomolybdic acid
PNB	Polynorbornene
PP	Polypropylene
PPO	Poly(phenylene oxide)
PSSA-MA	Poly(styrene sulfonic acid-co-maleic acid)
PSU	Polysulfone
PTFE	Polytetrafluoroethylene
PVA	Poly(vinyl alcohol)
PVDF	Polyvinylidene fluoride
QPVA	Quaternary ammonium poly(vinyl alcohol)
RH	Relative Humidity
RT	Room Temperature
ROMP	Ring-opening metathesis polymerization
SPEEK	Sulfonated poly(ether ether ketone)
SPPO	Sulfonated poly (2,6-dimethyl-1,4-phenylene oxide)
SPPS	Sulfonated poly(phenylene sulfone)
ST	Styrene
SWOT	Strengths, Weaknesses, Opportunities, & Threats
TCA	Techno-economic assessment
TMA	Tetramethylammonium
TPABr	Tetrapropylammonium bromide
TPAOH	Tetrapropylammonium hydroxide
TPQPOH	Tris(2,4,6-trimethoxyphenyl)phosphonium

Symbols

a	Activity. [dimensionless]
A	Surface area. [m^2]
ASR	Area Specific Resistance. [$\Omega/m^{-2}(-\|-)$]
C	Molar concentration. [$mol/m^{-3}(-\|-)$]
D	Diffusion coefficient. [m^2/s]
e	Elementary charge. [C]
E°	Standard potential. [V]
E_{th}	Thermoneutral voltage. [V]
f	Volume fraction. [dimensionless]
$\mathscr{F}$	Faraday constant. [C/mol]
g	Gravitational constant. [$m/s^{-2}(-\|-)$]
I	Intensity. [A]
IEC	Ion Exchange Capacity. [meq g^{-1}]
j	Current density. [$A/m^{-2}(-\|-)$]
j_0	Exchange current density. [$A/m^{-2}(-\|-)$]
J	Flux. [mol m^{-2} s^{-1}]
J'	Volumetric flux. [m^3 m^{-2} s^{-1}]
k	Mass transfer coefficient. [m/s]
K	Sorption coefficient. [dimensionless]
k_b	Boltzmann constant. [J/K]
l	Thickness. [m]
L_p	Membrane permeability. [L m^{-2} s^{-1} bar^{-1} or mol m^{-2} s^{-1} bar^{-1}]
m	Weight. [g]
M	Molar mass. [g/mol]
n	Molar amount. [mol]
n_{drag}	Electroosmotic drag coefficient. [dimensionless]
n_e	Exchanged electron number. [dimensionless]
N_{cp}	Number of cell pair. [dimensionless]
p	Pressure. [Pa]
P	Power. [W]
PS	Permselectivity. [dimensionless]
$\dot{q}$	Volumetric flow rate. [m^3/s]
r	Radius. [\AA]
R	Universal gas constant. [J/K mol^{-1}]
S	Separation selectivity. [dimensionless]
Sc	Schmidt number. [dimensionless]
SEC	Specific energy consumption. [$Wh/m^{-3}(-\|-)$ or Wh kg^{-1}]
t	Transport number. [dimensionless]
T	Absolute temperature. [K]
u	Absolute mobility. [m^2 [C V s]$^{-1}$]
U	Voltage. [V]
v	Velocity. [m/s]
V	Volume. [m^3]
WC	Water content. [dimensionless]

x	Distance. [m]
X	Fixed-ion concentration. [mol/m^{-3}(−|-)]
z	Ion valence. [dimensionless]

Greeks

α	Charge transfer coefficient. [dimensionless]
γ	Activity coefficient. [dimensionless]
δ	Thickness of diffusion boundary layer. [m]
ΔG	Variation in Gibbs free energy. [J]
Δh	Loss of hydraulic head across the stack. [m]
ΔH	Variation in enthalpy. [J]
ΔS	Variation in entropy. [J/K]
ΔV	Volume dilatation. [dimensionless]
$\Delta\pi$	Osmotic pressure. [Pa]
$\Delta\varphi_D$	Donnan potential. [V]
$\in$	Porosity. [dimensionless]
ε_r, ε_0	Relative and free space permittivity. [F/m]
η	Overvoltage. [V]
λ	Molar ion conductivity. [S m^{-1} mol^{-1}]
μ	Dynamic viscosity. [Pa s]
ξ	Current effiency. [dimensionless]
ρ	Density. [g/m^{-3}(−|-)]
σ	Ionic conductivity. [S m^{-1}]
φ	Electrical potential. [V]
χ	Conversion rate. [dimensionless]
ψ	Mole fraction. [dimensionless]

Superscripts

ano	Anolyte
cat	Catholyte
cte	Concentrate
dlt	Diluate
eo	Electro-osmotic
el	Electrical
h	Hydraulic
j	Area *j*
m	Membrane phase
os	Osmotic
s	Bulk solution phase
*	Electrode/membrane surface

Subscripts

a	Anodic
act	Activation
c	Cathodic
conc	Concentration
ct	Counter-ion
d	Dry
D	Donnan
f	Final
h	Hydrated
i	Species *i*
in	Inlet
ini	Initial
k	Species *k*
lim	Limiting
mig	Migration
ohm	Ohmic
out	Outlet
Ox	Oxidizing agent
Red	Reducing agent
t	Time
tot	Total
w	Water
$\oplus$	Cation
$\ominus$	Anion

significance, promising more efficient, cost-effective, and environmentally benign solutions for a wide range of chemical engineering applications as highlights by the upgoing number of publications extracted from Fig. 1. Since 2000, the research area has been evenly structured between materials engineering (membrane formulation [21], membrane fouling [22], ionic transport [23], etc.) and chemical engineering (process intensification [24], cell's configuration [25], scale-up [26], etc.) illustrating the industrial transfer of this technology [27–29].

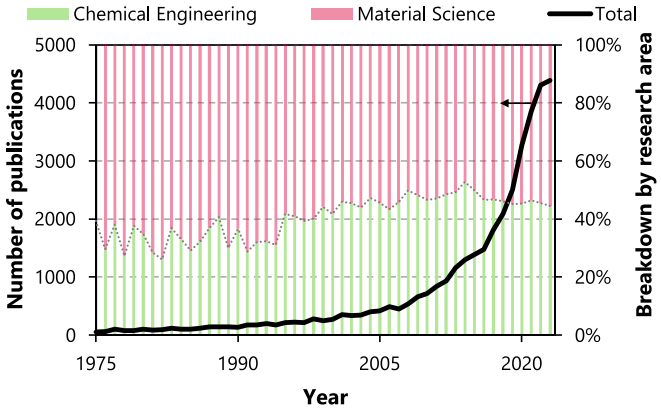

Fig. 1. Number of research articles when searching for the term 'Electrodialysis' as well as the distribution of search fields by query at Digital Science. (1975–2023) Dimensions available from https://app.dimensions.ai. Accessed on 2024/01/10, under license agreement.

1.2. Past research motivations

Tracing the ED's evolution, technologies of electromembrane separation processes have been fundamental. The earliest known use of a non-selective separator in electrochemical (EC) applications dates back to 1889, with an ED process applied to the demineralization of sugar syrup, implemented by Maigrot and Sabates [30]. The term 'electrodialysis' only became widespread about ten years later [31]. The production of ion-exchange materials, first in granular form and then as membranes, did not start until after 1930. This development led to the first use of ion-exchange membranes (IEMs) in 1939 by Manegold and Kalauch, in a three-compartment ED setup [32]. The 1950 s were marked by significant advancements with the work of Juda and McRae at Ionics Inc. [33], Winger et al. at Rohm [34], and Wyllie and Patnode at Gulf Research [35], who developed stable, highly selective, low-resistance membranes. These advancements made ED an essential industrial method for demineralizing and concentrating electrolyte solutions [36]. To assist the reader's understanding, a schematic view of the operation process of the ED procedure is presented for an anion exchange and cation exchange membrane in Fig. 2 – a.

Electrodeionization (EDI), an evolution of ED, was designed for producing ultra-pure water or desalinating low-conductivity media. EDI incorporates an ion-exchange resin bed within the diluate chamber (and occasionally in the concentrate chamber) of an ED setup, enhancing conductivity and creating a more effective three-dimensional phase interface for mass exchange than traditional ED [37]. This method uses an electric field to continuously transport ions from the ion-selective phase to the concentrate stream. Conceptually, EDI combines ED with traditional ion-exchange technology, an idea proposed in the 1970 s

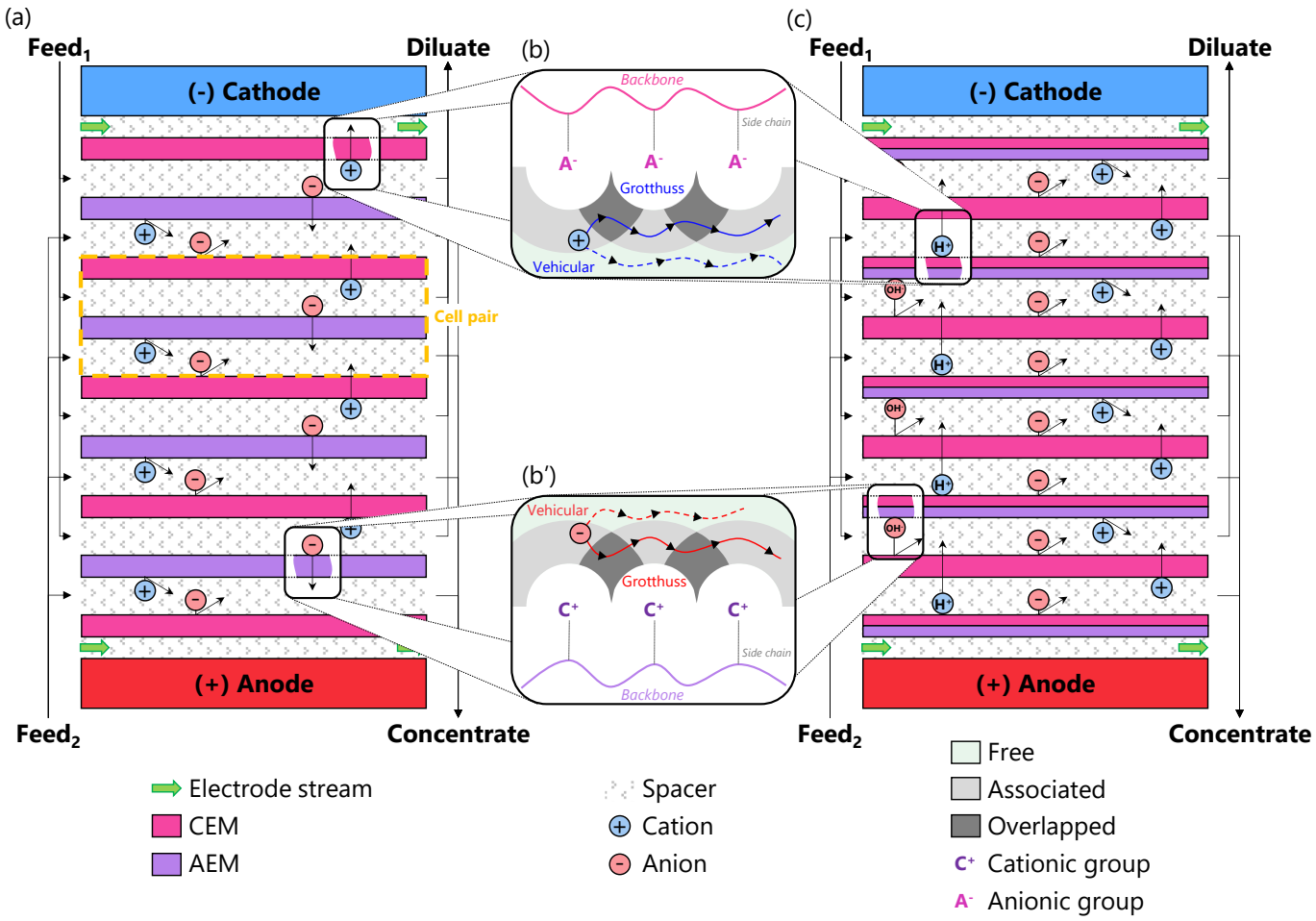

Fig. 2. Scheme illustrating: (a) the conventional ED principle; (b) cation and/or (b') anion transport through monopolar IEMs; and (c) the bipolar ED principle. Figure (b-b') adapted with permission from [58]. Copyright 2016 American Chemical Society.

[38,39]. The major advantage of EDI is its continuous operation without regenerative agents, reducing environmental impact and saving water needed for treating saturated ion-exchangers. Today, EDI is a commercially established technology [40] and this review will not develop this topic in the rest of this document.

In the field of ED, a notable advancement has been the integration of bipolar membranes (BMs). These specialized membranes are composed of distinct adjacent anion-selective and cation-selective layers [41]. The use of BED, as presented in Fig. 2 – c, allows the pH of solutions on either side of the membrane to be modified by dissociating the water within the BM. Depending on the pKa of the various salts present, their acid/base forms will be influenced, resulting in the production of acids and bases [42,43].

Parallel to the development of ED technology, the field of membrane electrolysis has also seen significant advancements. Unlike ED, industrial application of membrane electrolysis requires much higher operational current densities, often exceeding 2000 $A/m^{-2}(-|-)$. This approach has played a crucial role in diversifying and expanding the available membrane materials, particularly for cation- and anion-exchange membranes (CEMs and AEMs, respectively). Today, a wide range of such specialized membrane materials is available from various manufacturers [44]. To this end, several recent articles offer insightful reviews on IEMs (local material specifications [45–47], novelties in fabrication methods [48,49], etc.) or the application of ED in specific field (resource recovery [50,51], reverse ED [52,53], water treatment [54,55], etc.).

1.3. Scope and aim of this review

Bolstered by this momentum, research themes related to ED are increasingly leaning towards pilot scale applications today. However, reviews are currently lacking in studies that encompass the field of ED from a chemical engineering perspective. In particular, industrial scale-up is often neglected. To our knowledge, there is no review available that sheds light on the entirety of this technology as well as highlighting the main advancements in the field. The scope of this article encompasses a comprehensive review of ED as a critical operating unit in chemical processes, focusing primarily on advancements from lab to pilot scale implementations. It aims to provide a detailed analysis of the fundamental principles underlying ED (**Section 2**). Special emphasis is placed on recent developments in IEM materials and fabrication techniques (**Section 3**) and exploration of operational parameter process impacts (**Section 4**), which are pivotal for enhancing the efficiency, selectivity, and sustainability of ED processes. Additionally, the article seeks to address process intensification, system optimization strategies (**Section 5**), and the challenges associated with scaling up ED systems from lab to pilot scale (**Section 6**). By integrating diverse applications and case studies (**Section 7**), this review endeavors to offer a holistic view of the current state and future potential of ED in various industrial sectors. Finally, the main goal is to provide a balanced narrative that not only reflects the current technological advancements but also identifies future research directions and technological frontiers in the field of ED. For this purpose, the authors mainly focused on articles reported in the literature from 2019 to 2024 (year-by-year distribution of cited works in this document illustrated in Supporting Material – SM1).

The uniqueness of this study lies in its generalist approach to chemical engineering, yet it delves into the scientific nuances of ED technology, marking a contribution to the field. The manuscript is intended to serve not only as an educational resource for those new to ED but also as an update for seasoned researchers and practitioners. The recent literature often provides insufficient comprehensive and holistic guidance for researchers new to the field of ED. Predominantly, reviews focus on specialized applications or functional improvements, engaging in extensive scientific detail yet remaining confined to particular cases. This review endeavors to surmount this deficiency by offering a broader, more accessible, and recent overview of the field.

2. Fundamentals of electrodialysis

ED is an ionic purification of a liquid placed between sets of semi-permeable membranes, driven by ion transfers aimed at maintaining electroneutrality between the compartments. These compartments themselves are imbalanced by ED reactions on either side, induced by the application of an electric field. This section delves into the core principles underlying ED, focusing on IEM processes, including monopolar and bipolar configurations, and the mechanisms of ion transport within membranes and solutions. It outlines the basics of ED technology, discussing key aspects such as sorption-migration, ion selectivity, and the balance between membrane permeability and selectivity.

2.1. Concepts of ion-exchange membrane processes

2.1.1. Conventional electrodialysis

The core principles of ED are rooted in electrochemistry, ion transport, and membrane science, where a succession of heterogeneous interfaces (*i.e.*, electrode / electrolyte / membrane / electrolyte / … / electrolyte / membrane / electrolyte / electrode) is implemented, thereby generating reactions and heterogeneous transfer mechanisms. ED systems consist of an anode and a cathode, forming an EC cell as shown in Fig. 2 – **a**. However, it is important to note that ED process does not involve redox reactions, characteristic of electrolytic processes, except for reactions at the terminal electrodes (judiciously chosen so as not to be the system's critical overvoltage).

At the anode, oxidation reactions occur, while at the cathode, reduction reactions take place. Classically, between these electrodes are a series of IEM, alternating CEM, and AEM. In practical industrial applications, the number of membrane pairs in an ED stack often reaches hundreds. This scaling up is crucial to improving process efficiency and reducing investment costs per unit of production capacity [56]. Cations move towards the cathode and anions towards the anode by migration under the application of an electrical field. The membranes are arranged in a stack, creating alternating compartments of dilute and concentrate solutions. As ions migrate under the influence of the electric potential φ (V), they are either captured in concentrate compartments or allowed to pass into dilute compartments, effectively removing them from the solution to be treated [57]. Separation results from the selectivity of membrane ion transport and exclusion by electrostatic repulsion at the membrane surface due to like charges covalently bonded to the membrane material. When an electric field is applied, ions in the solution are driven towards the oppositely charged electrodes through migration and diffusion mechanisms which results in the generation of diffusion boundary layers (DBLs) on either side of each membrane. The diffusion of a species originates from the thermal agitation of molecules, which tends to equalize the concentration. It results in a flux of the species from regions of higher concentration to those of lower concentration. This is true both within the DBLs close to electrode and across the membrane. However, the polarity of the membrane restricts diffusion to ions of the opposite polarity, meaning that concentration cannot be increased indefinitely. At a certain point, Fickian diffusion of ions from the concentrate to the diluate becomes more significant than the flux by electromigration. Therefore, it would be more prudent to stop ED before this point to maintain its efficiency. It occurs primarily in the vicinity of the electrodes and membranes, in a DBL whose thickness varies from a few micrometers (in the case of agitation) to several centimeters.

2.1.2. Ion-exchange membranes

Alternatively, IEMs are typically categorized into five types, depending on the nature and arrangement of their fixed ionic groups (Fig. 3). These include CEMs [59], AEMs [60], amphoteric IEMs [61], BMs [62], and mosaic IEMs [63]. An IEM is composed of both hydrophilic ionic groups and hydrophobic polymer chains with charged ionic functional groups that allow the transport of oppositely charged species (counter-ions), while retaining like-charged ions (co-ions). Specific focus on the IEM materials will be presented in **Section 3**.

Bipolar electrodialysis (BED) is an advanced EC process that extends the principles of standard ED by incorporating bipolar membranes (BMs), illustrated in Fig. 3 – **c**, alongside the traditional CEMs and AEMs. This technique is particularly useful for generating bases and acids from salts. In BED, each BM consists of two layers: a cation-exchange layer and an anion-exchange layer. These layers are fused together, and at their interface, water molecules undergo disproportionation reaction into proton and hydroxide ions without any gas formation. This reaction is sometimes facilitated by catalytic sites within the ion-exchange layers. Upon applying electrical current across a BM, the ionic flow through the membrane is not supported by ions from the surrounding solution because neither cations nor anions can pass through both layers of the BM. Consequently, the transport of ionic current relies on proton and hydroxide ions produced at the membrane's internal interface. This process underlines the critical importance of the BM's orientation relative to the electrodes: to facilitate the migration of H^+ and OH^- ions in alignment with the electric field, the Cation Exchange Layer (CEL) must be oriented towards the cathode, while the Anion Exchange Layer (AEL) should face the anode. The resultant movement of H^+ and OH^- ions out of the membrane through their respective layers (H^+ through the CEL and OH^- through the AEL) leads to the formation of an acid and a base on alternate sides of the membrane, thereby establishing a pH gradient across the BM. This configuration, with the CEL positioned towards the

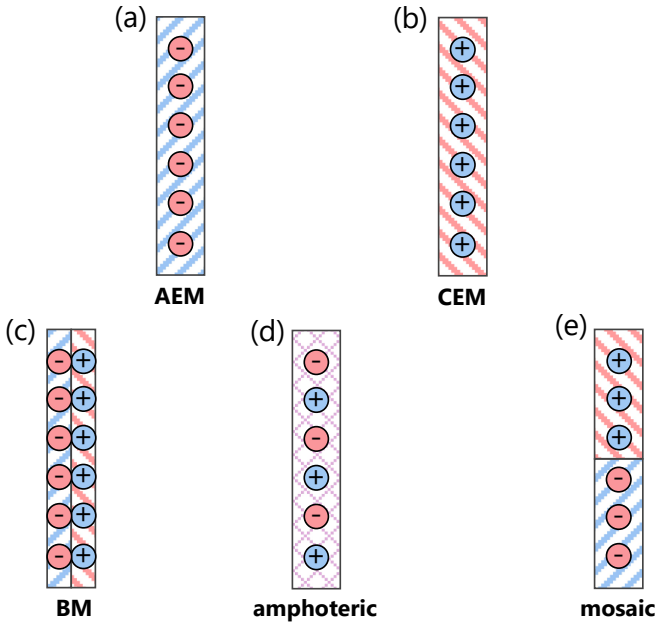

Fig. 3. Diagrammatic representation of various IEM varieties: (a) AEMs, (b) CEMs, (c) BMs, (d) amphoteric IEMs, and (e) mosaic IEMs. In this illustration, the circles represent the counter-ions embedded within the membrane structure, and the distinct background designs illustrate the fixed ionic groups in each type of membrane.

cathode, is often termed the 'reverse bias' condition (analogous to diode case). Altering the electric field's direction across the BM—either by switching the electrode's polarity or by rotating the membrane so that the CEL faces the anode and the AEL the cathode—results in a 'forward bias' condition. In the forward bias scenario, H^+ and OH^- ions migrate from the external solutions towards the bipolar junction, recombining into water. This water then diffuses out through the CEL and AEL, leading to the neutralization of the acid and base. BMs with their unique capability to synthesize compounds rather than merely facilitating ion transport, hold a unique place among IEMs [64]. BMs have garnered commercial attention recently, primarily due to their environmental benefits. They offer a chemical-free method for pH modification through direct H^+ and OH^- generation, avoiding the need for external chemical additives. Furthermore, BM technology is pivotal in the chemical industry's shift towards electrification, significantly contributing to the sustainable production of chemicals. Despite its benefits, the process is energy-intensive, making energy efficiency a crucial factor for its cost-effectiveness. Additionally, the stability and efficiency of BMs are key areas of focus, with ongoing research aimed at developing more durable and efficient membranes, subject to a multitude of recent reviews [65–67].

Amphoteric IEMs are characterized by the inclusion of both weak acidic and weak basic functional groups as shown in Fig. 3 **– d**. These groups are interspersed throughout the membrane's structure. This configuration enables the passage of both cations and anions, which can be modulated through pH adjustments. Notably, these membranes have been identified as promising in anti-fouling applications, effectively hindering the adherence of organic compounds and biological macromolecules (proteins) on their surfaces, as highlighted in various works [68,69].

Contrastingly, the structure of mosaic membranes is distinguished by the parallel arrangement of anion and cation exchange sites. These exchange resins are interspersed within a matrix that is either a neutral polymer or facilitates ion exchange, as depicted in Fig. 3 **– e**. The channels in these membranes that possess a positive charge typically exhibit a higher concentration of negatively charged anions, and the reverse is true for channels with a negative charge. This specific layout creates distinct pathways for the separate movement of anions and cations [36,70]. Mosaic membranes are particularly adept at separating salts from water-soluble organic materials and are valuable in the treatment of waste streams across various industrial sectors, thanks to their negative salt rejection and osmotic pressure capabilities [71]. Mosaic membranes demonstrate efficacy in concentrating dilute electrolytes when subjected to hydrostatic pressure and a gradient in chemical potential, a process known as piezodialysis. The proximity of anion and cation exchange sites within a singular membrane leads to a disproportionately elevated permeability to salts when compared to neutral molecules [72]. This process bears a resemblance to ED. However, a distinguishing feature in this case is the absence of electrodes typically associated with ED. However, the complexity of fabricating mosaic membranes, particularly in achieving a thin, selective layer with controlled domain size and preventing interfacial leakage between domains, presents significant challenges for commercial production [73].

Since most research on ED pilot plant development focuses on conventional IEMs and BMs, this review focuses on the two types of these IEMs.

2.2. Overcoming energy losses in ion transport for electrodialyzer

Ion transport in an electrodialyzer occurs under the application of a potential. This transport will generate energy losses within the system that must be overcome to bring the electrodialyzer into nominal operation. Before presenting the transport phenomena within the stack in detail, describing the energy losses in the form of overpotentials will allow for a better understanding of ion transport subsequently.

2.2.1. Energetic balance

To better understand the sources of energy loss in the process, it is necessary to establish a rigorous energetic balance on the ED plant. This potential field φ, illustrated in Fig. 4, gives a better idea of the main electrical overpotential in the process.

The operating voltage itself is composed of various elements, including the thermodynamic cell potential, the overpotential associated with both the cathode and anode reactions (Fig. 4 **– b**), and the potential losses due to the resistance of the electrolyte and the separator. This energy consumption can be related to the cell's potential and the system's overall overvoltage, as shown in **Eq. (1)**.

$$U_{stack} = U_{Nernst} + U_D + \eta_{act} + \eta_{conc} + \eta_{ohm} \tag{1}$$

where U_{stack} is the cell potential of the stack (V); U_{Nernst} is the redox potential at the electrodes (V); U_D is the Donnan overvoltage of the entire cell (V); η_{act}, η_{conc} and η_{ohm} are, respectively, the activation, concentration and ohmic overvoltages (V).

The ion transport in each stage of the ED process necessitates a specific amount of energy consumption/loss, which is described upon in the subsequent sub-sections.

2.2.2. Ohmic losses

Ohmic overvoltage represents the primary loss in ED. This overpotential can be broken down into various contributions occurring within the membranes and electrolytes, as outlined in Eq. (2).

$$\eta_{ohm} = \eta_{ohm}^{cte} + \eta_{ohm}^{dlt} + \eta_{ohm}^{CEM} + \eta_{ohm}^{AEM} + \eta_{ohm}^{ano} + \eta_{ohm}^{cat} \tag{2}$$

In each domain, the ohmic losses follow Ohm's law, as pointed in Eqs. (3) – (8)

$$\eta_{ohm}^{cte} = N_{cp} \times \frac{l^{cte}}{A_{cell}\sigma^{cte}} \times I \tag{3}$$

$$\eta_{ohm}^{dlt} = N_{cp} \times \frac{l^{dlt}}{A_{cell}\sigma^{dlt}} \times I \tag{4}$$

$$\eta_{ohm}^{CEM} = (N_{cp} + 1) \times \frac{l^{CEM}}{A_{cell}\sigma^{CEM}} \times I \tag{5}$$

$$\eta_{ohm}^{AEM} = N_{cp} \times \frac{l^{AEM}}{A_{cell}\sigma^{AEM}} \times I \tag{6}$$

$$\eta_{ohm}^{ano} = \frac{l^{ano}}{A_{cell}\sigma^{ano}} \times I \tag{7}$$

$$\eta_{ohm}^{cat} = \frac{l^{cat}}{A_{cell}\sigma^{cat}} \times I \tag{8}$$

where l is the thickness (m); A is the surface area of the cell (m^2); σ is the ionic conductivity (S m^{-1}) and I is the current (A).

In diluate electrolytes, ionic conductivity is influenced by both the concentration and the nature of each ion, as described in Eq. (9). In the case of concentrate electrolytes, more complex correlations need to be taken into account [74].

$$\sigma^j = \sum_i \lambda_i^j \times C_i^{j,s} \tag{9}$$

where λ is the molar ion conductivity (S m^{-1} mol^{-1}).

Note that the order of magnitude of each of these overvoltages is not identical, and they can be classified according to **Eqs. (10) – (11)**.

$$\eta_{ohm} > \eta_{act} > \eta_{conc} \tag{10}$$

$$10^2\ mV \approx \eta_{ohm}^{CEM} \approx \eta_{ohm}^{AEM} > \eta_{ohm}^{dlt} \geq \eta_{ohm}^{cte} > \eta_{ohm}^{ano} \approx \eta_{ohm}^{cat} > \eta_{act} > \eta_{conc} \approx 10^1\ mV \tag{11}$$

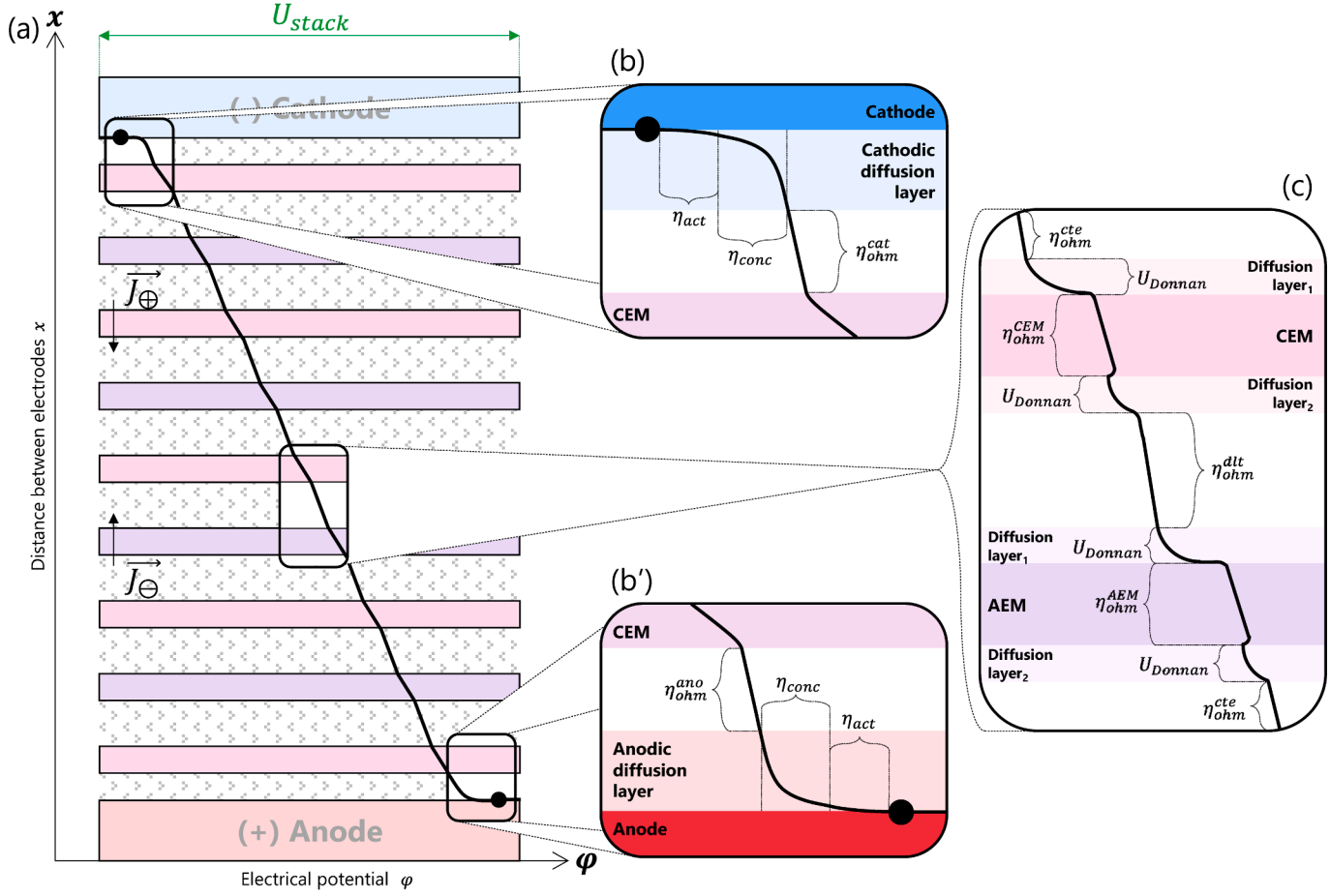

Fig. 4. Potential field φ (a) within the complete ED cell, at the interfaces of (b) the cathode, (b') the anode and (c) the monopolar IEM.

2.2.3. *Losses at the electrode surface*

Ion transport at the electrode undergoes three main phenomena: *(i)* thermodynamic equilibrium through Nernst overvoltage, *(ii)* kinetics and activation energy barrier through activation overvoltage and *(iii)* depletion of charge-carriers at the electrode surface generated by diffusion gradient or gas bubbles thorough concentration overvoltage.

Nernst potentials (depicted in Eq. (12)) and activation overvoltages are considered solely for the reactions at the electrodes, which are typically water oxidation and reduction. No other EC reactions occur in ED setup.

$$U_{Nernst} = \left\{E_a^{\circ} - \frac{RT}{z_i F}\ln\frac{a_{Red}^{ano}}{a_{Ox}^{ano}}\right\} - \left\{E_c^{\circ} - \frac{RT}{z_i F}\ln\frac{a_{Red}^{cat}}{a_{Ox}^{cat}}\right\} \quad (12)$$

where E_a° and E_c° are, respectively, the standard anodic and cathodic potential (V); a is the activity (dimensionless).

Kinetics of EC reaction can be typically modelized by a Tafel equation as written in Eq. (13).

$$\eta_{act} = \frac{RT}{\alpha_a z_i F}\times\log\frac{j}{j_{0,a}} + \frac{RT}{\alpha_c z_i F}\times\log\frac{j}{j_{0,c}} \quad (13)$$

where α_a and α_c are, respectively, the anodic and cathodic charge transfer coefficients (dimensionless); j is the electrode current density ($A/m^{-2}(-|\text{-})$); j_0 is the exchange current density ($A/m^{-2}(-|\text{-})$).

The concentration overpotential depends on the hydrodynamics in the electrode compartments and at the interface of each IEM sides (leading to concentration polarization) and thus on the concentration of reactants, as indicated in Eq. (14).

$$\eta_{conc}^{electrodes} = \left|\frac{RT}{n_e F}\times\ln\frac{C_{Red,a}^{*}}{C_{Red}^{ano,s}}\right| + \left|\frac{RT}{n_e F}\times\ln\frac{C_{Ox,c}^{*}}{C_{Ox}^{cat,s}}\right| \quad (14)$$

where n_e is the exchanged electron number (dimensionless) and C^* is the concentration at the electrode surface ($mol/m^{-3}(-|\text{-})$).

2.2.4. *Losses at the membrane interface*

Two main losses of energy are generated at the membrane interface: *(i)* caused by a concentration polarization and *(ii)* generated by the thermodynamic equilibrium of ions, called Donnan equilibrium, between solution and membrane interface [75].

The concentration overpotential depends on the hydrodynamics close to IEMs and at the interface of each IEM sides (leading to concentration polarization), as indicated in Eq. (15).

$$\eta_{conc}^{IEM} = N_{cp}\times\left\{\left|\frac{RT}{z_i F}\ln\frac{C_{\oplus}^{cte,*}}{C_{\oplus}^{cte,s}}\right| + \left|\frac{RT}{z_i F}\ln\frac{C_{\oplus}^{dlt,*}}{C_{\oplus}^{dlt,s}}\right| + \left|\frac{RT}{z_i F}\ln\frac{C_{\ominus}^{cte,*}}{C_{\ominus}^{cte,s}}\right| + \left|\frac{RT}{z_i F}\ln\frac{C_{\ominus}^{dlt,*}}{C_{\ominus}^{dlt,s}}\right|\right\} \quad (15)$$

$$\eta_{conc} = \eta_{conc}^{electrodes} + \eta_{conc}^{IEM} \quad (16)$$

where z_i is the ion's valence (dimensionless) and C^* is the concentration at the membrane surface ($mol/m^{-3}(-|\text{-})$).

Donnan formulated the equations for thermodynamic equilibrium in membranes by considering the IEM matrix as a solution containing uniformly distributed fixed charges. It was discovered that an electrical potential at the interface between the membrane and the solution causes the repulsion of co-ions from the membrane matrix as illustrated in Fig. 4 – **c** by Donnan equilibrium. The phenomenon where co-ions are

repelled by IEMs is known as the Donnan effect and the equilibrium leads to a Donnan potential $\Delta\varphi_D$ (V). For each membrane, two Donnan potentials occur at each interface. Since the EC potential of ions within the membrane is challenging to estimate, it is assumed to be identical at both interfaces, then we consider a single Donnan potential for the entire membrane. This latter depends on the ion activity on both sides of the membrane and can be expressed as **Eq. (17)**.

$$\Delta\varphi_D = \varphi^m - \varphi^s = \frac{RT}{z_i F} \times \ln \frac{C_i^s \gamma_i^s}{C_i^m \gamma_i^m} \tag{17}$$

where $\Delta\varphi_D$ is the Donnan potential (V) as the potential difference between the membrane φ^m and the solution φ^s potentials (V).

Each membrane in the ED setup possesses a Donnan potential that varies depending on the ion mobility present in the surrounding solutions [76]. Recently, Aydogan Gokturk et al. was the first to determine Donnan potential directly and experimentally by tender ambient pressure X-ray photoelectron spectroscopy [75]. In the scenario depicted in Fig. 4, there are four different membrane configurations. The top membrane is a CEM bordered by the catholyte on one side and the diluate on the other side. The bottom membrane is also a CEM but is bordered by the anolyte and the concentrate. Between the two, there are AEMs and CEMs, present in quantities corresponding to the number of cell pairs (N_{cp}) and the number of cell pairs minus two, respectively. All these membranes share a similar configuration, each flanked by a concentrate solution and a dilute solution. However, the mobile ions differ between the membranes: cations move through the CEMs, while anions traverse the AEMs. The Donnan potential in this arrangement is defined by Eq. (18). With a different configuration or in the case of a BM, the equation will vary, and a similar assessment must be conducted.

$$\begin{aligned} U_D &= \sum_j \Delta\varphi_D^j \\ &= (N_{cp} - 2) \times \left| \frac{RT}{z_i F} \ln \frac{C_\oplus^{cte}}{C_\oplus^{dlte}} \right| + N_{cp} \times \left| \frac{RT}{z_i F} \ln \frac{C_\ominus^{dlt}}{C_\ominus^{cte}} \right| + \left| \frac{RT}{z_i F} \times \ln \frac{C_\oplus^{cte}}{C_\oplus^{ano}} \right| + \left| \frac{RT}{z_i F} \right. \\ &\quad \left. \times \ln \frac{C_\oplus^{cat}}{C_\oplus^{dlt}} \right| \end{aligned} \tag{18}$$

where j represent each interface between an electrolyte and the IEM; N_{cp} is the number of cell pair (dimensionless); $C_\ominus$ and $C_\oplus$ are, respectively, the anion and cation concentration (mol/m^{-3}(−|-)).

On the other hand, when using BMs (not illustrated in Fig. 4), the main difference generates a different potential field $\Delta\varphi_D$ across the membrane. In the case of these membranes, the Donnan voltage at zero current is presented in **Eq. (19)**.

$$\Delta\varphi_D = 2.3 \times \frac{RT}{F} \times \Delta pH \tag{19}$$

where ΔpH is the pH difference across the BM (dimensionless).

In the literature, there are two primary theoretical frameworks utilized for characterizing the structure of the transition region in BMs. These are known as the 'abrupt junction' model and the 'neutral layer' model, as presented in Fig. 5. The 'abrupt junction' model posits that the cation- and anion-exchange layers are directly contiguous, leading to a negligible separation between them. This arrangement results in a pronounced shift in both voltage and concentration profiles at the junction of these layers, as depicted in Fig. 5 – **a**. The spatial extent of this transition region typically spans a few nanometers [77]. Conversely, the 'neutral layer' model, illustrated in Fig. 5 – **b**, hypothesizes the existence of a slender neutral solution layer interposed between the two ion-exchange layers. A notable observation in BM modelling studies is the prevalent assumption of perfect symmetry, wherein both the AEL and CEL are considered identical in terms of thickness, fixed charge density, and symmetric diffusion coefficients for both counter-ions and co-ions. This symmetric model, while prevalent, constrains the exploration of

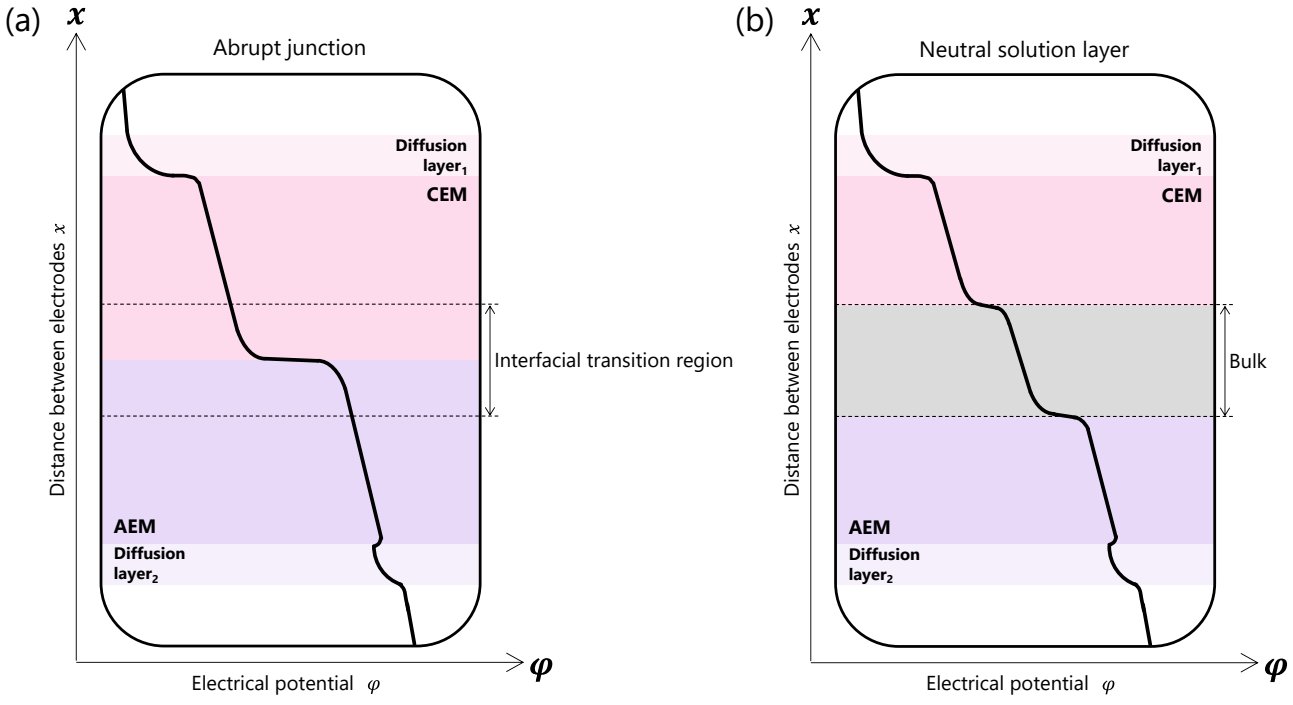

Fig. 5. Diagram illustrating the profiles of concentration and voltage in a BM, featuring (a) an abrupt junction model, and (b) a model with an intervening neutral solution layer. Adapted from [41], Copyright (2021), with permission from Elsevier.

asymmetric BM designs. Such asymmetrical designs hold potential for enhancing water transport across the bipolar junction from the surrounding solutions [41].

The interfacial layer situated between the dual layers of the membrane is often embedded with a catalyst to facilitate the dissociation/association reactions, thereby ensuring a continuous exchange or uptake of ionic charge carriers from each layer of the BM [78,79].

2.3. Sorption-migration phenomenon during ion transport in ion-exchange membranes

Ions undergo a two-step process involving initial sorption or partitioning into the membrane, followed by migration across the membrane driven by an electrical potential gradient. The process of ion sorption into the membrane's matrix is dictated by the equilibrium of EC potential between the bulk solution and the membrane matrix. This equilibrium is influenced by the difference in electrostatic potential at the interface between the solution and membrane [80].

The sorption coefficient, denoted as K, quantifies the ratio of the concentration of a specific ion *i* within the IEM to its concentration in the bulk-phase solution. This relationship is encapsulated in **Eq. (20)** as follows:

$$K_i \equiv \frac{C_i^m}{C_i^s} = \frac{f^w \gamma_i^s}{\gamma_i^m} \times \exp\left(-\frac{z_i F}{RT}\Delta\varphi_D\right) \tag{20}$$

where C is the concentration (mol/m^{-3}(−|-)); f^w is the water volume fraction in the membrane matrix (dimensionless); γ is the activity coefficient (dimensionless); z is the valence (dimensionless); F is the Faraday constant (C/mol); R is the universal gas constant (J/K mol^{-1}); T is the absolute temperature (K); and superscripts m and s denote membrane and bulk solution phases, respectively.

2.3.1. Transport modeling equations

A robust framework for quantitatively analyzing ion transport in IEMs is provided by two different scenarios: *(i)* Nernst-Planck (N-P) and *(ii)* Maxwell-Stefan (M−S) equations.

The extended N-P equation [81,82] articulates the ionic flux J (mol m^{-2} s^{-1}) as a cumulative function of three distinct components presented in **Eq. (21)** and quantifies the permeation across the membrane.

$$J_i = v^w \times C_i^m - D_i^m C_i^m \times \frac{d\ln(\gamma_i^m C_i^m)}{dx} - z_i e u_i^m C_i^m \times \frac{d\varphi^m}{dx} \tag{21}$$

$$D_i^m = D_i \times \left(\frac{f_w}{2 - f_w}\right)^2 \tag{22}$$

$$u_i = \frac{D_i}{k_b T} \tag{23}$$

where v^w denotes the water velocity in the membrane (m/s); D^m and u_i^m are the diffusivity (defined in Eq. **(22)** [83], m^2/s) and absolute mobility (defined in **Eq. (23)** by the Einstein relation, m^2 (C V s)$^{-1}$) of the ion within the IEM; e is the elementary charge (C); x being the spatial coordinate across the membrane (m); k_b is the Boltzmann constant (J/K) and f is the volume fraction of water (dimensionless).

Eq. (21) can apply to all ions under the condition of electroneutrality. The first term is indicative of ions' convective (advective) transport facilitated by electroosmotic solvent flow. The second term denotes ion diffusion driven by the activity gradient. The third term describes ion electromigration, an outcome of the electric potential gradient [84]. Notably, in the context of ion transport within the membrane, while both diffusion and convection contribute, their influence is minor compared to electromigration [85]. This is particularly true for IEMs, which are characterized by a dense structure, and exhibit an electrolyte diffusion coefficient in the membrane that is significantly lower (by one to three orders of magnitude) than in bulk solutions [86,87]. The N-P model operates under the presumption of an ideal solution, disregarding the interactions between ions. Its applicability is established for dilute ionic environments. However, in the realm of ED, one often encounters solutions with high ion concentrations. Under these circumstances, the M−S framework offers a more accurate representation, acknowledging the complexities arising from component interactions and deviations from ideal solution behavior. Furthermore, the M−S methodology accounts for the movement of water through its interactions with ions, in contrast to the N-P model which necessitates the addition of a distinct formula (namely the Schlögl equation [88]), to describe water transport. Although the traditional N-P equation (which omits the convective term) has limitations in accurately characterizing ion transport through inhomogeneous media, its extensive applicability and utility have been well-established [89,90].

The M−S theory articulates a balance of forces at the steady state, encapsulating the interplay between the driving forces and the resistive frictional forces encountered by a specific component within a mixture. Eq. **(24)** delineates the relation between the driving force experienced by a component i within the mixture and the cumulative frictional forces arising from interactions between component i and another component k, expressed in mole fraction terms.

$$\begin{cases} driving force on species i = friction forces with other species k \\ C_{tot}\psi_i \times \left(RT\frac{d\ln a_i}{dx} + z_i F\frac{d\varphi}{dx}\right) = \sum_{k\neq i}\frac{RT}{D_{i,k}}(\psi_i J_k - \psi_k J_i) \end{cases} \tag{24}$$

where ψ is the mole fraction (dimensionless) and a is the activity (dimensionless).

2.3.2. Modes of ion transport

For example, CEM functions by selectively allowing positively charged ions to pass through while blocking negatively charged ions [81]. It is composed of a polymeric matrix, often made from materials like polyethylene or fluoropolymers [91], which is embedded with negatively charged functional groups, such as sulfonic or carboxylic acids. These functional groups bind to cations in the solution as presented in Fig. 2 **– b**. The ion transport selectivity is largely influenced by electrostatic repulsion between the migrating ions and those fixed within the membrane. Steric hindrance also plays a role in affecting ion transport, which is related to the polymers' topology and the size of migrating ion through the membranes. Polymer chains exhibit both hydrophobic (carbon chains constituting the backbone) and hydrophilic (ionic functionalities) properties. Upon hydration of the polymer membranes, clusters form between water and the hydrophilic segments of the polymers. With sufficient hydration, these clusters evolve into aqueous channels, and the membrane adopts a biphasic structure. Water uptake in the membrane is defined by the ratio of water molecules per functional site. The water content is influenced by factors such as temperature, ion exchange capacity (IEC), membrane pretreatment, water vapor pressure, and the mechanical properties of the membrane, which depend on the ionomer's nature and manufacturing process.

Ion transport through the membrane can occur via two main mechanisms. The first mechanism, known as the Grotthuss mechanism, involves mobile ions moving from one ionic site to another via hopping. If the membrane is adequately hydrated, a second mechanism, termed the 'vehicular' mechanism, occurs where ions are directly transported in the aqueous phase, bounded to water molecules [92]. At this point, water is also transported by migration within the membrane. The dominance of one mechanism over the other depends on the polymer's nature, the ionic functionalities (polymer's hydrophobicity and hydrophilicity, acidity of ionic functionalities, cross-linking, chain size, etc.), and operational conditions, particularly the membrane's hydration. For fuel cells, electrolysers or EDs using a proton exchange membrane, adequate hydration of the membrane is crucial (it can reach up to 20 wt % in Nafion®, for example). Under such conditions, vehicular transport predominantly accounts for the membrane's good ionic conductivity

[58].

2.4. Performance efficiencies

The economic viability of an EC process largely hinges on its consumption of electrical energy [93]. This consumption is intricately linked to several factors: the operating voltage, the electrical charge necessary for the desired separation of the reactant, and the current efficiency of the process. The main criteria for evaluation are presented in this subsection.

2.4.1. Limiting current density

Increasing the voltage applied to a module's terminals results in a rise in current density, which in turn boosts the ion flux until the ion concentration at the membrane surface drops to zero. This point represents the peak current density attainable, referred to as the limiting current density, symbolized as j_{lim} and presented in Eq. (25).

$$j_{lim} = \frac{z_i D_i F C_i^s}{\delta \times (t_{i,ct}^m - t_{i,ct}^s)} \quad (25)$$

where δ is the thickness of the DBL (m) and t^s and t^m represent the transport number in the bulk and in the membrane, respectively (dimensionless); ct stands here for the counter-ion.

Studying the movement of ions from the diluate to the concentrate compartments involves tracking the change in current intensity I relative to the voltage U applied at the module's terminals. The curve generated from this analysis displays three distinct segments and is represented in Fig. 6 – a. The first segment, marked (A), exhibits an almost linear relationship, illustrating the combined resistance effects from the electrolyte, membranes, and the concentration polarization, as indicated by the straight line's slope. In this segment, Ohm's law ($U = R \times I$) holds true. The next segment, denoted as (B), shows a flat plateau indicating complete polarization of the cell. This plateau reveals the limiting current intensity, influenced by ion delivery to the membrane via electric potential-driven flux, diffusion, and convection. Following this, in segment (C), the intensity begins to rise once more. However, this rise is not attributed to resumed solution species transfer but to solvent redox reactions. This process results in excessive energy consumption, pH shifts leading to irreversible damage, and increased resistivity of the medium. Therefore, the procedure's efficiency is adversely affected, underscoring the importance of operating below the threshold of the limiting current density.

In practical terms, when plotting the ratio U/I against 1/I, the inflection point P, termed the polarization point, reveals the limit current intensity, as referred to Fig. 6 – b. This approach is based on the Cowan and Brown methodology [94]. For a more rapid and effective assessment, a potentiostat is commonly employed on a laboratory scale.

Consequently, the limiting current density is a direct measure of the ionic concentration of the solution undergoing demineralization. As the process of ED progresses and the ion concentration decreases in the diluate, the limiting current similarly reduces. Should this threshold be surpassed, the concentration at the solution-membrane interface approaches zero, and the solution's resistance moves toward infinity. This scenario can cause localized heating, potentially leading to the membrane's irreversible damage, such as burns or pH shifts. It is thus crucial to accurately determine and regulate j_{lim} throughout the ED operation. For optimal control, determining j_{lim} at a steady concentration is advisable, allowing the operational conditions to be adjusted to consistently stay below the j_{lim} threshold.

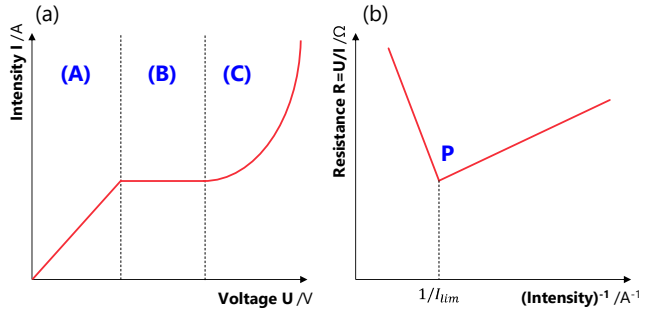

Fig. 6. (a) Evolution of current I as a function of applied voltage U across the stack terminals and (b) experimental determination of the limiting current density.

2.4.2. Current efficiency

In the context of electrokinetic separation techniques, the efficiency with which charged particles are separated or migrated is quantitatively evaluated by the metric known as current efficiency (ξ, also called Faradaic or Coulombic efficiency). In the case of ED in batch mode, this efficiency is a comparison between the actual amount of target charged species transported and the theoretical amount predicted by the charge delivered. In the case of continuous-mode ED, this efficiency compares a mass flow rate with a corresponding electrical current. For batch and continuous processes, this efficiency is usually represented as a percentage, as depicted in Eqs. (26) – (27).

Batch reactor:

$$\xi = \frac{n_i \times z_i \times F}{\int I \times dt} \quad (26)$$

Continuous reactor:

$$\xi = \frac{\dot{q} \times z_i \times F \times (C_{i,in} - C_{i,out})}{N_{cp} \times I} \quad (27)$$

where n is the transformed molar amount during batch operation (mol); $C_{i,\,in}$ and $C_{i,out}$ are the concentration of the target species i at the inlet and the outlet of the stack, respectively (mol/m^{-3}(−|-)); $\dot{q}$ denotes the stack volumetric flowrate (m^3/s); F is the Faraday constant (C/mol).

2.4.3. Specific energy consumption

The consumption of electrical energy by the ED stack can be determined through the product of the voltage applied to the stack, and the electric current flowing through it. Additionally, the energy expenditure for operating the hydraulic pumps was derived from the product of flow rate and the pressure differential. Furthermore, the specific energy consumption (SEC), defined in Wh/m^{-3}(−|-) (often Wh kg^{-1}), represents the energy required by the ED process to produce a specific volume of product solution.

The electrical power (P^{el}, W) utilized by the ED stack is computed as follows in Eq. (28)

$$P^{el} = U_{stack} \times I \quad (28)$$

The power required for hydraulic pumping (P^h, W) through the ED stack is given by Eq. (29).

$$P^h = \rho \times g \times \dot{q} \times \Delta H \quad (29)$$

where ρ stands for the mass density of the solution, g the gravitational constant (9.81 m s^{-2}), $\dot{q}$ the stack flow rate (m^3/s), and ΔH the hydraulic head loss across the stack (m).

The specific energy consumption (SEC) for a batch and a continuous reactors are calculated with Eqs. (30) – (31).

Batch reactor:

$$SEC = \int_0^t \frac{P^{el} + P^h}{V} \times dt \quad (30)$$

Continuous reactor:

$$SEC = \int_0^t \frac{P^{el} + P^h}{\dot{q}} \times dt \quad (31)$$

where $\dot{q}$ the stack flow rate (m^3/s).

2.4.4. Ion selectivity

In conditions where electromigration is the prevailing mechanism, outstripping the effects of diffusion and convection, the ion flux described in **Eq. (21)** can be simplified accordingly to $J_i \approx -\frac{z_i D_i^m F C_i^m}{RT} \times \frac{d\varphi^m}{dx}$. This simplification is feasible because each ion species is subjected to an identical gradient in the transmembrane electrostatic potential. Consequently, it becomes possible to express the fluxes of different ions, normalized by their concentrations [80], as in **Eq. (32)**.

$$S_{i,k} \equiv \frac{J_i C_k^s}{J_k C_i^s} \approx \frac{K_i}{K_k} \times \frac{z_i u_i^m}{z_k u_k^m} = \frac{\gamma_i^s \gamma_k^m}{\gamma_k^s \gamma_i^m} \times \exp\left[-\frac{(z_i - z_k)F}{RT} \times \Delta\varphi_D\right] \times \frac{z_i u_i^m}{z_k u_k^m} \quad (32)$$

Therefore, the ability of IEMs to selectively separate ions arises from disparities in the sorption and migration behaviors of ions *i* and *k*. The key determinants influencing the discrimination between ions include the valence (and polarity) of the ions (z), the activity coefficient in the membrane (γ^m), and the ions' absolute mobility within the membrane (u^m).

The ion selectivity capabilities of IEMs can be structured into *(i)* their charge selectivity (*e.g.*, chlor-alkali process [95]), *(ii)* valence selectivity (*e.g.*, recovering Li^+ from Mg^{2+} in lithium-rich brines [96]), and *(iii)* specific ion selectivity (*e.g.*, separation of Li, Ni, Mn, and Co from $LiNi_{0.33}Mn_{0.33}Co_{0.33}O_2$ for battery recycling [97]). Selectivity can also be studied between the crossover of uncharged molecule and ions within IEMs and can be systematically divided into two key areas: *(iv)* ion/solvent selectivity (*e.g.*, solvent crossover [98]) and *(v)* ion/uncharged solute selectivity (*e.g.*, mixing of dissolved H_2 and $O_{2,(g)}$ creating hazardous situation [99] or vanadium ions cross-over in vanadium redox flow battery [100]). Several detailed reviews focusing on the fundamentals [80,85] or modeling [101] of those aspects are reported in the literature.

2.4.5. Permeability-selectivity balance

The permeability of an IEM towards a specific ion is foundational to the efficiency of most IEM processes. Membrane permeance is defined as the ion flux per unit driving force, and when this value is multiplied by the membrane's thickness, it yields the membrane's permeability L_p (L m^{-2} s^{-1} bar^{-1}).

Ionic conductivity σ_i (S m^{-1}) emerges as a significant parameter. This measure is not an intrinsic membrane property but is influenced by operational conditions such as the concentrations of solutions involved [102]. A higher σ_i suggests more efficient ion transport, implying that a membrane with higher ionic conductivity for a particular ion would require less surface area to achieve a specific separation yield, potentially reducing both capital and operational costs [103]. However, the pursuit of increased ionic conductivity often leads to a decrease in selectivity, particularly in the discrimination between counter-ions and co-ions. The compromise between conductivity and selectivity is attributed to the alteration in the membrane's water content, steric effects and the density of fixed charges within the membrane which affects the ion transport pathways [104,105].

Within ED apparatuses, it has been noted that the membrane's thickness significantly influences the overall performance of the cell. Thicker membranes tend to elevate the cell's resistance. On the contrary, thinner membranes decrease the area-specific resistance but concurrently cause an increase in the crossover flux of reactants, which is proportionally related to selectivity [106]. This not only leads to diminished power efficiency but also accelerates the rate of degradation, affecting the system's longevity adversely. Employing thinner membranes can also serve to lower the costs associated with materials, presenting an advantageous aspect for the commercial viability. Consequently, there is a discernible compromise among cost reduction, enhanced performance, and longevity [107]. A recent examination conducted by researchers at General Motors [108] on fuel cell membranes revealed that the interplay between conductivity and permeability due to varying membrane thickness has a direct correlation with both the durability and the total cost of ownership. Enhancements in conductivity are beneficial for increasing power density and diminishing the cost of the stack, whereas an increase in gas crossover (*i.e.*, permeability) elevates fuel expenses and detracts from the membrane's and the system's operational lifespan.

This trade-off is analyzed through the lens of sorption-migration transport equation (Eq. **(32)**). The flux of ion *i*, and thus its conductivity σ_i, can be enhanced by either increasing *(i)* the ion's concentration within the membrane or *(ii)* its mobility. The sorption of ion *i* is governed by its activity coefficient ($C_i^m \propto 1/\gamma_i^m$), which dictates how readily the ion is absorbed into the membrane. For improved conductivity, conditions that lower the activity coefficient and increase the ion's mobility (u^m) are preferred. Conversely, enhancing selectivity ($S_{i,k}$) involves optimizing the relative sorption and mobility ratios of ions *i* and *k*, aiming for conditions where the activity coefficient ratio is low (γ_i^m/γ_k^m) and the mobility ratio is high (u_i^m/u_k^m).

This nuanced understanding of the conductivity-selectivity trade-off in IEMs underscores the challenges in optimizing membrane performance for specific applications. It highlights the need for a balanced approach in membrane design, where enhancements in selectivity or conductivity are achieved without significantly compromising the other metric [109].

3. Advances in membrane materials and fabrication techniques

In the context of ED, the development of new electrode materials is not an active area of research, as it is not a limiting factor in the process. However, concerning membrane technology and selectivity optimization, significant advancements have been made in the development of innovative membrane materials, each addressing specific challenges and applications in the field of separation processes. The recent advancements in both robust and efficient AEM and BPM have enabled the industrial-scale development of ED. The following sections will concisely present the state of the art concerning *(i)* membrane materials, *(ii)* advances in fabrication and finally *(iii)* IEM performance characterization methods.

3.1. AEM materials

AEMs must operate effectively within alkaline environments to fulfill their roles. To position AEM technologies as viable alternatives to current CEM and Nafion® solutions, ongoing research is intensively directed towards enhancing both the conductivity and longevity of these membranes under such challenging conditions [110]. The European Union's Horizon2020 initiative, through its FCG-02–4-2019 call for projects (ANIONE [111], CHANNEL [112] and NEWELY [113]), has established specific targets (stability of 2000 h, hydroxide conductivity of 50 mS cm^{-1}, etc. [114]). Among these, durability emerges as a paramount objective, pursued through a variety of strategies focusing on the selection of ionic functionalities and the structural composition of the polymer backbone.

3.1.1. Functionnal carriers

In AEMs, ionic functionalities comprise cationic groups containing heteroatoms such as nitrogen, phosphorus, sulfur, or metallic cations.

3.1.1.1. Quaternary ammoniums. Quaternary ammoniums are characterized by a N atom substituted by four groups, forming a cation, and are

widely studied for AEM development due to their straightforward and cost-effective synthesis. However, their lifespan in alkaline conditions is limited by various degradation mechanisms, with propyl-trimethyl amine exhibiting a half-life of only 33.2 h in strong alkaline conditions (6 mol/L NaOH), including nucleophilic substitution (S_N2 reaction), Hofmann elimination, Stevens rearrangement, Sommelet-Hauser rearrangement, and 1,4-elimination [115]. The most concerning are nucleophilic substitution and elimination reactions, involving carbons adjacent and next to the N atom, respectively.

To improve longevity, tetramethylammonium (TMA) [116] and benzyl trimethylammonium (BTMA) [117] derivatives have been studied, showing enhanced resistance to degradation, though challenges persist in integrating them into membranes. Innovations in membrane design, including the use of side chains and multi-cation chains, aim to counteract these issues but often face trade-offs between ionic conductivity and stability [118]. Notably, cyclic and spirocyclic ammonium structures have emerged as highly promising for their remarkable stability in harsh alkaline environments, attributed to their unique geometric configurations that resist common degradation reactions [119,120].

3.1.1.2. Imidazoles. Imidazoles are aromatic heterocyclic compounds with a 5-atom ring, including two N atoms. When both N atoms are substituted, imidazole forms a cation with charge delocalization across the ring. Imidazoles are readily synthesized and converted into cations through alkylation [121]. The stability of imidazole derivatives in alkaline conditions varies significantly with the substitution pattern on the ring. Unsubstituted imidazoles are particularly prone to degradation, including ring-opening and deprotonation reactions. However, strategic substitutions at specific positions on the imidazole ring can enhance stability. For instance, substituents at the carbon between the N atoms (C2) or on the N itself can prevent degradation, with aryl groups providing better protection than benzyl groups. Additionally, substitutions at the outer carbons (C4 and C5) effectively inhibit degradation, likely due to steric hindrance and electronic effects, including resonance stabilization [116,122]. Hugar et al. demonstrated that certain imidazole derivatives, especially those with mesityl groups or bis-substituted with aryl groups, exhibit remarkable resistance to alkaline degradation, showing less than 1 % degradation after extensive exposure to harsh conditions [122].

3.1.1.3. Guanidiums. Guanidiniums, derivatives of guanidine where nitrogen bounded by a double bond to a carbon is quaternary, feature a charge delocalized across the nitrogen and carbon. This characteristic can enhance the catalytic properties of platinum and other metals supported on carbon in oxygen oxidation and reduction reactions [121]. However, the guanidinium group is susceptible to addition reactions in alkaline environments, risking the elimination of the quaternary nitrogen. To counteract this, the introduction of sterically hindering groups, such as ethyl substituents on the N atoms, has been shown to limit degradation, with compounds exhibiting less than 10 % degradation after 312 h in a 1 mol/L KOH solution at 60 °C [123].

3.1.1.4. Quaternary phosphoniums. Beyond N, phosphorus atoms can also bear cationic charges as in quaternary phosphonium ions. These ions, susceptible to nucleophilic attacks and α- and β-eliminations like ammonium ions, face additional vulnerability to direct OH^- attacks on the phosphorus, leading to phosphonium group detachment due to phosphorus's oxophilic nature [121].

Enhancing the stability of these cations can be achieved through phenylic substitutions, which donate electrons to the phosphorus, thus conjugating and stabilizing it against degradation. For instance, the MTPP-(2,4,6-Me) degrades only 10 % after 2000 h in 1 mol/L KOH at 80 °C [124].

The tetra(dialkylamino)phosphonium family showcases a different stabilization strategy, where alkyl or cyclohexyl substituents mitigate degradation through structural reinforcement, reducing susceptibility to nucleophilic and elimination reactions [125,126]. This approach is exemplified by membranes such as TPQPOH, which exhibit low anionic conductivity (27 mS cm^{-1}) but high resistance to degradation (less than 1 % degradation over 720 h), underscoring the potential of tailored substituents in enhancing the durability of phosphonium-based materials in harsh environments [127].

3.1.1.5. Organometallic cations. Multivalent metal cations can coordinate with multiple anions, enhancing IEC, evident in ruthenium, nickel, and cobalt cations. Ru-based cations show good alkaline stability, but AEMs incorporating them have relatively low conductivities comparable to quaternary ammoniums and, due to their cost, remain of limited interest. Conversely, nickel serves both as an ionic conductor and a cross-linker to form ionic clusters, yet membranes containing it suffer from mechanical properties unsuitable for ED applications [121]. In addition, tetra-*tert*-butyl cobaltocene undergoes only 8.2 % degradation after 1000 h in 5 mol/L KOH at 80 °C [128], and octamethyl cobaltocene 8.5 % degradation after 1000 h in 1 mol/L NaOH at 140 °C [129].

3.1.2. Backbones

In the exploration of polymer backbones for enhanced stability in alkaline environments, the focus has shifted towards developing polymers beyond traditional aryl ether-based polymers like PEEK, PSU, and PPO. These conventional polymers are vulnerable to nucleophilic attacks, prompting the search for more resistant skeletal structures without ethers [130].

Radiative grafting has emerged as a promising method to modify commercial polyolefins and fluoropolymers, such as ETFE, HDPE, and LDPE, with BTMA [110]. This technique allows for the direct attachment of BTMA onto these polymers, yielding membranes with high conductivity and variable stability against alkaline degradation.

Polynorbornene (PNB) synthesized via ring-opening metathesis polymerization (ROMP) offer another avenue, leveraging the ROMP method's ability to create polymers with complex architectures. These polymers can achieve high conductivity and low degradation rates in alkaline solutions, with enhanced performance through strategic modifications such as side chains and cross-linking [110,130].

Synthesized through Diels-Alder polymerization, polyfluorenes and polyphenylenes *via* metal-catalyzed coupling reactions (Suzuki-Miyaura and Yamamoto couplings), represent advanced approaches to polymer backbone development [110,130]. These methods provide pathways to easily incorporate functional groups like quaternary ammoniums into the polymer structure, although they differ in synthesis complexities and polymer properties [131,132].

Acid-catalyzed polycondensation offers a route to synthesize ether-free, metal-free polyaromatics with high molecular weight, demonstrating significant potential [130,133].

3.2. CEM materials

CEMs are currently prevalent in a variety of industrial applications, including fuel cells, electrolysis, ED, and vanadium flow batteries. Predominantly, these membranes are based on perfluorosulfonic acid (PFSA, $-CF_2SO_3H$) materials. Originating from Dupont's innovation in the 1960 s, marketed under the brand name Nafion®, this copolymer foundation is similarly employed in the development of Solvay's Aquivion®, Flemion®, Hyflon®, Dow®, Aciplex® or BAM3G® and GoreSelect® membranes [134]. The key benefits of using this polymer include its notable ionic conductivity, excellent chemical resistance, especially against oxidation, and its satisfactory mechanical durability. However, its production is relatively expensive, and the degradation process releases environmentally harmful perfluorosulfonic and perfluorocarboxylic acids due to the presence of perfluorinated groups

[135]. Additionally, its application at temperatures exceeding 100 °C poses challenges due to a decrease in mechanical strength and the necessity for hydration to maintain conductivity. Altering the polymer structure to introduce new functional groups or to create a copolymer tailored for specific applications presents significant difficulties [136].

In this section, two strategies are presented for the creation of advanced generations of CEM. The first strategy involves subjecting PFSA to various treatments or engaging in its hybridization. The second strategy concentrates on the development of innovative polymers.

3.2.1. Enhancements to polymer properties

Modifying the PFSA polymer's electrical conductivity, resistance, water retention, and mechanical properties through alterations in its chemical structure presents considerable challenges. Nonetheless, advancements in treatment methodologies, preparation protocols, and hybridization approaches have shown potential to induce these changes effectively, as cataloged comprehensively by Karimi et al. [137]. Thermal treatments influence the crystalline architecture of PFSA membranes, with the effects varying substantially based on the temperature and method of the treatment. These processes, which include annealing in controlled environments such as ovens or through wet methods involving boiling solutions, modify the crystalline state towards equilibrium, thus affecting the membrane's water uptake and conductivity. High temperatures, however, might increase crystallinity, thereby hindering the polymer's flexibility and functional performance [138–141]. Employed primarily to prepare PFSA membranes for applications in fuel cells and electrochemical devices, acid and peroxide treatments target the removal of organic residues and enhance proton conductivity by protonation at the anionic sites of PFSA. The choice of acid is critical, requiring a dissociation capability superior to the PFSA's acidic groups to achieve effective protonation, as demonstrated by the distinct protonation levels achieved with different acids [142]. These treatments not only refine the IEC but also modulate the membrane's water absorption and electrical resistance, tailoring it for specific ion exchange applications. Alternative strategies, such as exposure to supercritical CO_2 or subjecting PFSA membranes to electric fields, have been utilized to manipulate the membrane properties further. These treatments aim to enhance crystallinity and align the copolymer blocks and ionic clusters within the membrane, thereby facilitating improved pathway formation for proton conduction and achieving significant increases in conductivity [143,144]. Hybridization of PFSA membranes with polymers like PTFE [137], or inorganic NPs like titanium dioxide (TiO_2) and silicon dioxide (SiO_2) introduces additional properties into the base material [145]. These composites enhance mechanical strength and water uptake through the formation of new ionic clusters around the NPs. Moreover, the size and surface functionalization of these nanoparticles are critical; smaller, functionalized nanoparticles significantly enhance conductivity by forming efficient conduction paths and promoting mechanisms beneficial under varying humidity conditions [146–148]. Such modifications also protect the membrane from radical-induced degradation, crucial for maintaining long-term stability and performance in electrochemical applications.

It should be noted that the primary objective must be to do without PFSA groups, which are now recognized worldwide as an eternal pollutant harmful to our environment.

3.2.2. Advancements in the field of new ionic groups and backbones

Despite the advantageous attributes of PFSA membranes, innovative polymer families have been introduced as alternatives for CEMs. These advancements aim to identify membranes that offer similar conductivity and degradation resistance as PFSA membranes during operational use, while being more cost-effective to produce and fluorine-free, thereby lessening their environmental footprint. Similar to the case with AEMs, the characteristics of these membranes are influenced by both their functional groups and structural frameworks. The frameworks designed for CEMs are similar to those for AEMs, and as such, will not be extensively elaborated on in this section.

3.2.2.1. Ionic groups. CEMs can incorporate various functional groups that are easily deprotonatable acids, such as the sulfonic group $-SO_3H$ in PFSA membranes. These groups' pKa values influence membrane conductivity; higher pKa correlates with higher conductivity, yet selection also considers stability and resistance to degradation [110]. For instance, sulfonimide groups offer superior proton conductivity but are oxidation-prone, limiting their application. Conversely, carboxylic acid groups, despite their moderate high pKa value (4–5) and resulting low conductivity, can enhance membrane chemical and thermal stability, especially when combined with sulfonic acid and used in high-temperature applications through cross-linking methods like terephthalic dihydrazide [149,150].

3.2.2.2. Backbones. Backbones containing heteroatoms, such as SPEEK or SPPS, are easily synthesized through polycondensation and require a higher IEC than PFSA due to their less hydrophobic nature, affecting phase separation and mechanical properties [110]. Strategies to enhance phase separation include *(i)* separating the functional group from the backbone with a flexible chain [151], *(ii)* utilizing copolymer architectures [152], *(iii)* adding side chains [153], and *(iv)* increasing sulfonation density [154]. Despite these strategies, the presence of heteroatoms makes the polymers prone to oxidation and radical attacks. Various works developing novel polymers such as fluorinated polystyrenes [110], organized sulfonated polyethylene [155] or polyphenylenes [156,157], have been published over the years.

3.3. Bipolar membrane materials

BMs bear resemblance to p-n junction semiconductors, with the junction at the BM's interfacial layer (IL) acting as a depletion zone. The fabrication of BMs traditionally involves the layer-by-layer deposition of CEL and AEL materials, or by physically bonding CEL and AEL through the application of external heat and pressure or employing adhesives. Through these fabrication techniques, a thin, modified IL emerges between the CEL and AEL, facilitating the production of protons and hydroxide ions. At the CEL interface, a higher pKa value for a functional group enhances the dissociation kinetics. Hence, the sulfonic group, with a pKa of 1–2, is less suitable compared to carboxylic and phosphonic groups, which have pKa values of 4–6 and 3–7, respectively [158]. On the AEL side, primary, secondary, or tertiary amines [159], tertiary ammoniums, pyridyls, or imidazole are preferred. It is crucial that the materials employed in both CEL and AEL facilitate efficient ion transport to achieve optimal ionic conductivity in membranes. To this end, strong ionic groups such as sulfonic acid for CELs and quaternary ammonium or pyridinium for AELs are essential. A promising approach involves the encapsulation of catalysts within the IL to introduce alternative pathways for the dissociation reaction. This necessitates incorporating a specific catalytic layer at the ion exchange layers' interface, which can be a polymer containing weak acid functions like pyridyl, amino, carboxylic, sulfonic, and ammonium groups, showing promise. Alternatively, the polymer may be designed as a dendrimer, such as PAMAM [160] or Boltorn® series [161], whose branched structure enables a high concentration of catalytic groups. The recent use of metal–organic framework (MOF on the metal or ligand site) [162] or graphene catalyst [163] has also been reported in the literature.

The above solutions are starting to be developed on an industrial scale. Recent literature [41,44,164–167] provides a wealth of tabulated information on the characteristics (*e.g.*, manufacturer, functional groups, composition, performance, etc.) of various commercial membranes, including AEM, CEM and BM, available on the market.

3.4. IEM specification for electrodialysis

The integration of ion exchange membranes into the ED process differs from other types of membrane (*e.g.*, ultrafiltration, nanofiltration, etc.) in 2 ways: *(i)* the use of BMs to vary the pH of adjacent solutions, and *(ii)* the use of AEM and CEM to selectively separate anions (OH^- and other negative ions) and cations (H^+ and other positively charged ions). ED remains the technology of choice for BM. For IEMs of the AEM/CEM type, the use of these membranes in electrolyzers or energy storage systems needs to be distinguished with their use in ED. In the first case, the membrane is preferentially used for transporting protons or hydroxides. In the case of ED, membrane selectivity needs to be optimized to allow the passage of specific ions (other than protons and hydroxides).

Unlike conventional membranes, IEMs are distinguished not only by their material composition or pore size but by their interactions with charged molecules and the specific nature of their functional groups. Ion transport through an IEM can be broken down into five steps: *(i)* ions move from the dilute compartment to the membrane surface across a solution boundary layer, *(ii)* ions partition into the membrane at the surface, *(iii)* ions traverse through the bulk of the membrane, *(iv)* ions exit on the opposite side of the membrane surface, and *(v)* ions move across a solution boundary layer to the concentrate. The selectivity of counter-ions is predominantly determined during the partitioning phase and their migration through the membrane matrix and boundary layer in the electrolyte solution [59].

Consequently, charge density is a crucial factor influencing ion transport to maintain electroneutrality. Enhancing ion removal efficiency involves adjusting the charge density and incorporating specific functional groups that form hydrophilic or hydrophobic domains, thereby improving selectivity for ions of varying valences [168,169]. The selectivity of IEMs for ions with different valences arises directly from how these ions interact with the hydrophilic domains. High-valence ions exhibit higher charge densities, leading to stronger electrostatic interactions with the fixed charged groups in the hydrophilic regions. This interaction creates a greater energy barrier for their passage compared to monovalent ions. As a result, the hydrated channels within these hydrophilic domains are more conducive to the transport of monovalent ions, as they require less energy to move through the membrane [170].

The morphology of the membrane also plays a significant role in ion removal. For example, perfluorosulfonic membranes like Nafion® 117 have a homogeneous structure with uniformly sized pores and evenly distributed functional groups [171]. In contrast, the heterogeneous HDX 100 membrane shows irregular ion depletion due to a broader distribution of pore sizes and functional groups, resulting in surface concentration polarization [172]. The literature frequently documents the reduced j_{lim} values observed in heterogeneous IEMs [173]. This reduction is ascribed to the existence of surface regions with varying conductance. The underlying mechanism involves the deflection of current paths as they near ion-impermeable zones, such as those associated with the reinforcing fabric or polymer binder-rich areas [174]. These deviations, from a direct trajectory observed in the case of homogeneous IEM, lead to the observed decrease in j_{lim} values.

Ionic selectivity during the separation of multiple counter-ions is governed by other mechanisms. One such mechanism is the electrostatic barrier effect, which results from the varying degrees of electrostatic interaction between counter-ions and the membrane surface [175]. Counter-ions with higher valency, larger size within the same valency, or lower hydration energy tend to have stronger electrostatic affinities [176].

Another influential mechanism is the ion's affinity for water (*i.e.*, solvation shell [177]), as described by Gibbs hydration energy, and the hydrophobicity of the membrane surface. Ions with lower hydration energy shed their water molecules more easily, facilitating their transport through the hydrophobic membrane [178].

Steric hindrance also affects ionic selectivity by restricting the partitioning of larger ions within the dense structures of IEMs. Smaller ions, typically less than a nanometer in size, can penetrate the hydrophilic pores of the membrane more rapidly. Therefore, the ease of counter-ion partitioning depends on factors such as ion size, valency, hydration energy, as well as the membrane's fixed-charge concentration and water uptake capacity [179,180]. For example, the fabrication and characterization of AEMs (fabricated with ion-exchange resins with different alkyl groups and a polymeric binder with charged functional groups) demonstrated enhanced selectivity for NO_3^- over Cl^-. This investigation focused on how varying the length of alkyl substituents in quaternary ammonium groups influenced membrane properties, particularly water content. The increased selectivity for NO_3^- was linked to a reduction in water content, resulting in greater membrane hydrophobicity as the alkyl chain length increased. This rise in hydrophobicity, coupled with enhanced steric hindrance from larger alkyl groups, likely caused a partial loss of water molecules from the hydration shells of the counterions [170].

Moreover, other solutions studied on a lab scale are still under development, such as *(i)* monovalent ion perm-selective membranes (permeation of mono-valent ions, while blocking passage of multi-valent ions) [181] and *(ii)* mixed matrix membranes (inorganics embedded into organic polymers) [182].

3.5. Advances in fabrication

Crafting new materials with advantageous features for IEMs is as critical as adopting appropriate fabrication techniques to assure the membranes' quality. The conventional fabrication process, called phase inversion, involves dissolving these innovative materials in solvents, spreading the solutions on a smooth surface to form films, followed by solvent evaporation and sometimes subsequent modifications (like sulfonation or amination) to enhance the membranes' properties [36,183]. At the same time, innovative methods for preparing IEMs are being developed to enhance their structural integrity and functional characteristics.

3.5.1. Polymer blending

Within the realm of IEMs, polymer blending is a pivotal technique [184], distinguished by two principal approaches: the mixing of fluorinated with non-fluorinated polymers and the combination of functional with non-functional polymers. The strategic amalgamation of these polymers aims to harness their respective strengths, enhancing IEM performance by improving ion conductivity through the introduction of water channels by ion-functionalized polymers, while mitigating water swelling and bolstering stability through the incorporation of hydrophobic polymers. This blend not only promises to refine the physical and chemical properties of IEMs but also faces the challenge of maintaining mechanical integrity amidst the diversity of materials employed, such as PVDF/SPPO [185], PAES/PPO [186] or PVA/PSSA-MA [187] for example. Yet, achieving harmony among diverse materials poses a significant hurdle, potentially leading to compromised mechanical strength in blended IEMs due to the proliferation of interfaces [164].

3.5.2. Pore filling

Numerous researchers have recently developed IEMs characterized by minimal swelling and enhanced selectivity through pore-filling techniques, involving the infiltration of electrolytes into porous substrates (PAN [188], high density PE [189], PP [190], PES [191], PI [192]) as illustrated in Fig. 7. This method leverages the chemical and mechanical robustness of these substrates to effectively limit the expansion of electrolyte polymers, using either polymeric or monomeric electrolytes.

3.5.3. In-situ polymerization

The conventional methods for producing IEMs often involve

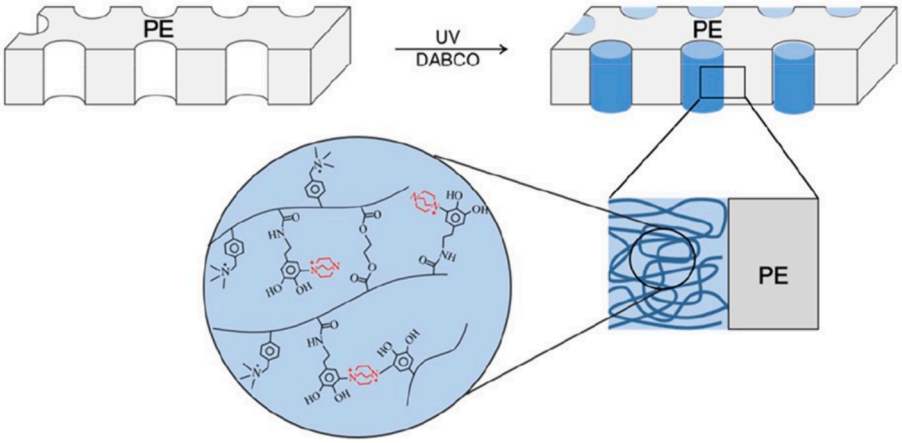

Fig. 7. Schematic structure of the pore-filling membrane preparation based on the reaction between DMA and DABCO motifs. Adapted with permission from [193]. Copyright 2024 American Chemical Society.

modifying pure polymers or synthesizing monomers with specific functions, processes that typically require significant amounts of harmful organic solvents (*e.g.*, DMF, DMAc, etc. [194]). To facilitate the production of IEMs on an industrial scale in an environmentally friendly manner, the development of straightforward, quick, and green fabrication techniques is crucial. A novel solvent-free *in-situ* polymerization approach has been introduced to address the environmental and practical challenges posed by traditional solvent-reliant methods. This innovative technique, already investigated with different systems (BPPO/ST/DVB [195], SPEEK/PMA/PANI [196]), distinguishes itself by using liquid monomers that become an integral part of the finished membrane, thereby eliminating the need for organic solvents.

3.5.4. *Electro-spinning*

This technic, illustrated in Fig. 8 – **a**, has emerged as a popular method for creating continuous nanofibers, offering key benefits like a high specific surface area, increased chemical reactivity, and a cost-effective production approach [197]. The solvent electrospinning process leverages electrostatic repulsion from surface charges in the polymer solution to extend a viscoelastic jet uniaxially. This method involves a high-voltage power supply, a spinneret equipped with a needle for the polymer solution, and a grounded collector. The polymer solution, fed through the needle by a syringe pump at a controlled rate, becomes charged under high voltage. This induces electrostatic repulsion among surface charges and Coulombic forces from the external field, forming a Taylor cone. Overcoming surface tension, the jet stretches, thins, and solidifies into nanofibers as the solvent evaporates, collected as a non-woven membrane [198]. This technique, already developed at commercial stage (Elmarco s.r.o., Liberec, Czechia and Inovenso Ltd., Istanbul, Turkey for example), allows for precise control over the nanofibers' structure (average fiber diameter often approaching 200 nm) and morphology by adjusting variables such as polymer type, solution concentration, solvent characteristics, and spinning conditions [199]. Several studies have explored the impact of size on ion-exchange nanofibers, finding that smaller diameters generally lead to improvements in IEC and ionic conductivity. For instance, research by Dong et al. [200] demonstrated in Fig. 8 – **b**; that Nafion® nanofibers with a diameter of 400 nm achieved a conductivity of 1.5 S cm^{-1} (measured by electrochemical impedance spectroscopy (EIS)), highlighting the potential of nanofibers for enhancing EC separation processes. The reduction in fiber size contributes to lower internal resistance (η_{ohm}^{IEM}) and higher efficiency in these applications. The versatility of electrospinning has led to the development of numerous polymers and composite materials (PECH/PAN/DABCO [201], QPVA/PDDA [202], PBI [203] nanofibers), finding applications across various domains.

3.6. *Basic specifications and characterization of ion-exchange membranes*

Once manufactured, membrane performance can be evaluated according to several criteria, for example to optimize manufacturing conditions. Fine-tuning the properties of IEMs is a complex task due to the conflicting effects of certain parameters. For example, enhancing mechanical strength through increased cross-linking can lead to higher electrical resistance due to a lower mobility of polymer chains. The core polymer matrix is fundamental in establishing the membrane's mechanical, chemical, and thermal properties, whereas the type and concentration of ionic groups within the matrix are key to its permselectivity and electrical characteristics, yet they also influence its mechanical integrity [183].

3.6.1. *Basic characteristics*

3.6.1.1. Ion exchange capacity. IEC quantifies the membrane's total active or functional groups facilitating ion exchange. It is typically measured *via* a standard acid-base titration, where the IEC value, expressed in meq g^{-1} or mol/g, is calculated based on the volume of titrant utilized in titration, the membrane's dry weight, and the titrant solution's concentration, as depicted in Eq. **(33)**. This metric is crucial for evaluating the membrane's ion exchange efficiency [205,206].

$$\mathrm{IEC} = \frac{\text{molar amount of ion carriers}}{m_d^m} \tag{33}$$

where IEC is expressed in mol/g and m_d^m is the dry membrane weight (g).

Additionally, the IEC aids in calculating the membrane's fixed-ion concentration X^m in terms of moles of sites per unit volume of the wet membrane, employing **Eq. (34)**. This calculation is essential for assessing the density of active ion-exchange sites within the membrane's structure.

$$X^m = \frac{\epsilon \times \mathrm{IEC} \times \rho_d}{\Delta V} \tag{34}$$

where ϵ is the porosity (*i.e.*, volume of free water within the membrane per unit of volume of wet membrane, dimensionless); IEC is expressed in equivalent per gram of dry membrane; ΔV is the volume dilatation of the membrane upon absorption of water per unit of volume of dry membrane (m^3); ρ_d is the density of the dry membrane ($g/m^{-3}(-|-)$).

3.6.1.2. Water content. The degree to which IEMs expand in presence of water can vary based on the solution's salinity and chemical makeup they come into contact with. This expansion, or water content WC (also known as water uptake), measured in grams of water per gram of dry

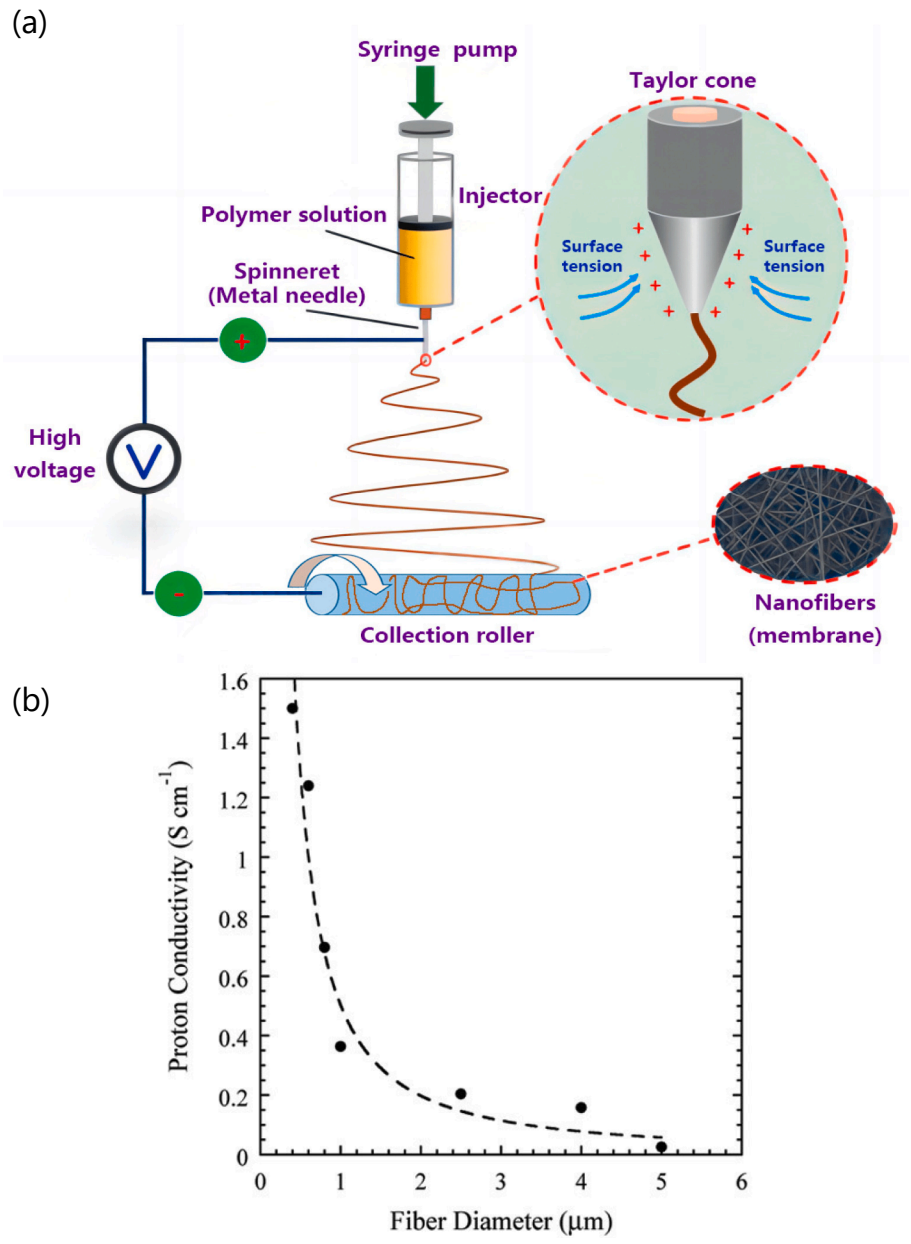

Fig. 8. (a) The electrospinning device and (b) proton conductivity (at 30 °C, 90 % RH) vs. fiber diameter for high-purity Nafion® nanofibers measured on individual nanofibers. Figure (a) reprinted with permission from [204] (CC-BY MDPI). Figure (b) reprinted with permission from [200]. Copyright 2010 American Chemical Society.

polymer, plays a critical role on ion mobility through the membrane. The water content of the membrane is determined, as illustrated in Eq. (35), by comparing its mass when dry and when swollen, a process done through gravimetric measurements.

$$WC = \frac{m^m_{wet} - m^m_{dry}}{m^m_{dry}} \quad (35)$$

where m^m is the mass of the membrane sample (g).

Note that the ionic strength (and therefore the osmotic pressure) of the medium in contact with the membrane has an impact on its swelling. In addition, it is possible to observe water in the membrane by simple equilibrium with a gaseous phase having a certain relative humidity.

3.6.1.3. Mechanical properties. Evaluating the mechanical properties of IEMs encompasses assessments of not only thickness and swelling but also dimensional stability, tensile strength, and hydraulic permeability, requiring membranes that have been pre-treated and equilibrated. The study of water permeability illuminates the movement of water through membranes influenced by hydrostatic pressure. Notably, the occurrence of pinholes and high porosity can heighten permeability (**Eq. (36)**) [207,208].

$$\epsilon = \frac{\Delta V}{(1 + \Delta V)} \quad (36)$$

$$\Delta V = \frac{(m_h - m_d) \times \rho_d}{\rho_w \times m_d} \quad (37)$$

where ϵ is the porosity (*i.e.*, volume of free water within the membrane per unit of volume of wet membrane, dimensionless); ΔV is the volume dilatation of the membrane upon absorption of water per unit of volume of dry membrane (dimensionless); m and ρ are, respectively, the weight (g) and density (g/m^{-3}(−|-)); h and d stands, respectively, for hydrated

and dry membrane states.

The membrane's swelling behavior (Eq. **(37)**) is another critical, influencing its dimensional stability, selectivity, electrical resistance, and hydraulic permeability [209],. This characteristic is dependent on the polymeric material's nature, its IEC, and the degree of cross-linking, typically measured by the variation in water content between the membrane's wet and dry states, indicating the extent of water absorption under specific conditions [210].

3.6.1.4. Electrical resistance. Resistance, measured in Ω, is conventionally referred to as 'electrical resistance'. This term characterizes the capacity of a conductor, such as a resistor, to hinder the flow of electrical current, denoted by I, when a voltage is applied across it. However, in scenarios where a salt solution is partitioned by IEMs, the conveyance of current is facilitated not only by the ions within the solution but also by those within the membrane's pores. In such context, the concept of 'ion transport resistance' might be more aptly applied than the traditional notion of electrical resistance. In the realm of liquids, the concept of resistance is often inverted to discuss conductance (measured in S), which encapsulates the capacity for current transport. The value of a membrane's electrical resistance is influenced by its IEC as well as the mobility u_i^m of ions crossing the membrane's structure [211]. Determination of this parameter can be performed by 2 different methods either *(i)* direct current, and *(ii)* EIS with alternating current and frequency variation [212,213].

The electrical resistance exhibited by IEMs plays a crucial role in influencing the energy requirements (especially η_{ohm}^{IEM}) of ED processes. Nevertheless, in many practical scenarios, the resistance encountered within the membrane is notably less than that of dilute solutions ($\eta_{ohm}^{dlt} > \eta_{ohm}^{IEM}$). This reduced resistance is attributed to the comparatively high concentration of ions within the membrane itself. Typically, this resistance is quantified in terms of specific membrane resistance (expressed in Ω m). However, for engineering applications, expressing membrane resistance as ASR in $\Omega/m^{-2}(-|\text{-})$ proves to be more practical and is commonly referenced in commercial product specifications. It often ranges from 1 to 100 Ω cm^{-2} depending on the characteristics of the membranes [214].

3.6.2. Permselectivity

The permselectivity PS of an IEM (dimensionless), indicative of its selectivity for counter-ion transport over co-ion transport, is defined through transport numbers as **Eq. (38)**. The transport number t (dimensionless) reflects the proportion of ionic current carried by an ion *i* as presented in **Eq. (39)**.

$$PS = \frac{t_{ct}^m - t_{ct}^s}{1 - t_{ct}^s} \tag{38}$$

$$t_i = \frac{|z_i| J_i}{\sum_i |z_i| J_i} \tag{39}$$

A membrane achieves perfect permselectivity PS = 1 when only counter-ions contribute to ion transport $t_{ct}^m = 1$, whereas it exhibits no selectivity PS = 0 when the transport behavior mimics that in the solution phase $t_{ct}^m = t_{ct}^s$ [215].

IEMs traditionally differentiate between counterions and co-ions, but they also facilitate selective ion separations. These membranes can distinguish ions with similar charges but different valencies, such as separating Li^+ from Mg^{2+} in lithium-rich brines. Further, IEMs capable of identifying ions of the same valence allow for specific separations, such as extracting Co^{2+} from Ni^{2+} in battery recycling fields. As presented in Fig. 11, several recent reviews [23,80,84,85,216] provide extensive insights into the different types of IEM selectivity, namely charge, valence, and specific ion selectivities:

(i) *Charge selectivity*: this selectivity is facilitated by the inherent negatively or positively charged functional groups present in IEMs. The underlying mechanism of selectivity is fundamentally based on the principles of charge attraction and repulsion as depicted in Fig. 11 – a. For example, in CEMs, the negatively charged functional groups draw cationic counterions towards the membrane while simultaneously repelling anionic co-ions. Enhanced charge selectivity is primarily achieved by increasing the densities of fixed charges within the membrane (X^m). This augmentation increases the magnitude of the Donnan potential difference, $\Delta\varphi_D$, which serves to exclude co-ions more effectively from the membrane.

(ii) *Valence selectivity*: the separation of similarly charged ions that differ in valence is also facilitate in IEMs. This differentiation is influenced by ion valence, as demonstrated in Eqs. **(20)**, (21) and (32), which show that valence plays a crucial role in both sorption and migration selectivities. Essentially, the valency of ions provides a dual pathway—*via* sorption and migration mechanisms—to modulate the relative transportation of different counterions. The examination of sorption selectivity (K), indicates that in mixed electrolyte solutions, counterions with a higher valence, z, are preferentially concentrated within the membrane matrix as observed in Fig. 11 – b. This effect can be intuitively understood considering the stronger coulombic attraction between the fixed functional groups of the IEM and species with a larger absolute value of z. There are primarily two strategies commonly used to selectively transport monovalent counterions over their polyvalent counterparts: *(i)* the first method leverages the increased exclusion of co-ions with higher valences, effectively reducing their mobility through the membrane, while *(ii)* the second method involves the application of dense coating layers on the membrane, which enhances the steric hindrance encountered by polyvalent counterions, thereby impeding their passage.

(iii) *Specific ion selectivity*: IEMs could also differentiate between counterions of the same valence which would revolutionize specific ion selectivity. However, since the valence sign and magnitude are the same for the ions intended for separation, ion charge does not serve as a viable criterion for distinguishing between them, unlike in cases of charge and valence-based selectivities. Consequently, achieving specific ion selectivity presents significant technical challenges, and currently, no such membranes are commercially available. To overcome this, coordination chemistry has been explored to facilitate the selective transport of targeted species. By employing ligands that preferentially form reversible complexes with specific ions, these ions can effectively "hop" from one site to another, as illustrated in Fig. 11 – c. This approach utilizes specific coordination interactions to discriminate between counterions with identical valences and selectively transport certain ions over others. It is notable that ions with the same z value typically exhibit similar sizes in their hydrated states, whether they are mono- or polyatomic, which limits the effectiveness of steric methods in enhancing ion discrimination as depicted in Fig. 10.

Moreover, phenomena affecting membrane selectivity (*i.e.*, electro-osmotic and diffusive phenomena) will be detailed in a dedicated Section 4.6 below.

3.6.3. Chemical stability

The expenses associated with IEMs represent a notable portion of both the initial setup costs and the ongoing costs for ED [217]. Consequently, there is a push towards not only lowering the cost of these membranes but also prolonging their lifespan. However, the performance and structural integrity of membranes during ED may be compromised by several factors, such as the accumulation of organic

and inorganic deposits, pH fluctuations, and interactions with treated solution components [218], leading to their deterioration by several mechanisms.

3.6.3.1. Fouling. This phenomenon involves the chemical interaction between the IEM and the components of the solution being treated, leading to compound deposition and membrane property deterioration. This degradation often manifests as reduced electrical conductivity (blockage of pores, ionic sites blocked by multivalent ions) or a decline in limiting current density [219], with models available to describe these effects based on the type of fouling film formed [220,221]. Fouling in IEMs can be categorized (Fig. 9) by its causes as: inorganic substance fouling (also known as scaling due to the formation of a 'scaly' precipitate) [222,223], fouling due to organic molecules and colloids (especially in the food industry) [224,225], and biofouling [226,227].

3.6.3.2. Chemical reactions and physical interactions. IEM degradation encompasses not just fouling but also involves mechanisms unrelated to substance deposition. These include interactions with the physicochemical properties of the solution, such as high ionic strength and reactions between membrane components and solution ions, including H^+ and OH^- ions. These reactions, catalyzed by the membrane's polar groups, extend beyond simple sediment formation, affecting the membrane significantly [217]. The concentration of H^+ and OH^- ions in solutions can alter due to inherent solution properties or generated during ED, impacting IEMs in applications like alkaline fuel cells [229–232], where this issue is extensively discussed. The presence of these ions can lead to protonation/deprotonation reactions and irreversible reactions with membrane materials (such as the cation groups attack *via* Hofmann elimination, nucleophilic substitution to cleave the cationic group from the tethered bond to the polymer backbone, and nucleophilic substitution of dealkylation [233,234]), highlighting the complex influence of physicochemical interactions on membrane longevity and functionality. The degradation of the membrane is influenced by two additional parameters: the elevated ionic strength of the solution [235], and the stretching of the membrane matrix caused by ions with bulky hydration shells [236]. Hydration shell can increase the ions radius by a factor of 14 in the most severe cases, as illustrated in Fig. 10. This significant expansion results in increased mechanical stress on the membrane, further contributing to its degradation.

4. Operational parameters and their impacts on efficiency and selectivity

The performance of the ED process, along with its product quality and economic viability, is significantly influenced by the operating conditions. Specifically, the factors affecting these outcomes can be divided into four main categories: *(i)* intensity of the electric field; *(ii)* concentration of the initial solution; *(iii)* presence of co-ions; and *(iv)* rate of solution feed. The various operating parameters that can influence the performance of the reactor, as well as the phenomena impacted, are synthesized in Fig. 12, and studies focusing more specifically on each phenomenon are provided as examples. To facilitate a comprehensive

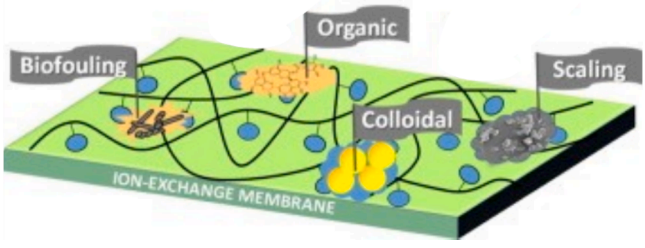

Fig. 9. Types of fouling. Reprinted from [228], Copyright (2016), with permission from Elsevier.

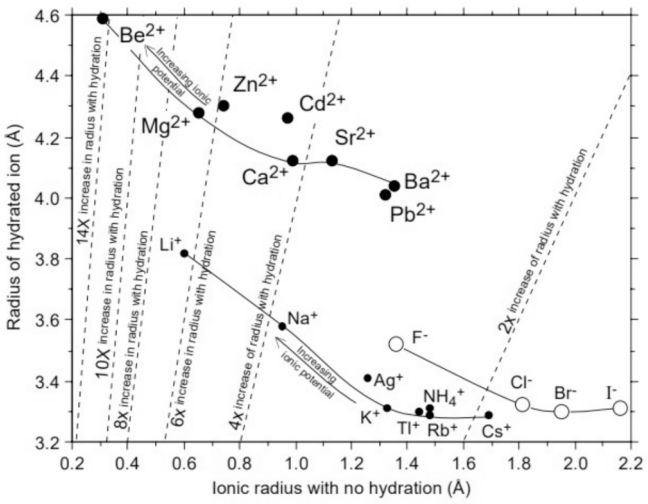

Fig. 10. Relationship between the radius of ions and their hydration status. Ions of smaller dimensions exhibit a greater propensity for hydration, attributed to their higher charge density. Reprinted with permission from [237].

understanding of ED and to foster enhancements in process efficiency, this section will present a detailed examination of each influencing factor and highlight the limiting factors of the process.

4.1. Electric field intensity

In ED, the primary force propelling ion migration is the electric field intensity as previously presented in **Eq. (21)**. The influence of this electric field intensity on the process is examined through two key parameters: current density j and cell voltage U_{stack} which are intrinsically combined. In ED processes, the practice of maintaining a constant current is widespread. Here, the current density is the applied current divided by the effective surface area of the membranes in use. The same types of conclusions presented in this section are therefore identical concerning process behavior in response to cell voltage. The literature on this topic suggests that the impact on the process encompasses several key dimensions: *(i)* ion migration, *(ii)* concentration of reaction products, *(iii)* energy consumption / current efficiency.

An elevation in current density is associated with enhanced ion migration, which contributes to a reduction in the operational duration of the ED process for the same conversion time by increasing the flux across the membrane. For example, the increase in current density was observed to elevate the potassium average flux, illustrating the promotion of ion migration during separation between K^+ and Mg^{2+} [238]. Furthermore, Liu et al. conducted research on the ED process for obtaining Ni^{2+}, NH_4^+, total phosphorus and NO_3^- from electroless nickel-plating wastewater. Their findings revealed that an increase in current density (from 20 to 25 mA cm^{-2}) reduced the operation time from 12 to 10 h for the same removal rate [239] (which is consistent with theory: one monovalent ion exchanged = one electron exchanged in an ideal situation). Leveraging the enhanced ion migration, Peng et al. explored the continuous production of 2-mercapto-5-methyl-1,3,4-thiadiazole (MMTD, intermediate of antibiotic) from MMTD wastewater (containing MTTD and K_2SO_4), observing an increase in the OH^- concentration of the base compartment from 0.4 to 0.8 mol/L as the current density was raised from 30 to 70 mA cm^{-2} [240]. Nevertheless, this elevation of current density was also associated with a noticeable increase in voltage drop, which in turn contributed to a higher electrical resistance and thus augmented energy SEC demands [241]. For instance, an investigation by Doornbusch et al. highlighted that the energy required for the seawater desalination surged from 0.2 to 0.9 kWh/m^{-3}(−|-) when the current density was increased from 2.5 to 7.5 mA cm^{-2} [242], under similar

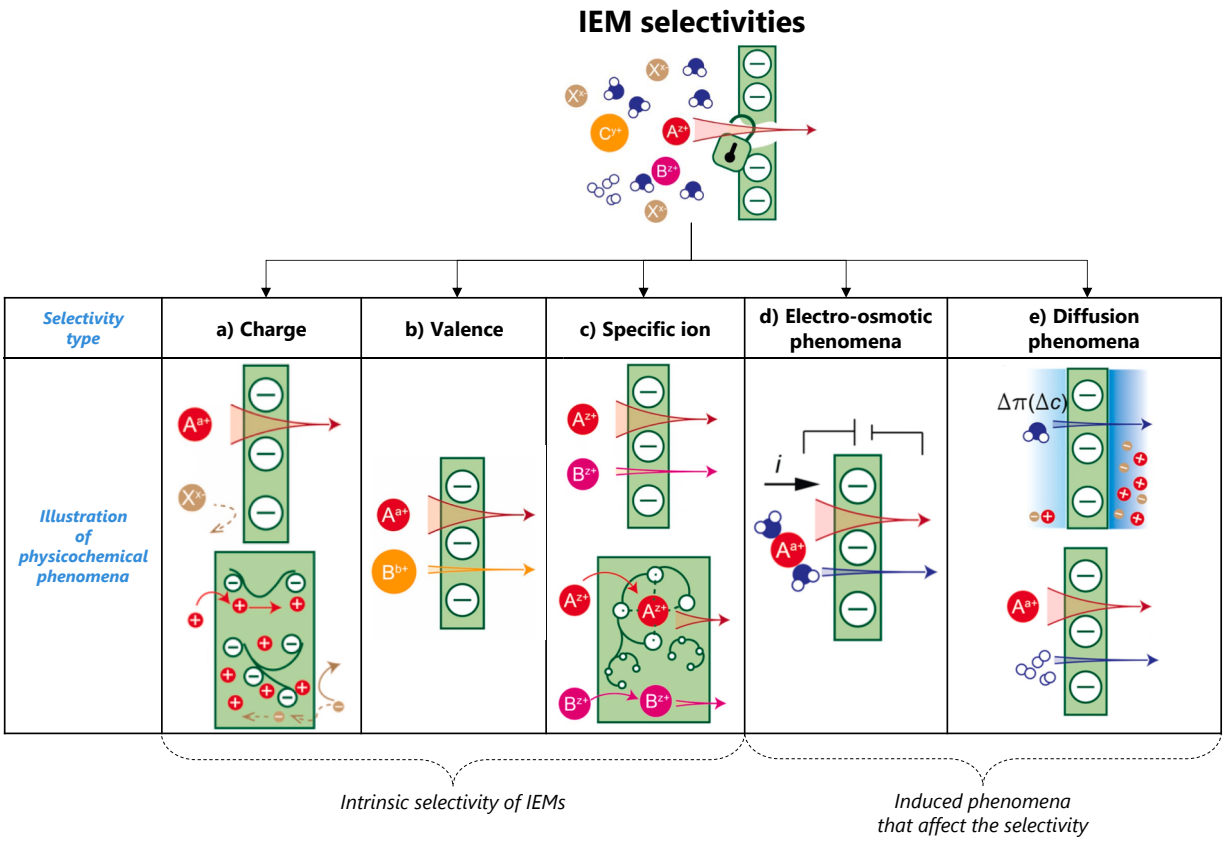

Fig. 11. Summary of the different types of IEM selectivity organized according to a) selectivity according to charge, b) selectivity according to valence, c) selectivity according to specific ion, and selectivities subjected to IEMs according to d) electro-osmotic phenomena and e) diffusion phenomena (via osmosis or gas separation). Adapted with permission from [80] (CC-BY 4.0 Springer).

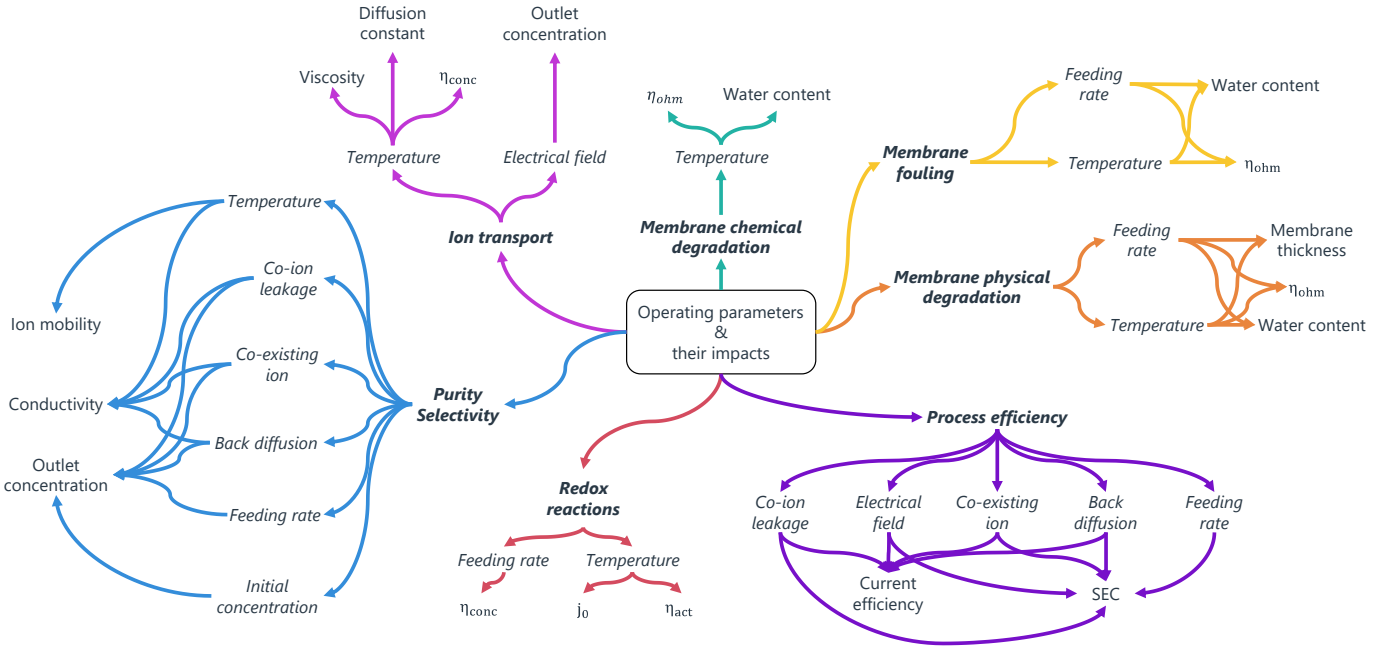

Fig. 12. Summary of the influence of each operating/limiting parameter on the ED process. Phenomena that are impacted are represented in italic and bold, operational parameters or limiting factors in italic, and the measurable parameter in plain text.

flow conditions. Additionally, Ibáñez et al. demonstrated, during the extraction of sulfuric acid from copper metallurgical plant effluents using ED, a bifurcated pattern in the energy consumption related to current density. Initially, at lower current densities, there is a sharp escalation in the SEC, culminating at 3.60 kWh kg^{-1} of H_2SO_4 when the current density hits 30 mA cm^{-2}. Subsequently, the trend shifts towards

a more gradual ascent in SEC as current density increases, with the SEC reaching approximately 4.11 kWh kg^{-1} at a current density of 70 mA cm^{-2}. This represents an approximate growth of 12.5 % in the SEC upon augmenting the current density by a factor of 2.3 [243]. The relationship between current efficiency and current density was examined in a study of Xu et al. reported a decline in current efficiency from 5.56 % to 1.84 % as current density increased from 16.1 to 483 mA cm^{-2} during the continuous production of LiBr from NH_3 −H_2O −LiBr ternary solution in ammonia absorption refrigeration system [244].

4.2. Initial solution concentration

The initial concentrations of solutions also affect the final product concentrations (Eqs. (40) – (41)), the conductivity, current efficiency, and the conversion rates (Eqs. (42) – (43)) throughout the ED process which is very classic and unsurprising.

Batch reactor:

$$C_{f,i} = C_{ini,i} \pm \frac{\xi_i \times \int_0^{t_f} I \times dt}{z_i F} \quad (40)$$

Continuous reactor (1 pass):

$$C_{out,i} = C_{in,i} \pm \frac{\xi_i \times I \times N_{cp}}{\dot{q} z_i F} \quad (41)$$

where ξ_i is the current efficiency (dimensionless) and $\dot{q}$ is the volumetric stack flow rate (m^3/s).

Batch reactor:

$$\chi_i = \frac{C_{ini,i} - C_{f,i}}{C_{ini,i}} \quad (42)$$

Continuous reactor (1 pass):

$$\chi_i = \frac{C_{in,i} - C_{out,i}}{C_{in,i}} \quad (43)$$

where χ_i is the conversion rate of the ion *i* (dimensionless).

Typically, elevating the concentration of the initial feed solution results in a higher concentration of the final product. The study of Wang et al. involved synthesizing NaOH from NaCl by using BED to achieve a rigorous comparison of caustic soda production by electrolysis. They demonstrated that the concentration of NaOH increased with the feed solutions' concentration (from 12 to 26 % NaCl concentration) rising from 1.81 to 4.35 mol/L [245]. In a parallel investigation, Kırmızı et al. separated chromium(VI) and nickel(II) ions from effluent and noted a comparable trend [246]. Notably, in these instances, the enhanced initial concentration underscores the principle that an increase in the initial concentration of ions contributes to a more significant ion flux. However, it is crucial to establish an equilibrium between the enhancement of solute concentration and the decline in ion selectivity. As the initial solute concentration increases, the observed decrease in ion selectivity is often attributed to phenomena such as back diffusion [98] and the diminished charge-exclusion capacity of the membrane when exposed to elevated solute concentrations, a consequence of charge screening (observed in several cases such sulfate ions and lead from battery manufacturing effluents [247] or seawater desalination [248]). Moreover, the current efficiency is improved with the rise in concentrations of ions. This enhancement in current efficiency is often attributed to a reduction in the electrical resistance of the solutions (η_{ohm}) [249].

4.3. Feeding rate

Numerous of studies claims that increasing the feeding rate leads to higher product concentration and lower energy usage in ED processes [246,250,251] because the ion flux is increasing. For example, Zhao et al. observed an increase in the concentration of ions within the solutions of the product chamber, correlating with a rise in the feeding rate from 10 mL min^{-1} to 20 mL min^{-1}, during the treatment of ammonia and saline wastewater [252].

Furthermore, adjusting the feeding rate can mitigate the risk of membrane fouling that arises from high product concentrations and solvent diffusion. It is worth noting that in an ED setup, the energy required for pumping a fluid rises with an increase in the Reynolds number (*i.e.*, the feeding rate). Indeed, a balance must be found between the energy consumption associated with pumping and the improvement of performance in terms of mass transfer, which is often itself limited by the resistive transfer of ions across the membrane. It is indeed possible that the reduction in overpotential does not offset the increase in pumping costs.

4.4. Temperature

The influence of temperature on the ED system manifests many aspects on the ED process as illustrated in Fig. 13, but mainly through two mechanisms:*(i)* the dissociation of water in the case of BM, and (ii) the velocity at which ions traverse the membranes.

It has been observed that an increase in temperature accelerates the water dissociation kinetics within BMs [253,254]. In fact, part of the energy is supplied in the form of thermal energy, reducing the cell voltage required to carry out the same reaction. As with electrolysis, the thermoneutral voltage (E_{th}, in V) of the water dissociation reaction into H^+ and OH^- ions decreases as the temperature increases, according to Eq. (44).

$$\Delta H = \Delta G + T\Delta S = -E_{th} \times n \times F \quad (44)$$

Where ΔG is the change in the Gibbs free energy (J), ΔH is change in enthalpy (J), T is temperature (K) and ΔS is the change in entropy (J/K).

The decrease in the DBL's thickness with temperature is not necessarily intuitive. In fact, by providing more energy to the molecules, their diffusion velocity (*i.e.*, their diffusion coefficient) and therefore the diffusion gradient will increase. In addition, the decrease in viscosity with an increase in temperature will enable the liquid in the compartments to move at a higher flow rate for the same pumping pressure differential (or hydraulic power P^h). Furthermore, an increase in the conductivity of IEM is observed with an increase in temperature [255,256]. This enhanced conductivity will allow for reduced energy losses for ion flow within the membrane.

Nonetheless, the operation at elevated temperatures is constrained by the thermal stability of commercial membranes, which cannot endure temperatures beyond 40–60 °C for extended periods for BMs [41], 60–80 °C for AEM [257] and up to 250 °C for some CEM [258], leading to a scarcity of research into BM performance at high temperatures. In terms of ion migration across membranes, a temperature rise from 24 °C to 41 °C has been shown to enhance ion migration rates, thereby increasing conductivity in the acid and alkali chambers. This enhancement potentially improves the current efficiency of the process [259] by increasing the diffusion and decreasing the viscosity of the solution at the same type.

4.5. Initial volume ratio

In the context of industrial applications, the implementation of multistage or batch operations in BED is commonly adopted to showcase scalability and minimize manufacturing costs [260]. Such operational modalities present challenges for replication in laboratory environments. Therefore, to simulate multistage and batch processes, adjustments in the volume ratios (or flow rate ratio in the case of continuous reactor) of the individual chambers can be employed as a practical approach. Adjusting the initial volume ratio of solutions is also a proven strategy for enhancing product concentration [261]. Note that there is

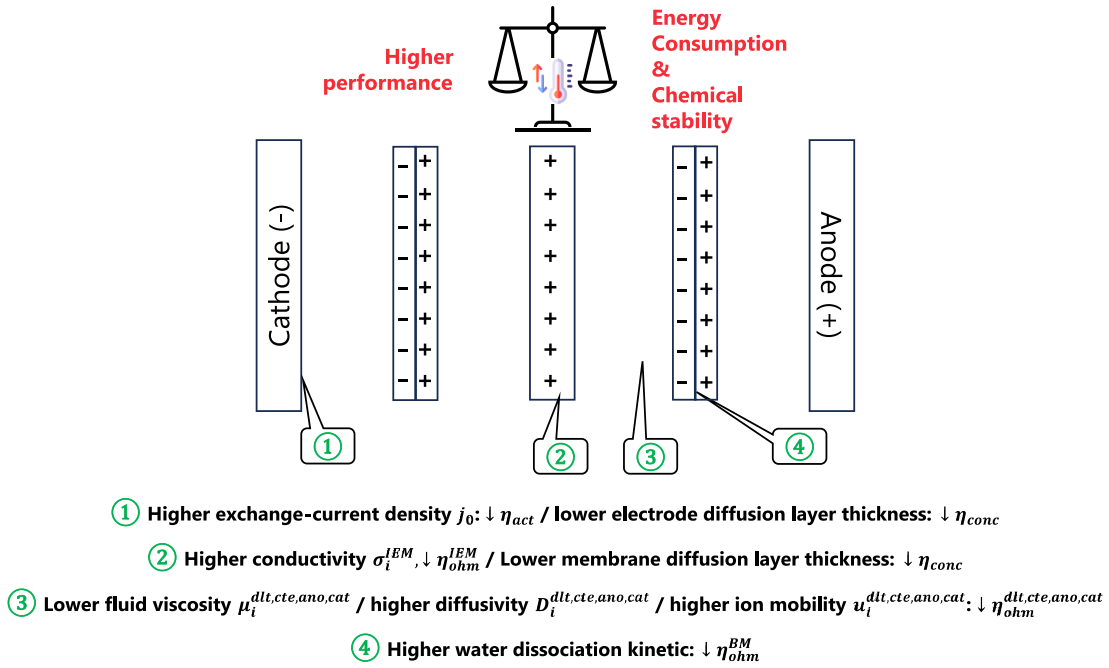

Fig. 13. Effect of temperature on various zones of an ED process. Green effects are favored by an increase in temperature. (For interpretation of the references to colour in this figure legend, the reader is referred to the web version of this article.)

also a concentration limit, as described in section 2.4.1 above. There is a concentration limit above which the backflow is of the same order of magnitude as the current-induced migration, and the efficiency decreases.

This parameter's impact can be divided based on modifications to the volume ratios within two-chamber or three-chamber setups.

In the two-chamber scenario, Dong et al. investigated how varying the volume ratios between the acid and alkali chambers affected product concentration during the production of hexacyanocobalic acid. They discovered that increasing the ratio (acid: base) from 1:2 to 2:1 led to an increase in the final concentration of acid from 0.11 to 0.2 mol/L [262]. The approach of modulating volume ratios in a three-chamber system mirrors that in a two-chamber setup. In a similar vein, Delgado et al. reported, using four-chamber setup during the recovery of acid mine drainage effluent, that enhancing the volume ratios of the diluate to concentrate chamber from 1 to 3 reduced SEC energy consumption from 35.01 to 27.44 kWh/m^{-3}(−|-) [263].

4.6. Limiting factors

The summary of ED applications and their influencing factors highlights benefits in environmental protection and resource conversion. However, ED technology faces challenges, including impurities in the product and the production of low-concentration outputs that require further concentration. These issues are often linked to several limiting factors, such as *(i)* the co-existing ion competition, *(ii)* the leakage of co-ions, *(iii)* the solvent transport, and *(iv)* the back diffusion. Generally, co-existing ions and leakage of co-ions compromises product purity, whereas solvent transport and back diffusion contribute to the reduced concentration of the product and efficiency losses.

4.6.1. Co-existing ion competition

As a reminder, IEMs are polymeric films with charged ionic functional groups covalently bond to their backbone. These structures facilitate the movement of ions carrying charges opposite to those of the membrane's functional groups (referred to as counter-ions), while blocking the passage of ions sharing the same charge as the membrane's functional groups (called co-ions). Typologically, the terms co-ion and counter-ion thus discriminate the membrane. Conversely, the co-existing ion is the ion that accompanies the ion of interest in its electro-neutrality. For example, in the case of NaCl salt, Na^+ is the co-existing ion of Cl^-. When using a CEM, Na^+ is then a counter-ion, while Cl^- is a co-ion.

The term 'co-existing ions' typically denotes the migration of ions within the system that possess the same charge as the targeted ion or acting as counter ions. This phenomenon can be categorized into co-existing cations and anions. Such coexistence primarily affects aspects of *(i)* ionic strength, *(ii)* conductivity, and *(iii)* diffusion reducing the resistance of the overall process. It therefore has an impact on product concentration and energy consumption.

The interaction of co-existing ions through the membrane significantly influences the recovery and transformation of targeted ions, notably through the competitive migration of ions sharing the same charge [264]. For example, Ji et al. examined how co-existing ions impact the synthesis of lithium from salt-lake brine and seawater. They introduced a separation coefficient corresponding to the concentration ratio of Mg^{2+}/Li^+ at a given moment to the initial time of Mg^{2+}/Li^+ in desalting compartment. At the same time, they discovered that the increasing presence of K^+ and Na^+ adversely affected the Li^+ concentration, reducing the separation coefficient of magnesium and lithium from 8.73 to 1.83 when the Na^+/Li^+ ratio increases from 1 to 5, and from 8.33 to 2.13 as the K^+/Li^+ ratio rises from 1 to 5 [265]. Notably, K^+ exerted a more pronounced effect than Na^+ in this ED process, a difference attributed to the ions' hydration radii ($r_{K^+} < r_{Na^+} < r_{Li^+}$, *i.e.*, Fig. 10). During the process, the energy usage is adversely influenced by the competitive migration of co-existing ions alongside the target ions, leading to increased energy consumption and diminished current efficiency. This outcome is attributed to the fact that co-existing ions lower the relative current carried by the target ions, thereby decreasing current efficiency and elevating energy costs. It should be noted that this aspect has also been studied using modeling approaches [101,266–268].

4.6.2. Co-ions leakage

The migration of co-ions across the membrane occurs in response to the reverse electric force illustrating the non-ideal behavior of the membrane (*i.e.*, transport number not equal to unity). This force is a

consequence of minor differences in the arrangement of charged groups within the membrane structure leading to transport number different from the unity. The primary impact of co-ions leakage includes *(i)* a reduction in the product's purity and *(ii)* a decrease in current efficiency [269].

Typically, the migration of co-ions leads to a diminished concentration of the desired product. For example, Yan et al. reported the detection of H^+ in the diluate solution, indicating the passage of proton through the AEM, which resulted in reduced product purity [270]. This issue is often linked to the imperfect selectivity of ion exchange membranes, allowing for co-ion leakage [271]. Cherif et al. observed the leakage of NO_3^- through the CEM to another chamber in the process of recovering HNO_3 and NaOH from $NaNO_3$ using BED, thereby compromising the purity of NaOH [272].

4.6.3. Solvent transport

An additional constraint within ED technology is the movement of solvent from the diluate chamber to the concentrate chamber (J_w, often water as in Eq. **(45)**). This solvent transfer usually results in an increased volume of the product solution, which can lead to a diluting effect, thereby limiting the attainable maximum concentration of the product, which have been study experimentally and by modeling [273–275]. More precisely, solvent movement encompasses two distinct categories: *(i)* electro-osmotic of water J^{eo} (Fig. 11 – d, Eq. **(46)**, mol m^{-2} s^{-1}) [276,277] and *(ii)* osmotic water J^{os} (Fig. 11 – e, Eq. **(47)**, mol m^{-2} s^{-1}) [81,278]. Electroosmosis involves the movement of water as it follows hydrated ions, consistently proceeding in the same direction as the ions themselves. On the other hand, osmosis results from the gradient of chemical potential that arises due to variations in salinity between adjacent compartments. In the initial stages of the process, water osmosis takes place in the direction opposite to ion migration, this reversal is due to the greater salinity (*i.e.*, lower water activity) present in the dilute compartment compared to the concentrate compartment [277,279].

$$J_w = J^{eo} + J^{os} \tag{45}$$

$$J^{eo} = n_{drag} * \frac{j}{F} * N_{cell} \tag{46}$$

$$J^{os} = L_p \times (\Delta\pi - \Delta p^h) \tag{47}$$

$$\pi = RT \times \sum_i C_i \tag{48}$$

where L_p is the water permeability of the IEM (mol m^2/s bar^{-1}); n_{drag} is the electroosmotic drag coefficient (dimensionless); $\Delta\pi$ is the osmotic pressure difference between both chambers (Pa); Δp^h is the hydraulic pressure difference between each interface of the IEM (Pa).

Concerning water electro-migration, Jaroszek et al. identified a direct linear correlation between the volume of water transported and the ion electromigration flux (K^+, Na^+, Cl^-, SO_4^{2-}) as the concentrations of KNO_3 and Na_2SO_4 solutions were increased (mainly attributed to the relation between concentration and hydration number) [280]. The linear regression analysis performed on the collected experimental data yielded average rates of water transport of $(2.04 \pm 0.01) \times 10^{-2}$ mol (A h)$^{-1}$ and $(3.73 \pm 0.03) \times 10^{-1}$ mol (A h)$^{-1}$ for the KNO_3 and Na_2SO_4 streams, respectively. The quantity of water molecules moved per mole of salt generated in the product stream was found to be 10.5 ± 0.8 (mol mol^{-1}) for KNO_3 and 16.9 ± 1.5 (mol mol^{-1}) for Na_2SO_4. In a similar vein, Zabolotskii et al. discovered a linear linkage between the rate of apparent water flux and the current density, evidenced by a high correlation coefficient ($J_w = 0.013 \times j + 0.206$ with $R^2 \approx 0.98$) during lithium chloride concentration [281].

Conversely, osmotic water movement is triggered by the osmotic pressure difference between neighboring chambers, a result of the variability in salinity levels between their solutions. At the outset of the ED process, osmotic water flux moves in the direction opposite to that of ion migration, attributed to the higher salinity of the feed solution [282]. When the concentration in the product solution surpasses that of the feed solution, the osmotic flux direction shifts to coincide with that of the electro-migration flux, which results in the dilution of the product solution. Unlike the well-studied electro-migration of water through membranes *via* hydrated ions, osmotic water flux has received less attention. Wang et al. highlighted the effect of osmotic pressure on the limiting of NaOH concentration during BED. Findings indicate a reduction in current efficiency from 90 % to 73 % and a decrease in the concentration of the base to a certain degree upon enhancing the osmotic pressure [245].

4.6.4. Back diffusion

Even if diffusion is not the main transfer phenomena compared to electromigration, back diffusion poses a considerable challenge to reaching high concentrations and purity of the product in ED processes [278], as presented in Eq. **(49)**. This phenomenon tends to manifest more prominently when there is a significant concentration disparity between the concentrate and dilute streams.

$$J^m_{back,\,i} = \frac{D_i}{\delta} \times (C_i^{cte} - C_i^{dlt}) \tag{49}$$

where $J^m_{back,\,i}$ is the surface molar flux caused by the back diffusion of the ion i (mol m^{-2} s^{-1}) and δ is the diffusion boundary layer thickness (m).

As highlighted by Yu et al., the phenomenon of back diffusion, driven by concentration gradients and a competition between migration and diffusion, can limit the current efficiency significantly (~40 % in their case) [283]. Chen et al. further observed that back diffusion is particularly raised by an increase of temperature [271] (as already discussed in section 4.4). To counteract the effects of back diffusion and enhance the final product's concentration during the ED process, a continuous operation mode is advised.

5. Process intensification and system optimization

Baldea presents in 2015 a definition of process intensification as 'any chemical engineering development that leads to substantially smaller, cleaner, safer and more energy efficient technology or that combine[s] multiple operations into fewer devices (or a single apparatus)' [284]. ED, like any other unit operation in chemical engineering, is not immune to innovations in its field. Thus, the various advances in terms of process intensification in ED can be structured with advances in terms of *(i)* cell design, *(ii)* modeling and *(iii)* operating modes.

5.1. Cell design and mixing promotion

The majority of electromembrane processes utilize plate-and-frame configurations (*e.g.*, filter press), where channel—supplied by a manifold and flow distributor—are formed by a pair of membranes serving as the channel walls, with an internal spacer maintaining the separation and enhancing convection within these channels. A balance must be struck between minimizing pressure losses, ensuring proper mixing of the solutions, and decreasing the distance between the membranes to reduce ohmic overvoltage. Consequently, choosing the right spacer geometry and material is critical in the design and optimization of these processes. This significance has led to thorough studies on the hydrodynamics and mass transport phenomena within the channels of membrane modules, providing detailed insights into their operational dynamics [285–287]. Recent advancements in ED technology have led to significant improvements in cell design, focusing on enhancing efficiency, and scalability (the latter being the subject of particular attention in the **Section 6**). These advances stand out in terms of *(i)* mixing promotion and *(ii)* process simulation.

Two primary configurations for electrolyte channels have been identified: sheet flow and tortuous path configurations. The sheet flow design, illustrated in Fig. 14 – a, features feed channels of a rectangular, through which the solution traverses in a substantially linear regime. Conversely, the tortuous path configuration, depicted in Fig. 14 – b, is characterized by feed channels that follow a narrow, winding route, incorporating multiple baffles and 180°-turns. The flow configuration can be organized into parallel, counter, or crossflow patterns. Counter-flow arrangements are generally favored in theory due to their advantage of avoiding the significant axial escalation in concentration difference that is characteristic of parallel flows. However, this configuration introduces greater pressure disparities across the concentrate and dilute sections, potentially leading to internal leaks and undue deformation of the membranes [288].

5.1.1. Non-conductive spacers

Initial research into ED applications has established that spacers vary significantly in their impact on mass transfer and pressure drop. This variation underscores the critical importance of optimizing channel design to enhance overall system performance. These spacers not only maintain a constant distance (usually varies between 0.3 and 2 mm [288]) between the membranes but also enhance mixing within the channels as illustrated in Fig. 15. To ensure the integrity of the channels, net spacers are equipped with gaskets around their edges, effectively sealing the channels and directing the flow of solutions through them [289]. Additionally, the incorporation of holes in spacers forms distinct conduits for the dual hydraulic circuits, serving as distribution and collection manifolds for the solutions entering and exiting the channels [25,290]. The assembly of the ED apparatus is completed by securing it with end plates and applying pressure using bolts and nuts. The design of spacers, crucial to ensure fluid flow and minimize concentration polarization, has evolved. Net spacers are categorized into four principal types: overlapped, woven, twisted, and multi-layer. Innovations include turbulence-promoting spacers and 3D printed spacers with optimized geometries that enhance mass transfer and reduce pressure drops, thereby improving energy efficiency by extensive numerical and experimental studies [291–294].

5.1.2. Ionic conductive spacers

A notable drawback of using net polymeric spacers in ED is their fabrication from non-conductive materials, which elevates the electrical resistance within the compartments by reducing area of the compartment (mainly through η_{ohm}). Alternatively, opting for spacers made from conductive materials presents a viable strategy to decrease energy consumption and thereby enhance the operational efficiency of ED units. In the 1970 s, Kedem introduced spacers fabricated from ion exchange materials [296,297]. These benefits included enhanced mass transfer, characterized by diminished polarization (decrease in ohmic resistance attributable to the absence of shadow effect) and an augmented limit current, owing to the expanded active surface area [298,299]. Over two decades later, the industry adopted conductive spacers, either through chemical modification or application of coatings, which reaffirmed the earlier findings [300,301]. Despite the highlighted benefits, conductive spacers have not been adopted in actual industrial ED units, likely due to their higher production costs, reduced durability, and increased complexity.

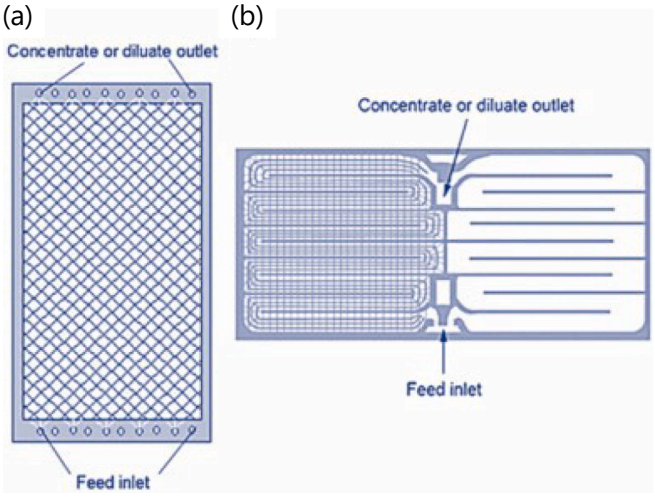

Fig. 14. (a) Sheet flow vs. (b) tortuous path flow spacers. Reprinted with permission from [54] (CC-BY 4.0 Elsevier).

5.1.3. Profiled membranes

It is also possible to construct ED stacks without the need for spacers by employing membranes with specific profiles. In more recent developments, profiled membranes, as illustrated in Fig. 16, have been introduced as a cost-effective and efficient substitute for conductive spacers. These membranes are designed with embossed features such as reliefs, pillars, or ridges on one or both sides, serving the function of spacers [302,303]. The integration of profiled membranes simplifies the assembly process of ED stacks by eliminating the need for separate spacers [304,305], while also offering benefits, illustrated Fig. 16 – e, akin to those of conductive spacers, including reduced ohmic resistance and the potential for increased active surface area [306]. These features affect the fluid mixing and then the mass transfer efficiency. It can vary depending on the specific profile design. The geometry of the profiles also significantly affects pressure drops [307].

Figures (a-b) reprinted from [308], Copyright (2014), with permission from Elsevier. Figures (c-d) reprinted from [307], Copyright (2017), with permission from Elsevier. Figure (e) reprinted from [305], Copyright (2010), with permission from Elsevier.

Although channel characteristics probably play an important role in controlling the performance of ED processes, attention also needs to be paid to hydrodynamic aspects concerning input–output distribution systems, commonly known as manifolds, and much work has been done to improve their performance in terms of flow distribution [294,308–311], with benefit from electrolysers or redox flow batteries [312–314].

5.2. Modeling and simulation techniques

A comprehensive understanding and subsequent simulation of the ED process necessitates the incorporation of sophisticated mathematical models. These models are essential for encapsulating various intricate phenomena, encompassing the equilibria between solutions and membranes, the effects of concentration polarization, the dynamics of fluid movement along the channels, the principles governing mass transport and the mass balance within the compartments, alongside electrical interactions among others. The literature to date has introduced a variety of modeling strategies, each uniquely tackling these elements to varying degrees. The primary objective behind these endeavors has typically been to forge potent tools for the design and optimization of ED operations.

The task of modeling ED, along with other electromembrane processes, presents a significant challenge due to the diverse array of phenomena occurring simultaneously across macroscopic, microscopic, and nanoscopic scales, which collectively influence the process's overall efficacy. A broad spectrum of ED modeling approaches is documented within the academic corpus, where the common goal across these methodologies is to predict output metrics such as outlet concentration (or concentration profiles) and current density from controlled input parameters like inlet concentration and voltage application. These models facilitate the derivation of crucial operational metrics including current efficiency and energy consumption SEC. Broadly, ED models fall

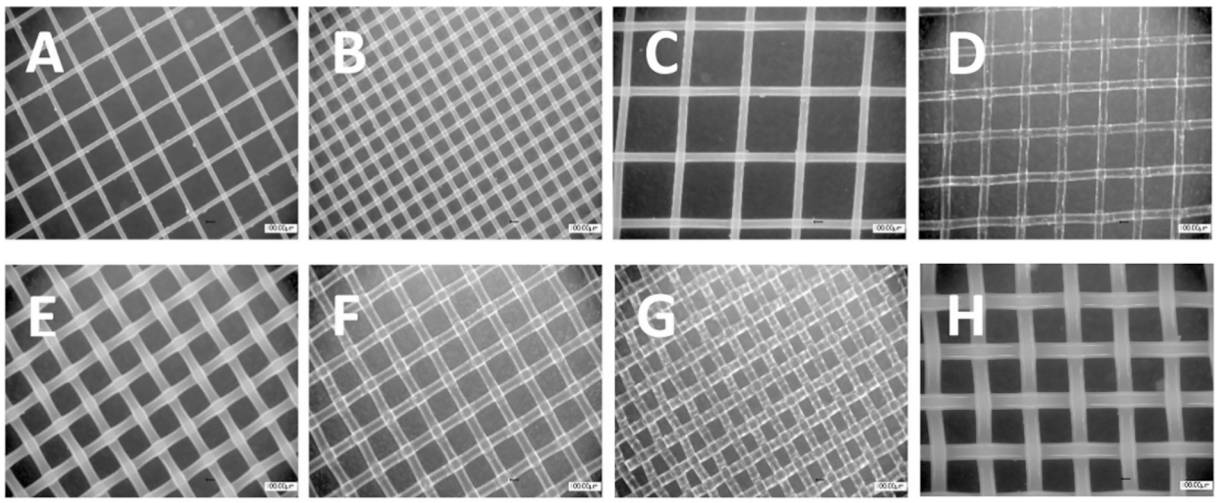

Fig. 15. Various types of spacers utilized in ED. Reprinted from [295], Copyright (2019), with permission from Elsevier.

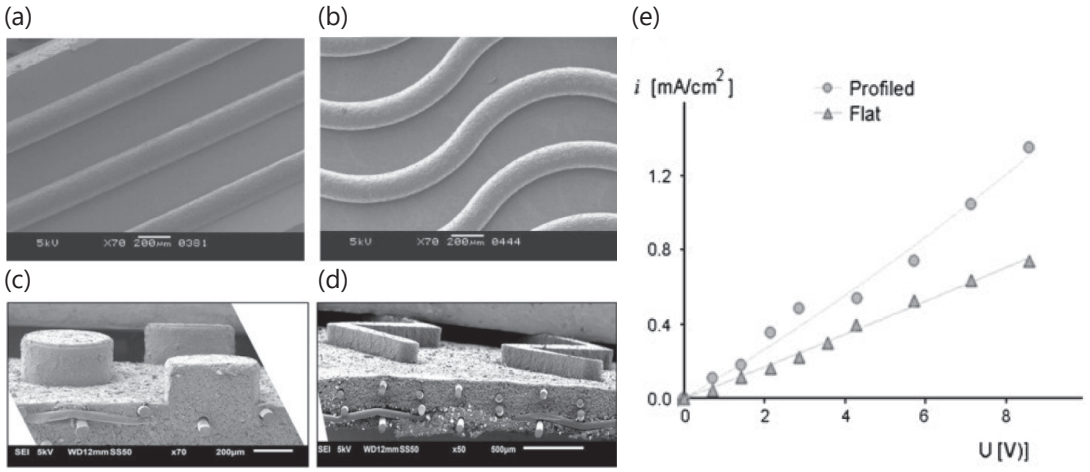

Fig. 16. Surface morphology of (a) ridges, (b) waves, (c) pillars and (d) chevrons profiled membrane. (e) Results obtained with profiled and flat sheet membranes showing the current density as a function of the voltage applied in a test cell with one cell pair and feed solutions of 350 μS cm^{-1} tap water.

into three distinct classifications as depicted in Fig. 17.

The first category of process models employs an equivalent circuit model, a streamlined representation of complex electrical systems, utilizing basic elements like resistors (representing resistive losses, typically ohmic ones), capacitors (standing for capacitive behavior), and voltage sources (used for EC potential difference) to emulate system behavior. By abstracting a system's electrical characteristics into a simplified circuit form, equivalent circuit models facilitate the prediction of system responses to electrical stimuli and the elucidation of internal dynamics. This approach often utilizes equations with lumped parameters. For instance, in electrochemical engineering, these models are key for examining cells and batteries, representing phenomena like ionic transport and charge storage through simple components, thereby aiding in performance assessment and lifespan prediction. Note that these models are empirical and do not directly describe the physics of the phenomena. It is therefore not possible to transpose them from one ED process to another.

The broader second category of process models is segmented into two distinct sub-categories which offers two-dimensional resolutions: *(i)* detailed models based on the N-P (*i.e.*, Eq. **(21)**) or M−S (*i.e.*, Eq. **(24)**) equations [315,316] and *(ii)* semi-empirical models [317,318]. The primary distinction lies in how they mathematically characterize phenomena occurring across the membrane. Theoretical models offer a comprehensive mathematical framework capable of describing transport phenomena within the membrane at a microscopic level with a high degree of precision, although reliance on empirical data for certain membrane properties such as ion diffusivity, mobility, and fixed charge density is still necessary. These models often utilize Finite Element Methods or similar computational techniques, integrating the model closely with thermodynamic and mass transfer principles, including fluid dynamics [319]. However, the extensive computational resources required for these models restrict their use to simplified channel geometries or small computational domains, rendering them less practical for simulations encompassing entire ED stacks. Conversely, semi-empirical models adopt a multi-scale approach that blends empirical data and small-scale theoretical analyses, such as computational fluid dynamics (CFD), to describe lower-scale phenomena like mass transfer and fluid flow behavior, which in turn helps in understanding mass transport phenomena in the DBL [320,321].

5.2.1. *Equivalent circuit models*

Studies on equivalent circuit models draw an analogy between ionic transport perpendicular to the direction of flow in ED cells and electron movement in a direct current electrical circuit, where solutions and membranes function as resistive components. These models rely on fundamental theoretical principles such as Ohm's and Faraday's laws to

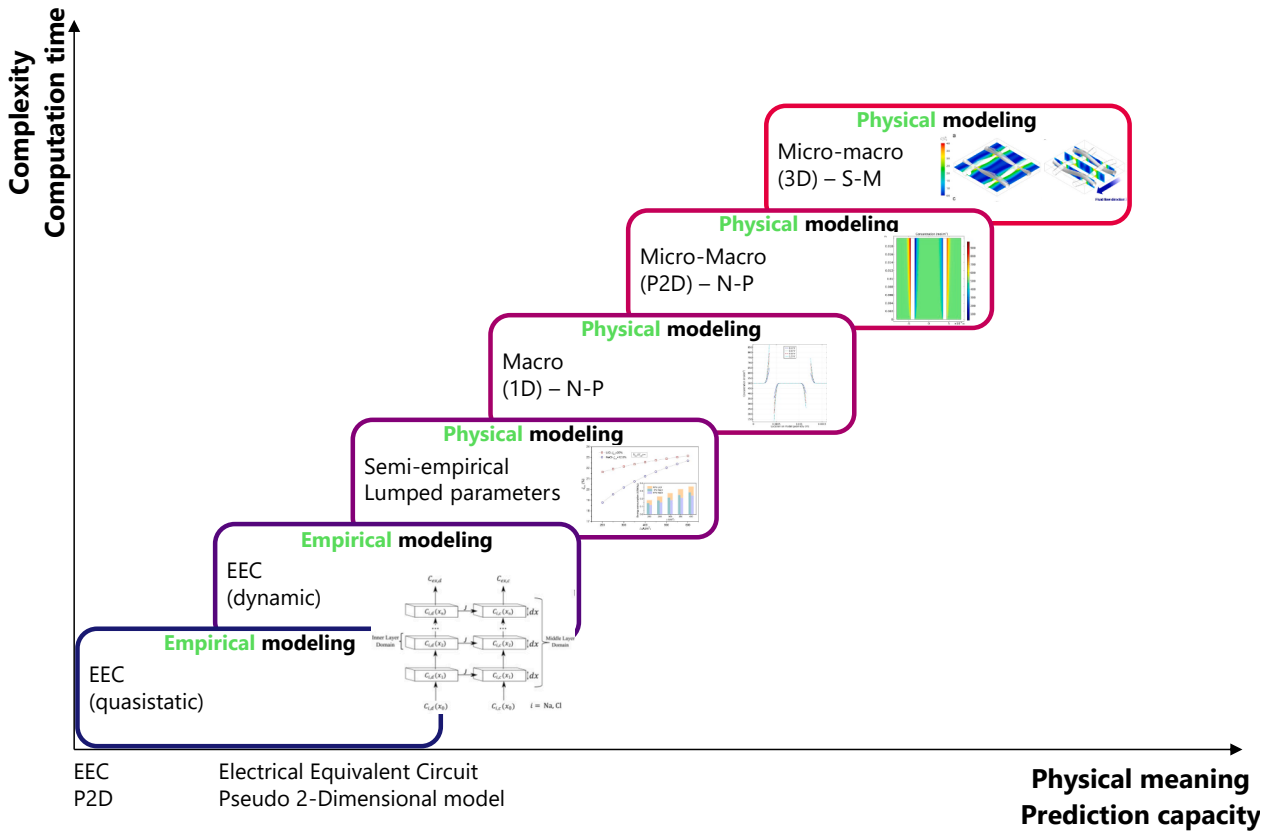

Fig. 17. Multiscale modelling applied to ED processes. Electrical equivalent circuit model figure is adapted from [322] (CC-BY 4.0 Elsevier). Semi-empirical model figure is adapted from [323], Copyright (2021), with permission from Elsevier. N-P model figures are adapted from [324], Copyright (2020), with permission from John Wiley & Sons, Inc. S-M model figure is adapted from [325], Copyright (2014) with permission from Elsevier.

establish relationships between key parameters like ionic flux, current density, electrical resistance, and voltage without any possibility of 2-dimensional modeling. They offer considerable adaptability, allowing for the inclusion of various phenomena by adding additional resistive components and adjustments in mass balances. They enable a comprehensive understanding of ED systems, while providing the capability to incorporate specific small-scale phenomena as needed. Distinguishing features of these models encompass the presumption of either constant voltage or current, the application of either a plug flow reactor model or a continuous stirred-tank reactor model for managing mass balances, the acknowledgment of DBLs adjacent to membranes, considerations of diffusive transport, the integration of water movement, attention to EC reactions and the implications of terminal compartment effects, and the portrayal of membrane selectivity, whether depicted as ideal, fixed, or through a transport number model [322,326–330].

5.2.2. Semi-empirical models

The focus in this section is placed on modeling approaches that choose an alternative to solving the theoretical equation, favoring instead the simulation of IEMs using experimentally measurable macroscopic characteristics, such as transport coefficients, electrical resistance, as well as ion and osmotic permeability. These models adopt a simplified approach by focusing on essential variables and incorporating aggregated empirical parameters. These parameters undergo calibration to align the models' forecasts with empirical data. Semi-empirical models primarily rely on a set of both algebraic and differential equations, organized as follows:

(i) Equations based on the principles of thermodynamics and electrostatics, enabling the derivation of parameters such as the cell potential (Eq. (1)), their resistance (Eq. (2)), and the generated electric current (Eqs. (13) and (25)) [331,332];

(ii) Mass conservation equations that account for variations in flow rates and concentrations in the main flow directions, inherently linked to mass transfer equations (Eqs. (50) – (51)) [333];

$$\frac{d\dot{q}^{dlt}(x)C_i^{dlt}(x)}{dx} = -\frac{d\dot{q}^{cte}(x)C_i^{cte}(x)}{dx} = -l^{IEM} \times J_w(x) \tag{50}$$

$$\frac{d\dot{q}^{dlt}(x)}{dx} = -\frac{d\dot{q}^{cte}(x)}{dx} = -l^{IEM} \times J_w'(x) \tag{51}$$

where $\dot{q}$ is the volumetric flow rate (m^3/s); x is the flow direction (m); l^{IEM} is the IEM length (m); J_w and J_w' are the molar and volumetric flux of solvent, respectively (mol m^{-2} s^{-1} and m^3 m^{-2} s^{-1}).

(iii) Transport equations calculating the mass flux of ions and water through the membrane from empirical data or autonomously determined values through dimensionless numbers (Sherwood Sh, Reynolds Re, Schmidt Sc; Eq. (52) – (53)) [334];

$$Sh = \frac{k \times d_c}{D} = f(Re;\, Sc) \tag{52}$$

$$j_{lim} = \frac{z_i \times F \times D_i \times C_i^s}{\delta \times (t_i^m - t_i^s)} = \frac{Sh \times z_i \times F \times C_i^s}{d_c \times (t_i^m - t_i^s)} \tag{53}$$

where Sh is the Sherwood number (dimensionless); k is the mass transfer coefficient (m/s); d_c is a characteristic length (m) and D is the diffusivity coefficient (m^2/s).

(iv) Lastly, equations aimed at assessing macroscopic performance criteria, such as energy needs (Eqs. (30) – (31)), pumping losses (Eq. (29)), and efficiencies (Eqs. (26) – (27)), formulated from empirical data [335].

These modeling approaches frequently employ the segmentation modeling technique (multi-layer system considering the DBLs presence)

using one-dimensional equations. Despite their effective representation of process dynamics, semi-empirical models necessitate extensive initial experimental calibration and further experimentation for validation across different operational conditions. One significant limitation of these models is their lack of universality, indicating that validations performed on experimental, lab-scale setups may not directly translate to industrial-scale applications. Additionally, the practice of aggregating empirical parameters into lumped forms masks the discrete effects of individual phenomena on the system's overall performance.

5.2.3. Theoretical models based on Nernst-Planck and Stefan-Maxwell equations

The resolution of the N-P equation facilitates the creation of a multi-dimensional concentration profile by integrating contributions from diffusion, convection, and electromigration to the cumulative flux, as indicated in Eq. **(21)** [336].

To attain a complete model, an additional condition related to charge is necessary. This can be met either by assuming electroneutrality (where the aggregate of all charges at any given point, inclusive of those contributed by the membrane, equates to zero) [324] or by the application of the Poisson equation [337], as described in Eq. **(54)**.

$$\sum_i z_i C_i = -\varepsilon_r \varepsilon_0 \nabla^2 \varphi \tag{54}$$

where ε_r and ε_0 correspond to the relative permittivity of the medium and the permittivity of free space, respectively (F/m).

The complexity of the intertwined partial differential equations necessitates their resolution *via* numerical methods such as the finite element method or finite volume method within CFD software packages like COMSOL Multiphysics, Ansys Fluent, or OpenFOAM while solving at the same time Navier-Stockes equations for hydrodynamic conditions [319,338]. These approaches enable detailed exploration at a micro-scale, proving invaluable for the examination of localized effects such as concentration polarization and the impact of space charge regions using two-dimensional equations [339,340]. Nevertheless, the granular focus of these analyses renders the extrapolation to full-scale process models as less efficient. In models based on the N-P framework, simplifications are typically made: *(i)* simulations are conducted either in one dimension (across the membrane) or *(ii)* two dimensions (along the axis and across the membrane) [341].

Note that the use of the N-P theory encounters specific limitations. Notably, in solutions of high concentration, ions are surrounded not only by solvent molecules but also by other ions, which increases the significance of short-distance interactions. Consequently, additional frictional forces come into play. To accurately model ionic transport in these dense media (specifically in DBLs), it is indispensable to incorporate a greater number of transport coefficients and to adopt a more precise approach, such as that proposed by the S-M equations [342]. Examples of using this method to analyze ion exchange systems remain scarce in scientific publications. Nonetheless, the N-P model remains widely preferred due to its ease of application and reliability across a broad range of operational conditions encountered in ED [315].

5.3. Operating modes

Electrodialysis with many hybrid modes allowing for improved performance and efficiency. This section presents them.

5.3.1. Electro-electrodialysis or redox-mediated electrodialysis

Electro-electrodialysis, also known as redox-mediated ED, represents an interesting development halfway between electrolysis and ED. In this configuration, a multi-compartment cell facilitates selective ion transport across IEMs, while interesting EC reactions take place at the electrodes, modifying the usual solvent oxidation and reduction reactions. [44,343,344]. This approach has facilitated the production of various organic and inorganic acids and bases, including acids, quaternary ammonium hydroxide, H_3BO_3, and LiOH [44,345–348]. Noticeable efficiency in terms of productivity, rooted in electrode reactions, alongside effective product separation due to the utilization of stacked electromembrane separation units, has been noted with redox reactions using ferri-/ferrocyanide or viologen solutions for example [349–352].

5.3.2. Electrodialysis metathesis

ED stands out in this domain for its notable environmental benefits and operational efficiencies [344,353]. Nonetheless, conventional ED techniques primarily focus on concentrating liquid salts without offering mechanisms for further enhancing the value of these resources [24]. Given the push for environmental conservation and the principles of sustainable development, there's a growing inclination towards transforming low-value saline wastewaters into high-value products [354]. ED metathesis has emerged as a prominent solution, acclaimed for its capacity to convert, and reclaim valuable mineral resources from saline waters. The essence of the ED metathesis process involves the ion exchange between two distinct saline streams, leading to the creation of new salt streams [355], echoing the conventional metathesis reaction as presented in Fig. 18 for the case of tetrapropyl ammonium hydroxide [356]. Thanks to these advantages, ED metathesis has found extensive application in the area of high-value salt conversion, treatment of saline wastewater, and the recovery of valuable resources, marking a significant stride towards resource sustainability and environmental stewardship [357,358].

5.3.3. Oscillating regimes

Recent literature emphasizes the improvement in transport phenomena and overall process efficiency within ED systems through the implementation of non-stationary operational conditions. By introducing oscillations, achieved through dynamic alterations in *(i)* electrical field or *(ii)* flow rate, an enhancement in the performance of ED systems has been documented. Applying pulsed flows or electric fields at relatively high frequencies, characterized by a time constant significantly smaller than the characteristic diffusion times observed in systems with high Schmidt numbers (Sc, Eq. **(55)**), disrupts the DBL and leads to a more uniform concentration profile. This departure from the usual sequence of steady states results in transient concentration fields that differ markedly. As a result, the concentration polarization phenomemon and its associated drawbacks can be substantially mitigated, leading to higher limiting currents and reduced electrical resistances. The extent of these benefits is influenced by the frequency, amplitude, and waveform of the applied oscillations [359].

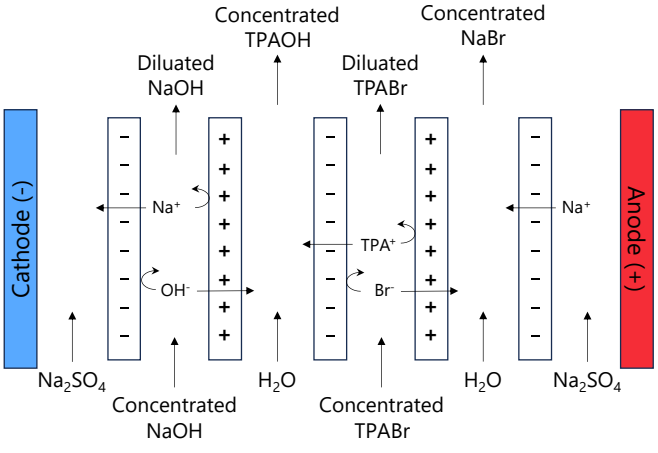

Fig. 18. Schematic principles of the ED metathesis process to prepare tetrapropyl ammonium hydroxide (TPAOH).

$$Sc = \frac{\mu_{electrolyte}}{\rho_{electrolyte} \times D_i} \quad (55)$$

where $\mu_{electrolyte}$ is the dynamic viscosity of the electrolyte (Pa s) and $\rho_{electrolyte}$ is the mass density of the electrolyte ($g/m^{-3}(-|-)$).

The pulsed electric field (PEF) operates in a dynamic regime by applying a discontinuous current or voltage, as illustrated in Fig. 19. During a specified period, the system experiences a steady current or voltage, followed by a period where the current or voltage is deactivated. The procedure involving a PEF employs a series of these pulse and pause intervals with uniform lengths [360]. Studies have documented that frequencies between 0.01 and 100 Hz are effective in reducing fouling across diverse fluid streams [361].

The dynamic electric fields in a non-stationary setup can reduce the effects of concentration polarization, as the interval between pulses allows for the continued migration of ions from the bulk solution to the membrane through both diffusion and convective processes, thus diminishing the concentration gradient prior to the next pulse's application [363]. Recent insights into PEF during pauses have shown a reduction in electrical resistance due to ion redistribution at the diluate membrane interface, leading to low electrical resistance. Voltage reapplied after pauses induces electroconvective vortices, causing current surges and affecting turbulence, facilitating ion transfer to membrane surfaces [364–366]. The concept of employing a non-stationary electric field was initially introduced in 1995 as a method to mitigate the phenomenon of concentration polarization and to facilitate the separation of Na^+ from Ca^{2+} [367]. Through theoretical analysis, Mishchuk et al. posited that the benefits of ED intensification are most pronounced when the duration of the electrical pulses is significantly shorter than the time it takes for the polarization layer to form [368]. Additionally, the application of PEF has been shown to improve the performance of ED in desalinating solutions containing various components such as whey proteins [369], humate [370], and wastewater effluents [371]. The equipment required for generating pulse-pause sequences, such as a pulse generator linked to the power supply or computer-controlled automatic pulse generation, is relatively simple and cost-effective, promoting the scalability of PEF technology [362].

Unlike PEFs, inducing oscillations in flow rates entails significant energy consumption [372], and the industrial feasibility of such application appears to be more distant. Nevertheless, several studies at the laboratory scale have shown substantial benefits in terms of mass transfer and fouling prevention [373–375].

5.3.4. *Complexation electrodialysis*

Complexation ED can be used in two different scenarios:

(i) Due to the inherent limitations in the separation capabilities of IEMs, substances that are neutrally or weakly charged do not move within the current field and, consequently, cannot be extracted from feed solutions. However, these substances can be effectively removed through an electro-membrane process by coupling the separation with chemical modifications such as protonation or complexation, transforming them into strongly charged entities. This strategy offers multiple benefits, including the ability to separate neutral or weakly charged substances *via* electro-driven forces.

(ii) Specifically, when treating metal ions, the valences of the latter are often similar, and the creation of a complexation reaction can lead to improved selectivity in the ED system [168].

Jiang and colleagues introduced an innovative complexation ED method, where a complexation reaction between functional organic compounds and heavy metal ions occurs. This process was demonstrated by combining Cr^{3+} (from electroplating waste) with acetylacetone (acac, from pharmaceutical waste) in a stirred reactor to form positively charged $Cr(acac)_n^{(3-n)+}$ complexes. These complexes were then processed in a complexation ED system, which benefits from induced turbulence to augment mass transfer and maximize the limiting current density. The system achieved removal efficiencies of 99.4 %–99.5 % for metal ions and 97.8 %–99.9 % for organics [376]. Additionally, a notable application of complexation ED is the treatment of aniline-containing wastewater through BED, leveraging the protonation interaction between aniline and carbon dioxide. Injecting CO_2 into aniline wastewater leads to the protonation of aniline, making it positively charged, while CO_2 is converted to bicarbonate/carbonate ions or carbonic acid. The resulting mixture can subsequently be processed in a BED system [377]. Babilas et al. utilized Na_2EDTA for complexing with Cu^{2+} and Zn^{2+} ions present in a zinc plating bath, achieving selective

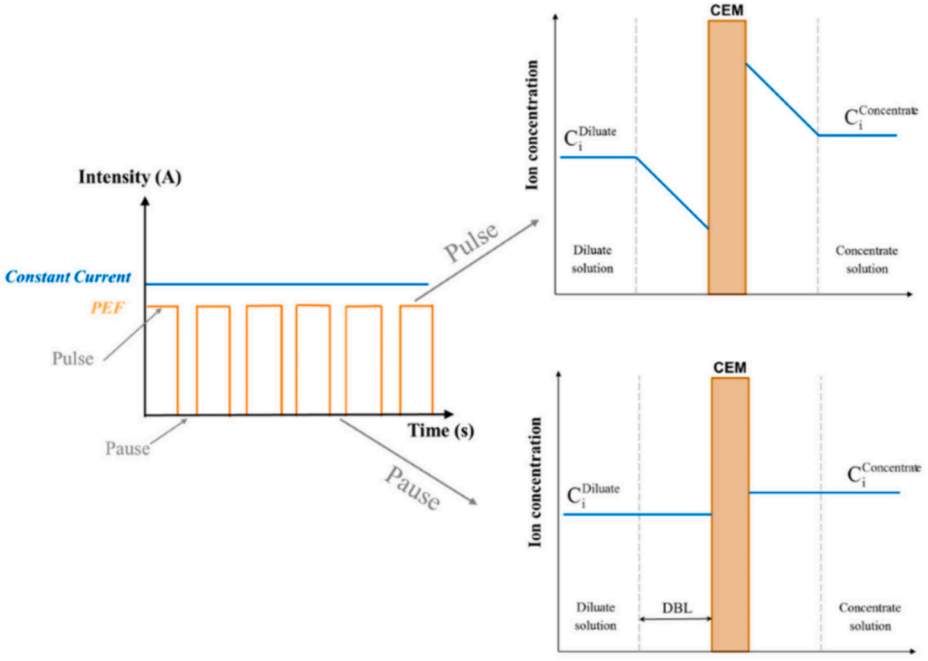

Fig. 19. Principle of PEF and effect on concentration polarization. Reprinted with permission from [362] (CC-BY MDPI).

removal of Zn^{2+} salts to the concentrate compartment and retention of Cu^{2+} complexes in the dilute compartment [378] A diversity of complexing agents has been explored to enhance the selectivity in the recovery of metal salts. EDTA stands out as the most frequently used complexing agent, proving its efficacy in the selective extraction of various metal salts including Ni^{2+} and Co^{2+} [379], Sr^{2+} and Cs^{+} [380], Ca^{2+} and Cd^{2+} [168], as well as Ag^{2+} and Zn^{2+} and Cu^{2+} and Cd^{2+} salts [381]. Additionally, other complexing agents such as citric acid – glycine [382], acid and acetylacetone [376] have also been shown to be effective.

6. Scaling-up: From laboratory to pilot scale

Scaling up a process is a critical phase in the development of ED technology, bridging the gap between theoretical research and practical application. This section delves into the essential aspects of this transition for ED. First, a practical dimensioning approach is discussed to ensure the successful scale-up of ED processes. Following this, the economics and sustainability of the scaled-up ED process are evaluated, providing insight into the financial and environmental implications through techno-economic assessment (TEA) and life cycle assessment (LCA).

6.1. Practical dimensioning approach

Scaling up an ED setup from laboratory to pilot scale requires meticulous planning and optimization across several practical dimensions.

Initially, it's crucial to systematically optimize parameters such as applied voltage, current density, flow rate, and solution pH, which are instrumental in achieving the desired balance between separation efficiency, energy consumption, and membrane longevity. This optimization process, informed by laboratory-scale experiments, guides the selection of suitable membranes and spacers that offer the best performance in terms of ion selectivity, fouling resistance, and mechanical stability, as adjustments may be necessary to accommodate increased flow rates and solution volumes at the pilot scale. The transition from lab to pilot scale involves designing an appropriately scaled ED stack, alongside engineering considerations for pumps, piping, electrical supply, and control systems to handle the increased operational scale with ease of maintenance and monitoring in mind. By keeping dimensionless numbers constant (*e.g.*, Newton, Peclet, Reynolds, Schmidt, Sherwood, Stanton numbers [383] or Thiele modulus [384]) and employing mathematical modeling aids in predicting the performance of the scaled-up system, facilitating adjustments based on pilot results for further optimization. This phase often requires re-tuning of operating conditions, membrane cleaning protocols, or system configurations to align with expected performance levels. There are two principal approaches to enhance the volume capacity treated by an ED system. The first approach focuses on adding more repeating units (N_{cp}) to the membrane stack, which, while increasing power consumption due to system overpotentials, minimally impacts electrode resistance and cell components. The second involves operating multiple ED units in parallel, which can significantly escalate equipment costs due to the need for additional stack materials. The most crucial criterion to improve during scale-up, regardless of the chosen method, remains the specific surface area criterion (the ratio of the active membrane surface area to the compartment volume) that must be imperatively sought to be maximized.

To date, several studies highlight research work on the ED process at the pilot scale (1000 cell pairs reverse ED with municipal wastewater effluent and seawater, achieving a power production of 95.8 W [385]; ED in a 30-cell pair pilot reactor demonstrated efficient concentration of NH_4^+ ions from wastewater with an power consumption of 4.9 kWh $kg^{-1}_{NH_4-N}$ [386]; large-scale ED using BMs and exhibiting 19 m^2 of total area [387]; separation of etc.). However, to the authors' knowledge, there is no mention anywhere of a developed and complete methodology for a process change of an ED cell from understanding mechanisms at the local scale to the development at an industrial scale of a pilot demonstrator on a specific application.

When scaling up the process, certain phenomena that are very rarely observed at the laboratory scale can be highlighted. This is notably the case for leakage currents (also called shunt currents). In an ED system, a series of IEMs are arranged in an alternating mode, facilitating ion migration based on their respective charges. Two primary sources contribute to the presence of parasitic currents. The first source is attributed to the transport of co-ions in an IEM. While the desired transport involves counter-ions, membranes exhibit less than absolute selectivity, allowing co-ions to pass through as well as depicted in the previous Section 4.6.2. The second source stems from ionic shortcut currents, which are generated by the movement of ions across the feed and drain channels. These channels serve as conduits for ionic transfer between compartments, facilitated by a difference in potential across cells. In a large stack, the potential difference between end cells could reach several hundred volts (*e.g.*, 0.6 V per cell pair [247]). In ED stack, both types of parasitic currents lead to diminished power efficiency. While reducing co-ion transport primarily involves improvements in membrane technology, the impact of ionic shortcut currents is closely linked to the design of the stack and is therefore the focus of this section. In case of current leakage, not only does this current traverse the membranes' active regions, but it also extends into these channels, as depicted in Fig. 20. Such detouring of current is influenced by the stack's geometric arrangement, the count of cell pairs (N_{cp}), and the conductivity properties of both the membranes and the solution. Consequently, this leakage current undermines the apparatus's efficiency since a portion of the electric current is diverted away from its primary role of driving ion transport across the membranes [388,389]. It has been highlighted in numerous studies that leakage currents predominantly occur configurations featuring a single hydraulic circuit [390–393]. Several strategies are proposed to mitigate the effects of ionic shortcut currents:

(i) Introducing air bubbles into the feed stream.
(ii) Implementing rotating valves functions as physical obstacles that interrupt the flow of electrolytic currents [394].
(iii) Using serial feeding, by directing concentrate/diluate sequentially through all compartments within the stack, which are interconnected in an alternating top-to-bottom manner, leading

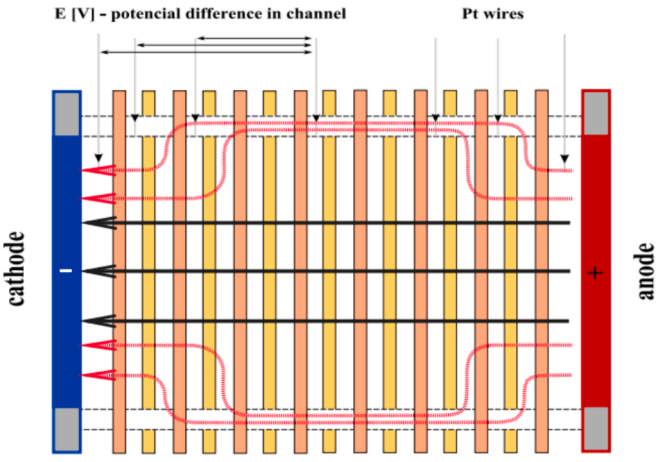

Fig. 20. Scheme of ED module with leakage currents (red arrows). Probes, designed as platinum wires, were incorporated into non-conductive separators and enabled the measurement of voltage directly inside the module. Used with permission of IOP Publishing, Ltd, from [390]; permission conveyed through Copyright Clearance Center, Inc. (For interpretation of the references to colour in this figure legend, the reader is referred to the web version of this article.)

to a zigzag flow pattern. Such a configuration forces any potential ionic shortcut currents to traverse a significantly elongated path, leading to a substantial reduction in their intensity. Nonetheless, this setup introduces greater fluid resistance. A hybrid approach, combining elements of both parallel and serial feeding, may offer an optimal solution in terms of stack design.

(iv) Employing spiral wound modules [395].

These strategies have been proposed to minimize the cross-sectional area of the liquid phase in channels and manifolds to enhance the performance, as mentioned in Section 5.1.3. However, these solutions introduce its own set of challenges, notably an increase in the pressure drop across the stacks. This elevation in pressure drop results in higher energy consumption for pumping and imposes more stringent demands on the mechanical durability of the stack's end plates and frame. A review of the literature indicates that adjusting the dimensions of the channels, specifically their length and diameter, presents a relatively straightforward method to enhance the current efficiency of large stacks. Nonetheless, determining the optimal channel dimensions often depends on empirical knowledge, highlighting a gap in the development of optimization models that balance current efficiency with pressure drop considerations in stack design [396].

6.2. *Evaluation of sustainability and economics*

6.2.1. *Techno-economic assessment*

Towards industrial application of green ED, its success hinges on the optimization of the system's design. Research and development efforts are crucially directed towards enhancing several key dimensions:

(i) The improvement of efficiency at various scales, including the cell, stack, and overall system, is paramount for reducing operational costs as well as the selectivity of the process.

(ii) Extending the lifespan of any developed system to surpass 10 years is another critical goal.

(iii) Reduction in investment costs (through capital expenditure (CAPEX) and operational expenditure (OPEX)), covering both the stack and the entire system, is necessary to make green ED technologies accessible and appealing for industrial applications.

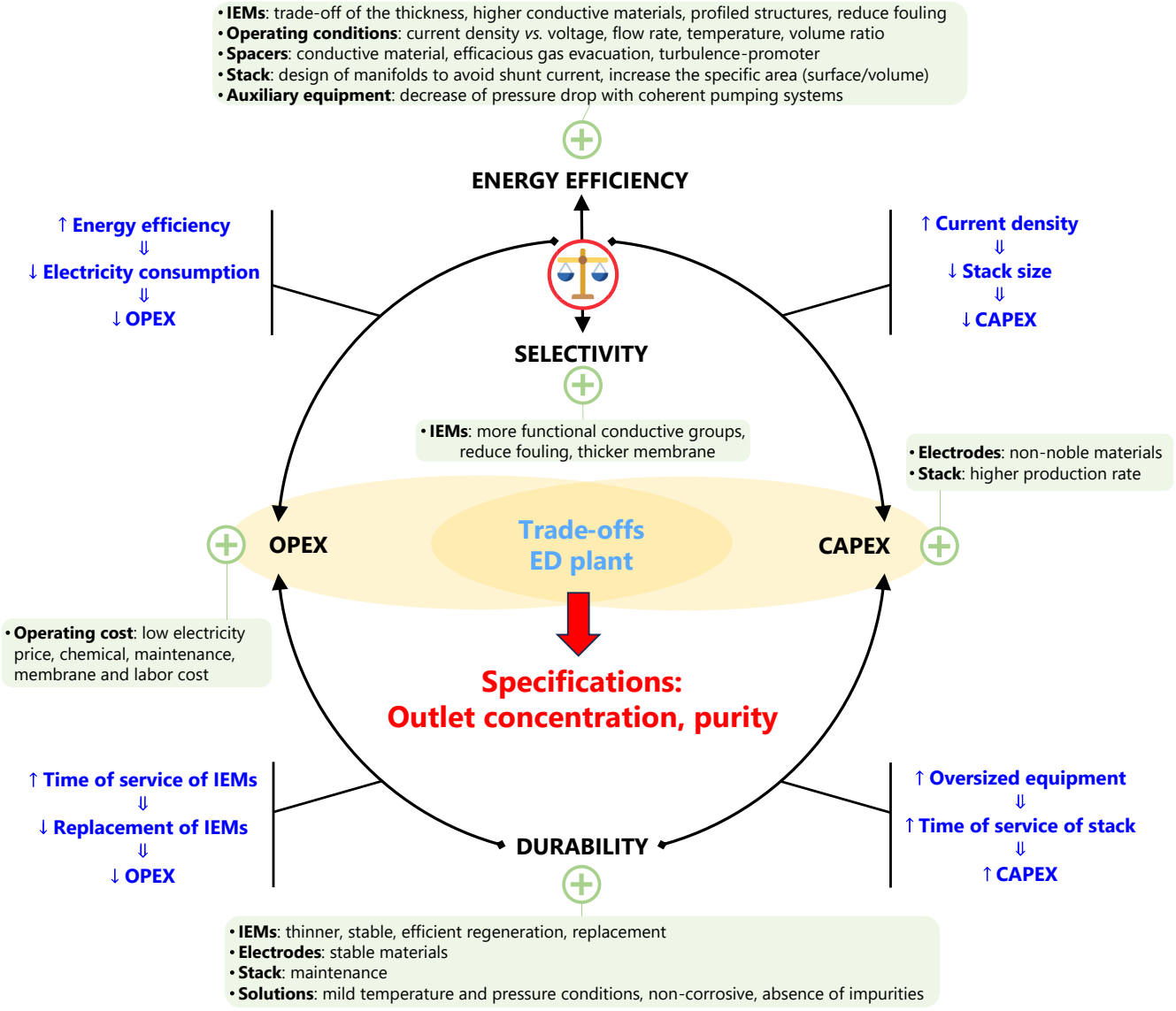

Fig. 21. Trade-offs between energy efficiency, selectivity, durability, and cost of ED process to meet product concentration and purity specifications. The green frames display the various actions to be taken to improve the associated criterion. (For interpretation of the references to colour in this figure legend, the reader is referred to the web version of this article.)

However, advancements in one area often entail trade-offs in others. Thicker membrane may enhance mechanical strength and durability but also increase resistance to charge transport, thereby diminishing efficiency. Similarly, while a longer lifespan reduces the cost attributed to investment by diluting it over time, any decrease in efficiency can lead to elevated operational costs due to increased energy consumption. Fig. 21 illustrates the beneficial or detrimental impacts that specific independent decisions, made during the manufacturing and research phases, exert on each of the aforementioned dimensions. Furthermore, the selection of materials, particularly catalysts and IEMs, plays a vital role in balancing efficiency and durability. More active functional groups of IEMs (see **Section 3**), can boost efficiency but may face challenges in maintaining stability over time. The pursuit of catalysts devoid of critical raw materials aims at sustaining high efficiency levels; however, it frequently results in materials that are less durable and more susceptible to degradation. Efficiency and selectivity are often conflicting dimensions. An increase in the thickness of the membrane will lead to better selectivity but will increase the ohmic over-potential of the membrane and therefore decrease its efficiency. Once again, it is all a matter of compromise. These dynamics underscore the complex interplay between various factors in the development of green ED technologies at large scale.

Concerning the TEA itself, the economic assessment of the cost per cubic meter produced necessitates calculating both the investment and operating costs. These parameters are derived from factors such as membrane surface area, flow rate, recovery rate, cell velocity, and outlet concentrations. Capital costs encompass process-related expenses (including pre-treatment and treatment), building construction, and auxiliary equipment. Operating costs cover consumables, energy expenses, and maintenance of installations (such as membrane and electrode replacements). Interestingly, few studies have ventured into the TEA of the ED process, which may indicate a certain impediment to the development of this technology on a larger scale. However, it should be noted that among the niche studies addressing TEA, most focus on applications in the field of water treatment [397–399]. For example, the works of Generous et al. [93] (28.6 %, 24.9 %, and 46.5 % of unit product water costs are contributed by power, fixed, and other charges[1]) and Ankoliya et al. [400] (cost of acid and base produced is comparable with the commercially available reagent) have demonstrated the benefits of this technology over conventional process. Studies applied to very specific case studies are emerging, such as those for the production of $H_3Co(CN)_6$ [262], the capture of CO_2 [401] or the coupling of BED with photovoltaic energy source [402].

6.2.2. Life cycle assessment

The challenges in reducing the environmental impact of production processes, *via* separation unit operation, present even greater opportunities for physical methods like ED compared to more polluting chemicophysical methods (*e.g.,* liquid–liquid extraction, precipitation, etc.). In the same way as TEAs, LCAs are good indicators of the maturity advancement of a technology. These data-intensive analyses enable us to approximate industrial operating conditions as closely as possible (*e.g.*, inputs such as flow rate, chemicals, power, heat demand, and outputs such as product and waste specifications) and necessitate the fixing of selected environmental impacts (*e.g.*, climate change through greenhouse gas emission quantification, discharge through mass balance, etc.) for each specific study.

A similar behavior to that of TEAs is observed for LCAs. Indeed, the majority of LCAs presented in the literature focus more on wastewater treatment applications. LCAs of wastewater treatment by ED primarily estimate carbon and water footprint distribution, with the objective of technology scale-up [4,403,404]. These studies include the work of Alrashidi et al. [405], which shows that in addition to frequent membrane replacements, membrane costs contribute significantly (50 % of equipment cost). Another study by Akula et al. [406] demonstrates that the use of BED is more eco-efficient than conventional processes for nitrate removal from wastewater.

However, ED is inherently energy-consuming technologies *via* external bias application. This results in indirect environmental impacts due to the emission of various air pollutants from conventional energy production processes, contributing to the greenhouse effect. For example, estimates indicate that estimated carbon footprint of seawater desalination is around 0.4 – 6.7 $kg_{CO_{2eq}}\ m^{-3}$ [407] (large gap due to variability in location, technologies, life cycle stages, etc.). This impact can be reduced *via* the implementation of renewable energy sources [408].

7. Diverse applications and case studies

In recent years, numerous developments have been made in the fields of conventional ED and BED. The implementation of these technologies into processes for the purification or production of organic molecules has, among other benefits, led to a reduction in saline effluents typically produced using ion exchange resins, or has minimized the need for solvents by replacing liquid–liquid extraction in certain scenarios. Saline effluents, which are often difficult to process in waste treatment facilities, can be repurposed into acids and bases through BED, which also limits the consumption of these reagents in the process. Numerous recent reviews discuss the advancements in water treatment (advancements in brackish and seawater desalination [54,409,410], energy generation through reverse ED [411–413]) and food (salt adjustment, acidification in sugar, beverages, and whey treatment [218,414–417]) applications, which remain today the major applications of this technology. We have chosen to present only the applications in more niche areas to highlight the potential for industrialization of this technology.

Table 1 summarizes the energy consumption by mass of the various products obtained by ED, depending on the application and compares them with ‘conventional processes’.

7.1. Gas desorption

ED could emerge as a significant technological advancement for the separation of gases in various applications, such as extracting CO_2 from the atmosphere (~400 ppm), isolating CO_2 and SO_2 from flue gases (and more recently removing NH_3 from ammonium sulfate [444,445]). The conditions under which the process operates frequently lead in gases desorbing within the membrane stack of the ED system. This phenomenon results in the entrapment of gas bubbles on the membrane surfaces, diminishing the available membrane surface area for the process. Consequently, this leads to an increase in resistance and the formation of localized areas of elevated current density. These hot spots can cause damage to the membranes, ultimately shortening their lifespan and compromising the system’s efficiency. In fact, an amount of work is being done to improve these separation processes.

7.1.1. CO_2 capture

While numerous pilot projects have been initiated in recent years, amine scrubbing remains the sole technique for capturing CO_2 that has seen widespread application at the industrial level. This method, a post-combustion strategy, employs amine-based chemicals (*e.g.*, monoethanolamine – MEA) to capture carbon dioxide from flue gases. Subsequently, the absorbed CO_2 is separated from the solvent through a regeneration step, which is facilitated either by altering the temperature or by changing the pressure (requiring energy that may emit additional greenhouse gases [446]). The process allows for the reuse of the solvent, and the desorbed CO_2 is prepared for transportation and storage. The primary challenges associated with amine scrubbing involve the

[1] *i.e.*, labor cost, membrane replacement cost, maintenance cost, chemical cost, and insurance cost.

Table 1
Summary and comparison table of energy consumption in relation to the products of interest *via* ED and 'conventional process'. Note that the SEC can vary significantly depending on factors such as experimental conditions, process configuration, and inlet/outlet concentration solution.

Product obtained *via* ED		**SEC[kWhkg$^{-1}_{product}$]**	Product specifications	Ref.	Product obtained *via* 'conventional process'	**SEC[kWhkg$^{-1}_{product}$]**	Product specifications		Ref.
CO_2capture	in NaOH solution	~ 0.3 kWh kg$^{-1}_{CO_2}$	100 vol% $CO_{2,(g)}$, from flue gas	[418]	CO_2capture	in NaOH solution (causticization)	~ 0.7 kWh kg$^{-1}_{CO_2}$	100 vol% $CO_{2,(g)}$, from DAC	[419]
	in KOH solution	~ 1.5 kWh kg$^{-1}_{CO_2}$	100 vol% $CO_{2,(g)}$, from DAC	[401]		in KOH solution	0.5 – 0.9 kWh kg$^{-1}_{CO_2}$	100 vol% $CO_{2,(g)}$, from flue gas	[420]
	in seawater	~ 1.5 kWh kg$^{-1}_{CO_2}$	100 vol% $CO_{2,(g)}$, from seawater	[421]					
	in amine solvent	~ 0.2 kWh kg$^{-1}_{CO_2}$	100 vol% $CO_{2,(g)}$, from flue gas	[422]		in amine solvent	0.8 – 1.1 kWh kg$^{-1}_{CO_2}$	100 vol% $CO_{2,(g)}$, from flue gas	[418]
SO_2 capture (amine solvent)		~ 1.1 kWh kg$^{-1}_{amine}$	N.A.[1]	[423]	SO_2 capture (limestone-gypsum wet desulfurization process)	~ 3.8 kWh kg$^{-1}_{SO_2}$	N.A.		[424]
Metal recovery	Lithium	~ 7.0 kWh kg$^{-1}_{Li_2CO_3}$	~98 %$Li_2CO_{3,(s)}$	[346]	Metal recovery	Lithium (Keliber process *via* hard rock deposit)	~ 21.8 kWh kg$^{-1}_{LiOH}$	~99 %$LiOH_{(s)}$	[425]
	Silver	~ 9.2 × 10^{-2} kWh kg$^{-1}_{Ag}$	~96 % of silver recovery	[426]		Silver (electro-winning)	~ 4.6 kWh kg$^{-1}_{Ag}$	99.9 % of silver	[427]
	Copper	~ 5.3 kWh kg$^{-1}_{Cu}$	~57 % of copper recovery	[428]		Copper (leaching and electro-winning)	~ 4.5 kWh kg$^{-1}_{Cu}$	100 % of copper	[429]
	Chromium	10 – 20 kWh kg$^{-1}_{CrO_3}$	~57 % of CrO_3 recovery	[430]		Chromium (leaching)	~ 0.6 kWh kg$^{-1}_{Cr}$	93 % of leached $Cr^{(III)}$	[431]
Na_2SO_4 splitting		~ 1.6 kWh kg$^{-1}_{Na_2SO_4}$	99 % NaOH + 90 % of H_2SO_4	[432]	Acid recovery	Hydrochloric acid (chlor-alkali diaphragm)	2.2 – 2.8 kWh kg$^{-1}_{acid}$	100 %HCl	[433]
Acid recovery	Hydrochloric acid	4.4 – 7.3 kWh kg$^{-1}_{acid}$	100 %HCl	[6]		Sulfuric acid (double absorption process)	~ 3.1 kWh kg$^{-1}_{acid}$	~98 wt% of H_2SO_4	[434]
	Nitric acid	~ 1.7 kWh kg$^{-1}_{acid}$	~90 % of conductivity recovery	[435]	Organic acid production	Acetic acid (ethanol oxidation)	~ 59 kWh kg$^{-1}_{acid}$	~93 % of acid yield	[436]
	Sulfuric acid	~ 1.7 kWh kg$^{-1}_{acid}$	~78 % of acid recovery	[437]		Oxalic acid (CO_2 reduction)	~ 6 kWh kg$^{-1}_{acid}$	~75 % of acid	[438]
Organic acid production	Acetic acid	3.8 – 15.7 kWh kg$^{-1}_{acid}$	100 % of acid	[439]		Citric acid (fermentation)	~ 2.0 kWh kg$^{-1}_{acid}$	~98 % of acid	[440]
	Oxalic acid	7.3 – 21.1 kWh kg$^{-1}_{acid}$				Lactic acid (fermentation)	~ 6.8 kWh kg$^{-1}_{acid}$	99 % of acid	[441]
	Citric acid	8.1 – 22.7 kWh kg$^{-1}_{acid}$							
	Lactic acid	~ 1.4 kWh kg$^{-1}_{acid}$	100 % of acid	[442]					
	Tartaric acid	~ 8.8 kWh kg$^{-1}_{acid}$	100 % of acid	[443]					

[1]N.A.: Not Applicable.

corrosive properties of the solvents and the substantial cost associated with the process, producing at the same time persistent and corrosive heat stable salts decreasing the reversibility of the process [447,448].

Given these limitations, there is a pressing need for research to pave the way for CO_2 capture technologies that are not only more effective but also more economical and decarbonated (~78 % reduction in energy consumption in the case of amine solvents according to Table 1). Concerning SEC, it seems that the use of NaOH or amine solvents are the most energetically viable solutions to develop. Typically, EC CO_2 separation involves a two-stage procedure using a liquid electrolyte to absorb and release CO_2, as depicted in Fig. 22, with IEMs facilitating the regeneration of the electrolyte [449].

The capture and release of CO_2 can be effectively managed through the EC modulation of absorbent proton concentration, acting as the central mechanism. This method, often termed as 'pH-swing', capitalizes on the proton-coupled EC reactions (*e.g.*, $X + ne^- + nH^+ \rightarrow XH_n$) to adjust the absorbent's pH. Such approaches exploit the pH-dependent thermodynamic equilibrium of CO_2 speciation in aqueous environments. An applied voltage across a series of monopolar and BM membranes initiates the CO_2 capture by generating OH^- ions and facilitates its release by producing H^+ [451,452]. Nevertheless, the presence of air bubbles within a BM reactor can diminish the usable membrane surface area and elevate the ohmic resistance across the stack, leading to an accumulation of heat on the membrane's surface. These challenges can be effectively mitigated by funneling the acidic solution through the hydrophobic side of a hollow fiber membrane reactor [453].

The development of the ED system aims at the CO_2 separation from both significant point sources, like power plant flue gases [454], and directly from the atmosphere (direct air capture, DAC) [401,455], with results suggesting the feasibility of scaling up this process (*e.g.*, decrease

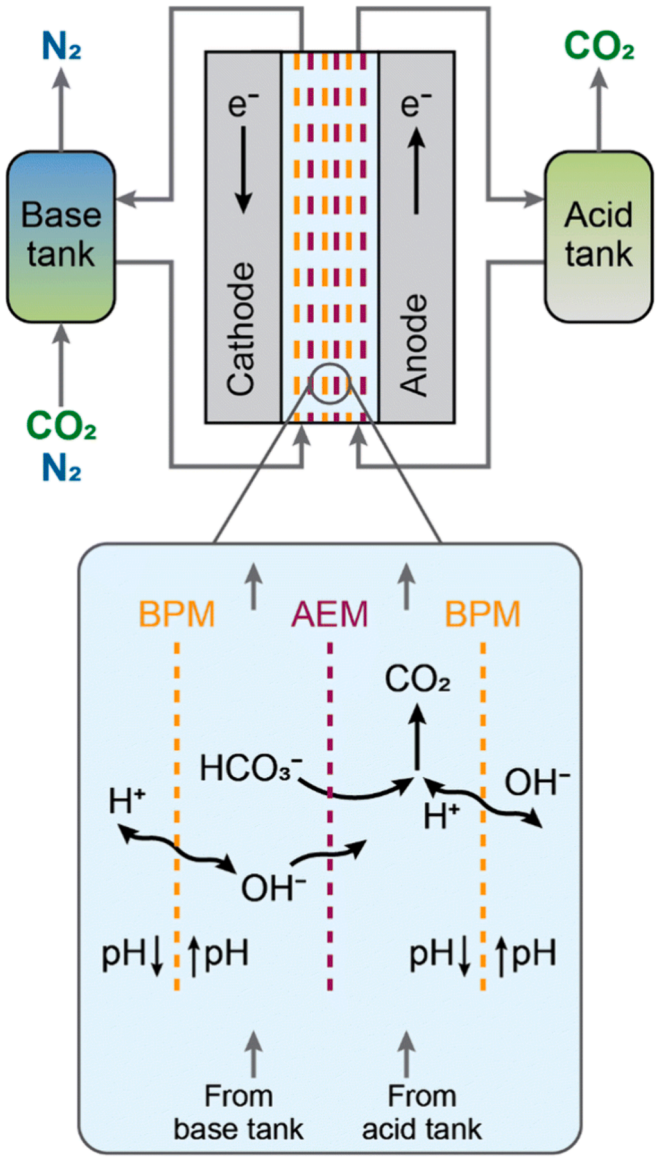

Fig. 22. Diagram illustrating the 'pH-swing' via ED for the purpose of carbon capture. Reproduced from [450] with permission from the Royal Society of Chemistry.

of energy consumption [456,457], carbon–neutral liquid fuel synthesis [421], etc.). Despite exploring various membrane configurations and electrolyte choices [458–461], the separation costs associated with ED are anticipated to be considerable, owing primarily to the need for multiple IEMs.

7.1.2. SO_2 separation

Analogous to CO_2 capture, flue-gas desulfurization plays crucial role in mitigating SO_2 emissions. BM process has been utilized for the removal and enrichment of SO_2-rich acid gases, achieved by acidifying the solution through water dissociation within the BM, which in turn enhances the rate at which these gases are desorbed *via* a 'pH-swing' and this application have been studied for the SO_2 desorption [462,463]. Initial studies suggest a reduction of about ~70 % in energy consumption when using the ED process.

Alkanolamines serve as a prevalent choice for the desulfurization (and decarbonization) of various fuel gases, including natural gas and synthesis gases derived from the gasification of coal and heavy oils. Nonetheless, these fuel gases often contain SO_3, which can react with alkanolamines to produce heat-stable alkanolamine sulfates ($-(RH)_2SO_4$) that resist simple thermal regeneration, increasing process irreversibility. Without intervention, these compounds accumulate, leading to a reduction in both the efficiency of desulfurization processes and the lifetime of the amine absorbents. Huang et al. demonstrated the regeneration of three alkanolamines through the application of BED. Their investigation focused on how various operational parameters, such as electrolyte concentration, the concentration of alkanolamine sulfate, and current density, influenced the regeneration process [423].

7.2. Hydrometallurgy applications

Numerous reviews specific to the application of ED in hydrometallurgy and metal recovery are presented in the literature [59,168,464]. In the hydrometallurgical industry, endeavors utilizing ED typically align with one of two primary objectives: *(i)* the recovery of desired species or *(ii)* the elimination of undesirable species. The latter, unwanted species, can interfere with other segments of the process industry or pose concerns from an environmental standpoint.

7.2.1. Metal value recovery

Research indicates that ED can achieve recovery rates of 70–99 % for valuable metals, including gold, noble metals, rare-earth elements, copper, and silver [465].

7.2.1.1. Li-ion battery recycling. While mining remains vital for supplying the raw materials necessary for lithium-ion batteries (LiBs), recycling is poised to play a critical role in addressing the soaring demand for lithium, cobalt, nickel, manganese, and graphite, driven by the anticipated surge in electric vehicle production over the next decade. Currently, LiB recycling is predominantly conducted through pyrometallurgical methods [466]. According to Table 1, the use of ED could lead to a reduction of SEC by about ~67 %.

Incorporating ED into a global hydrometallurgical flowsheet, which also includes solvent extraction and precipitation, could enhance the recycling process of nickel manganese cobalt (NMC) materials, as depicted in Fig. 23. Following the leaching of the black mass with H_2SO_4 and H_2O_2 [26], $Ni^{(II)}$, $Mn^{(II)}$, and $Co^{(II)}$ could be selectively extracted and separated using Cyanex® 272 as the extractant [466,467]. The resulting effluent, containing $Li^{(I)}$ along with residual amounts of $Ni^{(II)}$, $Mn^{(II)}$ and $Co^{(II)}$, could then be further purified through ED to produce high-purity lithium salts [468].

However, several challenges must be addressed before fully implementing ED in the recycling of LiBs. Particularly, the use of highly selective membranes for $Li^{(I)}$ presents difficulties due to the disparate transport properties of $Li^{(I)}$ and divalent cations ($Ni^{(II)}$, $Mn^{(II)}$ and $Co^{(II)}$). These differences can lead to the precipitation of divalent cations within the membrane's pores, which significantly reduces the limiting current

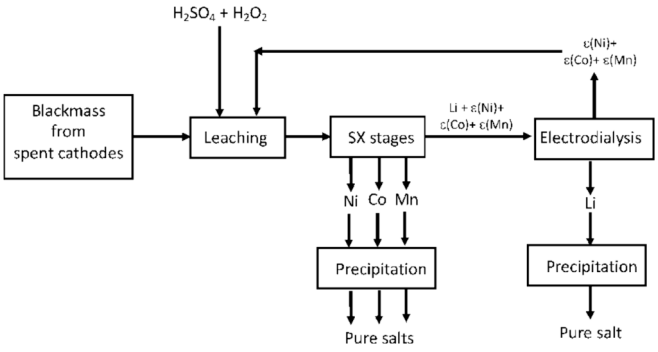

Fig. 23. Principles behind the use of ED in hydrometallurgical systems for generating high-grade lithium salts. Reprinted with permission from [466] (CC-BY MDPI).

during ED, posing operational challenges (*i.e.*, monitoring of j_{lim} over time during ED operation) [466].

ED has also emerged as a sustainable alternative for lithium recovery from diverse sources such as brines, ores, and spent LiBs [469,470]. A novel development in this field is the application of ED technique that demonstrates high selectivity for lithium (16 Wh g^{-1} of Li) over magnesium in high Mg/Li ratio brines [471]. However, the efficiency of lithium recovery can be significantly impacted by the presence of co-existing ions in solutions. Research indicates that increasing concentrations of certain co-existing ions (Na^+, K^+, SO_4^{2-}, HCO_3^-) can adversely affect the separation process of magnesium and lithium [265], highlighting the competitions occurring during the ED treatment in the presence of diverse ions. Moreover, the combination of precipitation and ED techniques for recovering lithium from spent LiBs presents an effective method for separating lithium and phosphorus (Li_3PO_4 precipitation) [472].

7.2.1.2. Other metals. Recent research into the ED process for reclaiming metals such as Cu, Ag [426], Co, Zn, and Fe demonstrates varied outcomes and limitations based on the metal in question and the specific conditions of the process.

For example, Shestakov et al. focused on the recovery of iron, nickel, and copper from printed circuit board manufacture wastewater. The study highlighted the efficient separation of these metals using ion-exchange membranes, though it noted the differential retention efficiencies for Ni^{2+} and Cu^{2+} cations in multicomponent solutions compared to single-salt solutions [473]. Similarly, Zimmermann et al. explored the separation of copper from silver in electrowinning solutions by using monovalent-selective IEMs. They highlighted the potential for continuous ED to remove divalent cations like copper, thus maintaining high purity of the recycled silver. The study also pointed out the significant drawbacks of scaling and fouling [474]. Gomes et al. combined ED with bioleaching (recycling technique that uses bacteria to recover some metals) for enhanced metal recovery from municipal solid waste incineration fly ashes. This approach showed promising results in increasing the performance of metal removal and recovery, including Co and Zn [475].

Despite the promising outcomes, common limitations across these studies include the complexity of separating multicomponent solutions (with often close valence) and challenges related to membrane scaling and fouling.

7.2.2. Approaches for treating wastewater with metal contaminants

A multitude of works dealing with ED has shown significant promise in treating wastewater containing various metal contaminants during the past few years [59,476–478].

Separation of metals from electroplating wastewater using ED was explored, demonstrating the effectiveness of ED in treating such wastewater and recovering over 90 % of metals, specifically copper and nickel [479]. The study highlighted a limitation where high voltages led to the formation of white sediments due to high current density, indicating a threshold for operational voltage to avoid precipitation issues. Recently, Cerrillo-Gonzalez et al. explored the broader application of ED in metal removal from both water and wastewater [464]. They highlighted the technique's potential in not only treating wastewater but also in recovering critical metals, thereby contributing to a circular economy. The performance of ED, as noted in their review, depends on various factors including membrane properties, cell configuration, and operational conditions. Moreover, a combined approach using ED and electrocoagulation (*i.e.*, coagulation of particles through electro-generated ions which neutralize the charge of pollutants) for the treatment of wastewater containing arsenic and copper was investigated. This innovative method achieved complete copper removal and substantial arsenic removal through ED, with further arsenic elimination *via* electrocoagulation [480]. Wang et al. focused on the treatment of electroplating wastewater with low-concentration nickel, using a combination of ED and electrodeposition. They managed to reduce the nickel concentration to below 0.1 mg/L, meeting the most stringent discharge standards [481].

7.2.3. Na_2SO_4 splitting

Base-metal refining processes, such as nickel production, are significant sources of sodium sulfate waste. In these operations, it is common to generate approximately 2 kg of Na_2SO_4 for each kg of Ni produced [432]. This waste originates from the neutralization of sulfuric acid with NaOH in the leaching solutions after metal extraction. The production and disposal of Na_2SO_4 not only reflect an inefficient conversion of valuable chemicals—imported sulfur is turned into H_2SO_4, which is then neutralized with costly NaOH to produce a low-value product—but also pose environmental risks (*e.g.*, soil salinization).

ED has emerged as a significant method for splitting Na_2SO_4, with various studies highlighting its potential and the challenges encountered. One of the noteworthy applications is the high-value conversion of Na_2SO_4 wastewater into K_2SO_4 solution (fertilizer) [482]. This work demonstrated the successful conversion of Na_2SO_4 to a K_2SO_4 solution with a concentration of 96.9 g/L and a purity of 95.2 % (limited mechanism caused by co-existing ion competitions). However, the presence of co-existing ions (Cl^-, CO_3^{2-}, Mg^{2+}, and Ca^{2+}) was found to influence the ED metathesis process, underscoring the complexity of handling mixed ion solutions, especially in terms of fouling and IEM stabilities. Another application involves the use of ED for sodium sulfate splitting in a base metal refinery, aiming to achieve a zero brine solution to prevent salinization [261,432,483]. Studies highlighted the potential of splitting Na_2SO_4 into NaOH, H_2SO_4, and water *via* SEC of ~1.6 kWh $kg^{-1}_{Na_2SO_4}$. The challenges identified included non-ideal membrane behavior and the effects of electro-osmosis, particularly at high concentration levels.

7.3. Recovery of other valuable products

ED has been effectively utilized in various recovery applications, showcasing its versatility and efficiency across different industries for producing valuable products [484,485].

In the realm of recovery from wastewater treatment, pilot-scale electrodialysis process has shown promise in recovering nutrients, such as N [486,487], P [464,488] and K [238,489,490], from wastewater with high current efficiency and low energy consumption. Furthermore, the recovery of acid (HCl [270,491], HNO_3 [272,435,492], H_2SO_4 [493,494], etc.) from process or waste streams through ED has been demonstrated to have high accuracy and the potential for energy optimization as highlighted by Table 1.

ED has also been explored for the recovery of dyes from solutions, demonstrating its potential in treating dye-laden wastewater and enabling dye reuse [354,495]. It should be noted that dyes are often not charged but purified of their saline impurities. The separation efficiency in this process is highly dependent on the molecular weight of the dye. Nevertheless, the fouling of IEMs is a significant issue, stemming from the natural electrostatic attraction between anionic (cationic) dyes and their respective anion (cation) exchange membranes. This accumulation notably impedes the transfer of ions, significantly reducing the effectiveness and, consequently, affecting the separation of dyes and inorganic salts in the treatment of dye-rich wastewater [496].

Moreover, ED has expanded its applications to include promising prospects in the pharmaceutical industry. It is particularly effective in treating wastewater containing pharmaceuticals, significantly retaining target micropollutants such as diclofenac, carbamazepine, and furosemide and limiting their transport to the concentrated ED product [497–499]. Additionally, ED has proven beneficial in the production of pharmaceutical substances, enhancing the purification process and increasing the quality of products like taurine, tuberculin, and cobalt

octa-4,5-carboxyphthalocyanine octasodium salt [15,500]. This underscores its efficiency and environmental friendliness in the pharmaceutical industry. In the production of vitamin C, BED has been applied to improve traditional acidification methods [501–503], demonstrating ED's role in enhancing product quality and its potential to streamline manufacturing processes in the pharmaceutical sector.

7.4. Acid productions

Organic acids are a group of compounds characterized by their weak acidic properties. The biodegradability of these acids has led to their increased adoption in various sectors over recent years. For example, succinic acid plays a crucial role in the development of biodegradable polymers used in resins, dyes, and pharmaceuticals, while lactic acid is being utilized in the production of biocompatible medical sutures and eco-conscious plastics [504,505]. Additionally, citric acid finds applications beyond its traditional use as a flavoring agent in food, being used for cleaning and maintaining surfaces [506]. Formic acid, on the other hand, is primarily used in the textile and paper industries [507]. The production of organic acids can be achieved through two main methods: *(i)* chemical synthesis and *(ii)* fermentation. Chemical synthesis faces challenges related to scalability, the generation of unwanted by-products, and high costs. In contrast, fermentation is gaining popularity due to its safety, efficiency, and flexibility. However, the complexity of the fermentation broth necessitates the development of sophisticated separation and purification strategies to obtain organic acids at the purity levels required for their specific applications [508,509].

For example, the process, also known as the sulfur-iodine thermochemical cycle for the H_2 production, employs iodine I_2, sulfur dioxide, and water as its primary reactants. Its fundamental operations include the production of sulfuric acid and hydroiodic acid (HI) through the Bunsen reaction. This is succeeded by the 'sulfuric section', dedicated to the reclamation of sulfur dioxide and water. Of paramount importance is the 'HIx section', recognized for its critical role in defining the process's efficiency and energy demands. This stage involves the enrichment of HI, culminating in its thermal breakdown to yield regenerated iodine and H_2 gas as the final product [510,511]. The application of electro-electrodialysis, particularly when outfitted with a CEM, has demonstrated considerable efficacy in enhancing the concentration of HI acid, a capability showcased in Fig. 24.

ED, particularly when combined with BM, is instrumental in the production of a variety of organic acids at such level of purity. For instance, in the case of citric acid, ED facilitates the efficient extraction of citric acid [512,513] from sodium citrate found in fermentation broths. This process capitalizes on the selective transport of citrate ions through membranes and their conversion to citric acid, utilizing the water dissociation capability of BM to supply the necessary protons. Similarly, acetic acid, vital for food preservation and as a precursor in the production of vinyl acetate monomer, can be recovered from dilute solutions resulting from fermentation processes [283,514,515]. Moreover, the production of specialty organic acids such as tartaric and oxalic acid, employed in the food industry and as cleaning agents respectively, also benefits from ED technology [348,439,516]. Additionally, gluconic acid, used in the food industry, pharmaceuticals, and concrete manufacturing, can be produced through fermentation followed by ED recovery. The BED process enables the direct conversion of gluconate salts to gluconic acid, improving the production process's sustainability and efficiency [517,518].

7.5. Electrodialysis membrane separations in biotechnology

ED technology's role in bio-product separation has seen significant advancements, as evidenced by recent scientific research. A notable application of ED is in the separation and purification of bioactive components, such as amino acids, proteins, and peptides, using ED with

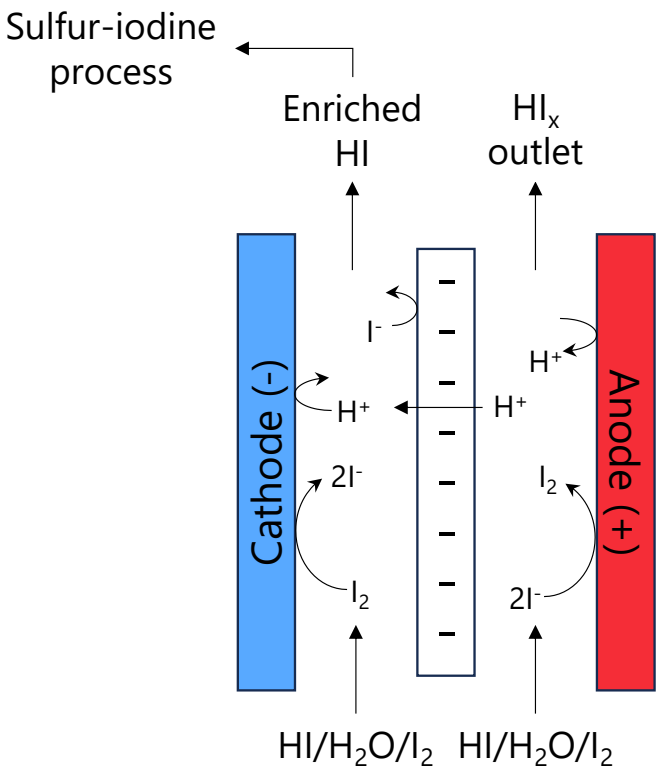

Fig. 24. Application of electro-electrodialysis studied on iodine–sulfur process for HI concentration.

porous membranes. This innovative approach, combining ED, porous filtration, and electrophoresis, has been explored by Sun et al. [519]. Their work addresses challenges like low productivity and membrane fouling.

In biotechnology, the extraction of electrically charged bioproducts, such as organic acids and antibiotics, is a one of ED application. Lazarova et al. provided an overview of recent achievements in ED for bioproducts separation and recovery (such as albumins), emphasizing its potential for more selective and efficient downstream processing [520]. ED with ultrafiltration membranes for peptide separation represents a promising approach to meet the large-scale production demands of bioactive peptides. Dlask and Václavíková investigated this hybrid process that combines the principles of ED and electrophoresis, offering an efficient method for the separation and concentration of peptides (*e.g.*, haemoglobin, β-lactoglobulin) [521]. However, it should be noted that experimental results are often compared with 'conventional processes' in terms of separation efficiency and almost never in terms of energy consumption, notably through life cycle analyses, a point that is lacking in the literature.

7.6. Pilot and industrial case studies

Numerous applications have been listed, but still remain limited in terms of larger-scale development. Nonetheless, the non-exhaustive Table 2 presents a number of large-scale case studies (*i.e.*, active surface area $> 1\ m^2$) that will familiarize the reader with some of the actors applying ED on a pilot scale. More detailed information can be found in recent comprehensive market overview studies [41,362].

One can also be pleased to see ED technology increasingly developing towards industrial applications, given the fundraising efforts by several companies and startups attempting to scale up [522,523], as well as the number of patents filed by private entities (publication dynamics of ED-related patents illustrated in Supporting Material – SM2).

Table 2
Examples of large-scale applications of ED reactors.

Industry domain	Company example	Application	Parameter of interest[1]	Ref.
Food processing	Eurosérum	Lactoserum production	> 20,000 tons per year	[524]
	Juclas	Wine stabilization by treating tartaric acid	76,000 m^3 per year	[525]
	Suez WTS Systems USA Inc	Demineralization of whey-based solution	> 250 m^3/h	[526]
Wastewater treatment	(academic plants)	Nutrient recovery from wastewater	7.2 m^2	[386]
		Production of potable water from brackish water sources	> 1 m^2	[527]
	General Electric Company	Water purification needs	Abrera, Spain: 220,000 m^3 per day San Diego, USA: 25,000 m^3 per day	[528]
Metal recovery	Lilac solutions Inc	Extraction of lithium from brine resources	200 m^3 of concentrated LiCl product at 2.8 g/L	[529]
	EnergyX	LiOH production	500,000 tons per year	[530]
Electroplating	(academic plants)	Metal recovery in electroplating processes, creating a closed-loop system	1.2 m^2	[531]
Organic acid production	BASF	Purification of an amino acid-containing solution	Unknow	[532]
Process supplier	PCCell GmbH	Continuous downstream processing, demineralization & production of valuable components.	160 m^2	[533]
	MemBrain®		19 m^2	[534]
	Ionics Electrodialysis – Veolia		64 m^2	[535]
	ASTOM Co. Ltd		>40 m^2	[536]
	Group Eurodia (EEDB, Ameridia, Oenodia, Chemistria)		>10 m^2	[537]

[1] *e.g.*, active surface area, production rate, etc.

8. Conclusion and prospects

Through this comprehensive examination, this review elucidates the pivotal role of ED in modern chemical engineering, underscoring its versatility, efficiency, and adaptability to a myriad of separation challenges. Integrating renewable energy sources with ED while managing their intermittency can foster a more sustainable and economically viable ED process, contributing significantly to a greener future. Notably, advancements in membrane materials and fabrication techniques have substantially augmented the performance of ED systems, enabling higher selectivity, reduced energy consumption, and enhanced operational stability.

Operational parameters such as electric field intensity, solution concentration, and temperature have been identified as key factors influencing the efficiency and selectivity of the ED process.

The integration of novel cell designs, mixing promotion strategies, and advanced operating modes presents a promising avenue for process intensification and system optimization.

As the ED technology matures from laboratory-scale explorations to pilot-scale implementations, the scalability and economic viability of these systems come to the forefront. Addressing these challenges requires a concerted effort in innovative design, rigorous testing, and comprehensive economic analyses to ensure the transition of electrodialysis technologies from niche applications to mainstream separation processes.

A strategic framework with targeted activities to enhance the ED process can be structured to increase ED performances:

(i) **Electrodes**: One of the proposed activities involves exploring the use of new materials for electrodes, aiming to reduce polarization and enhance conductivity. By doing so, the current efficiency could be increased, alongside a reduction in energy consumption, especially in systems that utilize redox-mediated processes.

(ii) **Spacers**: Another activity suggests designing spacers that induce turbulence while minimizing pressure drops, which could lead to improved mass transfer and reduced energy costs. This approach is critical for maintaining system efficiency without compromising the flow dynamics within the ED cells.

(iii) **Gas separation**: Further, addressing the challenges of gaseous ED separation, it is recommended to investigate novel reactor and spacer geometries to avoid gas accumulation and the screen-effect, which are known to impact system performance negatively. By exploring these new geometries, the process could potentially see a reduction in energy consumption.

(iv) **IEM materials**: Additionally, enhancing the mechanical strength of ion-exchange membranes (IEMs) is identified as a necessary improvement to facilitate gas separation at higher pressures, which could expand the applicability of ED in industrial settings. Meanwhile, improving membrane performance through advancements in nanotechnology and polymer chemistry—such as increasing rugosity and specific surface area—aims to enhance selectivity and conductivity while reducing permeability.

The roadmap also highlights the need for finding alternative membrane materials that do not rely on fluorinated compounds. This shift would improve the sustainability of the CEM life cycle and reduce pollution associated with PFAS.

(v) **Towards industrialization**: Currently, most ED applications are reported as batch operations, with limited investigation into continuous operations due to the complexity of the wastewater matrix. This limitation could hinder the broader application of BMED and delay its large-scale industrialization.

(vi) **Integration of online-monitoring tools**: As new tools for *in situ* process monitoring and control are developed, attention must be paid to their efficient incorporation into system designs and their scalability.

(vii) **Process electrification**: It is encouraged a reevaluation of certain processes to see how ED could be integrated through the electrification of processes, promoting an atom economy *via* the promotion of this technology to the chemical engineering community

(viii) **Green chemistry**: Lastly, incorporating the concept of atom economy into the ED approach emphasizes the efficient utilization of all reactants, minimizing waste and enhancing the overall sustainability of chemical processes by ensuring that each atom in the feed materials is effectively used in the final products [538,539]. The evaluation of eco-efficiency of the ED process needs to be developed mainly through the exploitation of LCA. Moreover, the future of ED appears to be moving towards integrating the technology with renewable electricity production methods, such as solar and wind power.

By methodically addressing these activities, substantial improvements in performance, efficiency, and applicability of ED systems are anticipated, steering the technology towards a future that is not only more sustainable but also economically viable. These efforts underscore

a concerted push to refine and evolve ED technology in line with contemporary environmental and industrial demands.

In conclusion, the ED process discussed has seen a growing trend towards industrialization, driven by a better understanding of local phenomena and improved energy management with considerable potential for further advancement. To realize this potential, intensive collaboration between material scientists, electrochemists, and electrochemical engineers is highly desirable. Such close cooperation is essential for overcoming the challenges inherent in advancing this multidisciplinary field. Notably, new applications of ED in areas such as wastewater treatment and battery material recycling are emerging. These advancements are facilitating scale-up changes, with several start-ups or industrial pilots now developing ED technologies (*e.g.*, REvivED water by FUJIFILM Manufacturing Europe B.V. [540], Eurodia group [541], AQUABATTERY [542], etc.). Finally, ED is a unit operation designed to be integrated into larger-scale processes. Therefore, it is essential to raise awareness of this separation technique among engineers and researchers within the chemical engineering community to fully realize its potential and integration into broader industrial applications.

CRediT authorship contribution statement

Guillaume Hopsort: Writing – review & editing, Writing – original draft, Visualization, Investigation, Data curation, Conceptualization. **Quentin Cacciuttolo:** Writing – review & editing, Supervision, Project administration, Conceptualization. **David Pasquier:** Writing – review & editing, Supervision, Project administration, Conceptualization.

Declaration of competing interest

The authors declare that they have no known competing financial interests or personal relationships that could have appeared to influence the work reported in this paper.

Data availability

Data will be made available on request.

Acknowledgements

This work was supported by the Agence Nationale de la Recherche under the project CATALPA - CO2 cApTure At Low or decarbonized energy PenAlty [grant number ANR-22-PESP-0007]. The authors gratefully acknowledged the partners of this proposal for their helpful discussion, especially Dr. F. Guillou and Dr. G. Petaud.

Appendix A. Supplementary data

Supplementary data to this article can be found online at https://doi.org/10.1016/j.cej.2024.153111.

References

[1] D.A. Vermaas, J. Veerman, N.Y. Yip, M. Elimelech, M. Saakes, K. Nijmeijer, High Efficiency in Energy Generation from Salinity Gradients with Reverse Electrodialysis, ACS Sustainable Chem. Eng. 1 (2013) 1295–1302, https://doi.org/10.1021/sc400150w.

[2] W. Wang, G. Hong, Y. Zhang, X. Yang, N. Hu, J. Zhang, P. Sorokin, L. Shao, Designing an energy-efficient multi-stage selective electrodialysis process based on high-performance materials for lithium extraction, J. Membr. Sci. 675 (2023) 121534, https://doi.org/10.1016/j.memsci.2023.121534.

[3] M.A. Morales-Mora, J.J. Pijpers, A.C. Antonio, J.d.C. La Soto, A.M.A. Calderón, Life cycle assessment of a novel bipolar electrodialysis-based flow battery concept and its potential use to mitigate the intermittency of renewable energy generation, J. Storage Mater. 35 (2021) 102339, https://doi.org/10.1016/j.est.2021.102339.

[4] K.E. Mueller, J.T. Thomas, J.X. Johnson, J.F. DeCarolis, D.F. Call, Life cycle assessment of salinity gradient energy recovery using reverse electrodialysis, J. Ind. Ecol. 25 (2021) 1194–1206, https://doi.org/10.1111/jiec.13082.

[5] M.M. Kabir, G.M. Sabur, M.M. Akter, S.Y. Nam, K.S. Im, L. Tijing, H.K. Shon, Electrodialysis desalination, resource and energy recovery from water industries for a circular economy, Desalination 569 (2024) 117041, https://doi.org/10.1016/j.desal.2023.117041.

[6] M. Herrero-Gonzalez, P. Diaz-Guridi, A. Dominguez-Ramos, R. Ibañez, A. Irabien, Photovoltaic solar electrodialysis with bipolar membranes, Desalination 433 (2018) 155–163, https://doi.org/10.1016/j.desal.2018.01.015.

[7] D.W. Bian, S.M. Watson, N.C. Wright, S.R. Shah, T. Buonassisi, D. Ramanujan, I. M. Peters, A.G. Winter, Optimization and design of a low-cost, village-scale, photovoltaic-powered, electrodialysis reversal desalination system for rural India, Desalination 452 (2019) 265–278, https://doi.org/10.1016/j.desal.2018.09.004.

[8] M. Alrbai, H.S. Hayajneh, A. Omar, M.A. Alkader, H. Al-Riaty, Experimental investigation of lab scale solar powered Electrodialysis system with corrugated membrane configuration, Sol. Energy 224 (2021) 390–400, https://doi.org/10.1016/j.solener.2021.06.028.

[9] P. Malek, J.M. Ortiz, H. Schulte-Herbrüggen, Decentralized desalination of brackish water using an electrodialysis system directly powered by wind energy, Desalination 377 (2016) 54–64, https://doi.org/10.1016/j.desal.2015.08.023.

[10] A. Campione, A. Cipollina, F. Calise, A. Tamburini, M. Galluzzo, G. Micale, Coupling electrodialysis desalination with photovoltaic and wind energy systems for energy storage: Dynamic simulations and control strategy, Energy Convers. Manag. 216 (2020) 112940, https://doi.org/10.1016/j.enconman.2020.112940.

[11] M.M. Rashidi, I. Mahariq, N. Murshid, S. Wongwises, O. Mahian, M. Alhuyi Nazari, Applying wind energy as a clean source for reverse osmosis desalination: A comprehensive review, Alex. Eng. J. 61 (2022) 12977–12989, https://doi.org/10.1016/j.aej.2022.06.056.

[12] Z.M. Ghazi, S.W.F. Rizvi, W.M. Shahid, A.M. Abdulhameed, H. Saleem, S.J. Zaidi, An overview of water desalination systems integrated with renewable energy sources, Desalination 542 (2022) 116063, https://doi.org/10.1016/j.desal.2022.116063.

[13] M.K. Shahid, B. Mainali, P.R. Rout, J.W. Lim, M. Aslam, A.E. Al-Rawajfeh, Y. Choi, A Review of Membrane-Based Desalination Systems Powered by Renewable Energy Sources, Water (basel) 15 (2023) 534, https://doi.org/10.3390/w15030534.

[14] M. Sedighi, M.M. Behvand Usefi, A.F. Ismail, M. Ghasemi, Environmental sustainability and ions removal through electrodialysis desalination: Operating conditions and process parameters, Desalination 549 (2023) 116319, https://doi.org/10.1016/j.desal.2022.116319.

[15] A.A. Konarev, Use of electrodialysis in the pilot- and commercial-scale production of pharmaceutical substances, Russ. J. Electrochem. 51 (2015) 1124–1134, https://doi.org/10.1134/S1023193515110051.

[16] S. Mikhaylin, L. Bazinet, Electrodialysis in Food Processing, https://doi.org/10.1016/B978-0-08-100596-5.03116-4, in: Reference Module in Food Science, Elsevier, 2016, ISBN: 9780081005965.

[17] T. Rózsenberszki, P. Komáromy, É. Hülber-Beyer, A. Pesti, L. Koók, P. Bakonyi, K. Bélafi-Bakó, N. Nemestóthy, Bipolar membrane electrodialysis integration into the biotechnological production of itaconic acid: A proof-of-concept study, Chem. Eng. Res. Des. 190 (2023) 187–197, https://doi.org/10.1016/j.cherd.2022.12.023.

[18] N. Kim, J. Jeon, R. Chen, X. Su, Electrochemical separation of organic acids and proteins for food and biomanufacturing, Chem. Eng. Res. Des. 178 (2022) 267–288, https://doi.org/10.1016/j.cherd.2021.12.009.

[19] B. Chen, Z. Zhang, C. Jiang, R. Fu, J. Yan, H. Wang, R. Li, G. Cao, Y. Wang, T. Xu, Electro-membrane reactor: A powerful tool for green chemical engineering, AIChE J 69 (2023) e18140.

[20] H. Wang, J. Yang, H. Zhang, J. Zhao, H. Liu, J. Wang, G. Li, H. Liang, Membrane-based technology in water and resources recovery from the perspective of water social circulation: A review, Sci. Total Environ. 908 (2024) 168277, https://doi.org/10.1016/j.scitotenv.2023.168277.

[21] M.N.Z. Abidin, M.M. Nasef, J. Veerman, Towards the development of new generation of ion exchange membranes for reverse electrodialysis: A review, Desalination 537 (2022) 115854, https://doi.org/10.1016/j.desal.2022.115854.

[22] U. Hani, Comprehensive review of polymeric nanocomposite membranes application for water treatment, Alex. Eng. J. 72 (2023) 307–321, https://doi.org/10.1016/j.aej.2023.04.008.

[23] N. Zhao, A. Platt, H. Riley, R. Qiao, R. Neagu, Z. Shi, Strategy towards high ion selectivity membranes for all-vanadium redox flow batteries, J. Storage Mater. 72 (2023) 108321, https://doi.org/10.1016/j.est.2023.108321.

[24] F. Dalanta, D.T. Handoko, H. Hadiyanto, T.D. Kusworo, Recent implementations of process intensification strategy in membrane-based technology: A review, Chem. Eng. Res. Des. 202 (2024) 74–91, https://doi.org/10.1016/j.cherd.2023.12.014.

[25] S.K.A. Al-Amshawee, M.Y.B. Mohd Yunus, Impact of membrane spacers on concentration polarization, flow profile, and fouling at ion exchange membranes of electrodialysis desalination: Diagonal net spacer vs. ladder-type configuration, Chem. Eng. Res. Des. 191 (2023) 197–213, https://doi.org/10.1016/j.cherd.2023.01.012.

[26] C. Simões, B. Vital, T. Sleutels, M. Saakes, W. Brilman, Scaled-up multistage reverse electrodialysis pilot study with natural waters, Chem. Eng. J. 450 (2022) 138412, https://doi.org/10.1016/j.cej.2022.138412.

[27] T. Elmakki, S. Zavahir, M. Gulied, H. Qiblawey, B. Hammadi, M. Khraisheh, H. K. Shon, H. Park, D.S. Han, Potential application of hybrid reverse electrodialysis (RED)-forward osmosis (FO) system to fertilizer-producing industrial plant for

efficient water reuse, Desalination 550 (2023) 116374, https://doi.org/10.1016/j.desal.2023.116374.
[28] M. Tedesco, A. Cipollina, A. Tamburini, G. Micale, Towards 1 kW power production in a reverse electrodialysis pilot plant with saline waters and concentrated brines, J. Membr. Sci. 522 (2017) 226–236, https://doi.org/10.1016/j.memsci.2016.09.015.
[29] S. Bazhenov, A. Rieder, B. Schallert, V. Vasilevsky, S. Unterberger, E. Grushevenko, V. Volkov, A. Volkov, Reclaiming of degraded MEA solutions by electrodialysis: Results of ED pilot campaign at post-combustion CO_2 capture pilot plant, International Journal of Greenhouse Gas Control 42 (2015) 593–601. https://doi.org/10.1016/j.ijggc.2015.09.015.
[30] E. Maigrot, J. Sabates (German Patent), Apparat zur Lauterung von Zuckersaften mittels Elektrizitat, 50443, 1890.
[31] V.A. Shaposhnik, K. Kesore, An early history of electrodialysis with permselective membranes, J. Membr. Sci. 136 (1997) 35–39, https://doi.org/10.1016/S0376-7388(97)00149-X.
[32] E. Manegold, K. Kalauch, ber Kapillarsysteme XXII, Kolloid-Zeitschrift 86 (1939) 93–101, https://doi.org/10.1007/BF01512006.
[33] W. Juda, W.A. McRae, COHERENT ION-EXCHANGE GELS AND MEMBRANES, J. Am. Chem. Soc. 72 (1950) 1044, https://doi.org/10.1021/ja01158a528.
[34] A.G. Winger, G.W. Bodamer, R. Kunin, Some Electrochemical Properties of New Synthetic Ion Exchange Membranes, J. Electrochem. Soc. 100 (1953) 178, https://doi.org/10.1149/1.2781103.
[35] M.R.J. Wyllie, H.W. Patnode, The The Development of Membranes Prepared from Artificial Cation-Exchange Materials with Particular Reference to the Determination of Sodium-Ion Activities, J. Phys. Chem. 54 (1950) 204–227, https://doi.org/10.1021/j150476a004.
[36] T. Xu, Ion exchange membranes: State of their development and perspective, J. Membr. Sci. 263 (2005) 1–29, https://doi.org/10.1016/j.memsci.2005.05.002.
[37] V. Vinayagam, N.K. Kishor Kumar, K.N. Palani, S. Ganesh, O.S. Kushwaha, A. Pugazhendhi, Recent breakthroughs on the development of electrodeionization systems for toxic pollutants removal from water environment, Environ. Res. 241 (2024) 117549, https://doi.org/10.1016/j.envres.2023.117549.
[38] Z. Matějka, Continuous production of high-purity water by electro-deionisation, J. Appl. Chem. Biotech. 21 (1971) 117–120, https://doi.org/10.1002/jctb.5020210408.
[39] E. Korngold, Electrodialysis processes using ion exchange resins between membranes, Desalination 16 (1975) 225–233, https://doi.org/10.1016/S0011-9164(00)82094-9.
[40] B.S. Rathi, P.S. Kumar, Electrodeionization theory, mechanism and environmental applications, A Review, Environ Chem Lett 18 (2020) 1209–1227, https://doi.org/10.1007/s10311-020-01006-9.
[41] R. Pärnamäe, S. Mareev, V. Nikonenko, S. Melnikov, N. Sheldeshov, V. Zabolotskii, H. Hamelers, M. Tedesco, Bipolar membranes: A review on principles, latest developments, and applications, J. Membr. Sci. 617 (2021) 118538, https://doi.org/10.1016/j.memsci.2020.118538.
[42] R. Fu, H. Wang, J. Yan, R. Li, C. Jiang, Y. Wang, T. Xu, Asymmetric bipolar membrane electrodialysis for acid and base production, AIChE J 69 (2023) e17957.
[43] T. Chen, J. Bi, Z. Ji, J. Yuan, Y. Zhao, Application of bipolar membrane electrodialysis for simultaneous recovery of high-value acid/alkali from saline wastewater: An in-depth review, Water Res. 226 (2022) 119274, https://doi.org/10.1016/j.watres.2022.119274.
[44] M. Paidar, V. Fateev, K. Bouzek, Membrane electrolysis—History, current status and perspective, Electrochim. Acta 209 (2016) 737–756, https://doi.org/10.1016/j.electacta.2016.05.209.
[45] C. Espinoza, D. Kitto, J. Kamcev, Counter-ion Conductivity and Selectivity Trade-Off for Commercial Ion-Exchange Membranes at High Salinities, ACS Appl. Polym. Mater. 5 (2023) 10324–10333, https://doi.org/10.1021/acsapm.3c02102.
[46] E.Y. Safronova, A.A. Lysova, D.Y. Voropaeva, A.B. Yaroslavtsev, Approaches to the Modification of Perfluorosulfonic Acid Membranes, Membranes (basel) 13 (2023), https://doi.org/10.3390/membranes13080721.
[47] Z. Qiu, Y. Yun, M. He, L. Wang, Recent developments in ion conductive membranes for CO2 electrochemical reduction, Chem. Eng. J. 456 (2023) 140942, https://doi.org/10.1016/j.cej.2022.140942.
[48] J.G. Hong, T.-W. Park, Ion-exchange membranes for blue energy generation: A short overview focused on nanocomposite, J. Electrochem. Sci. Eng. (2022), https://doi.org/10.5599/jese.1447.
[49] M.A. Shehzad, A. Yasmin, X. Ge, L. Wu, T. Xu, A Review of Nanostructured Ion-Exchange Membranes, Adv Materials Technologies 6 (2021) 2001171, https://doi.org/10.1002/admt.202001171.
[50] J. Ying, Y. Lin, Y. Zhang, J. Yu, Developmental Progress of Electrodialysis Technologies and Membrane Materials for Extraction of Lithium from Salt Lake Brines, ACS EST Water 3 (2023) 1720–1739, https://doi.org/10.1021/acsestwater.3c00013.
[51] Y. Luo, Y. Liu, J. Shen, B. van der Bruggen, Application of Bipolar Membrane Electrodialysis in Environmental Protection and Resource Recovery: A Review, Membranes (basel) 12 (2022), https://doi.org/10.3390/membranes12090829.
[52] M.M. Rahman, Membranes for Osmotic Power Generation by Reverse Electrodialysis, Membranes (basel) 13 (2023), https://doi.org/10.3390/membranes13020164.
[53] S.Y. Yeon, J. Rho, Y. Kim, T.D. Chung, Reverse electrodialysis for emerging applications, Bulletin Korean Chem Soc 43 (2022) 769–776, https://doi.org/10.1002/bkcs.12524.
[54] N. Mir, Y. Bicer, Integration of electrodialysis with renewable energy sources for sustainable freshwater production: A review, J. Environ. Manage. 289 (2021) 112496, https://doi.org/10.1016/j.jenvman.2021.112496.
[55] H. Peng, J. Guo, Removal of chromium from wastewater by membrane filtration, chemical precipitation, ion exchange, adsorption electrocoagulation, electrochemical reduction, electrodialysis, electrodeionization, photocatalysis and nanotechnology: a review, Environ Chem Lett 18 (2020) 2055–2068, https://doi.org/10.1007/s10311-020-01058-x.
[56] A. Daniilidis, R. Herber, D.A. Vermaas, Upscale potential and financial feasibility of a reverse electrodialysis power plant, Appl. Energy 119 (2014) 257–265, https://doi.org/10.1016/j.apenergy.2013.12.066.
[57] M. Schorr (Ed.), Desalination, Trends and Technologies, InTech, 2011.
[58] C. Chen, Y.-L.-S. Tse, G.E. Lindberg, C. Knight, G.A. Voth, Hydroxide Solvation and Transport in Anion Exchange Membranes, J. Am. Chem. Soc. 138 (2016) 991–1000, https://doi.org/10.1021/jacs.5b11951.
[59] Ö. Tekinalp, P. Zimmermann, S. Holdcroft, O.S. Burheim, L. Deng, Cation Exchange Membranes and Process Optimizations in Electrodialysis for Selective Metal Separation: A Review, Membranes (basel) 13 (2023), https://doi.org/10.3390/membranes13060566.
[60] X. Chen, Y. Zhan, J. Tang, X. Yang, A. Sun, B. Lin, F. Zhu, H. Jia, X. Lei, Advances in high performance anion exchange membranes: Molecular design, preparation methods, and ion transport dynamics, J. Environ. Chem. Eng. 11 (2023) 110749, https://doi.org/10.1016/j.jece.2023.110749.
[61] W. Yu, L. Xiong, J. Teng, C. Chen, B. Li, L. Zhao, H. Lin, L. Shen, Advances in synthesis and application of amphoteric polymer-based water treatment agents, Desalination 574 (2024) 117280, https://doi.org/10.1016/j.desal.2023.117280.
[62] X. Gao, J. Chen, R. Xu, Z. Zhen, X. Zeng, X. Chen, L. Cui, Research progress and prospect of the materials of bipolar plates for proton exchange membrane fuel cells (PEMFCs), Int. J. Hydrogen Energy 50 (2024) 711–743, https://doi.org/10.1016/j.ijhydene.2023.09.005.
[63] H. Strathmann, Chapter 3 - Preparation and Characterization of Ion-Exchange Membranes, https://doi.org/10.1016/S0927-5193(04)80034-2, in: H. Strathmann (Ed.), Membrane Science and Technology Ion-Exchange Membrane Separation Processes, Elsevier, 2004, ISBN: 0927-5193, pp. 89–146.
[64] I. Miesiac, B. Rukowicz, Bipolar Membrane and Water Splitting in Electrodialysis, Electrocatalysis 13 (2022) 101–107, https://doi.org/10.1007/s12678-021-00703-5.
[65] D. Shi, L. Cai, C. Zhang, D. Chen, Z. Pan, Z. Kang, Y. Liu, J. Zhang, Fabrication methods, structure design and durability analysis of advanced sealing materials in proton exchange membrane fuel cells, Chem. Eng. J. 454 (2023) 139995, https://doi.org/10.1016/j.cej.2022.139995.
[66] E. Kuhnert, V. Hacker, M. Bodner, A Review of Accelerated Stress Tests for Enhancing MEA Durability in PEM Water Electrolysis Cells, Int. J. Energy Res. 2023 (2023) 1–23, https://doi.org/10.1155/2023/3183108.
[67] F. Li, S.H. Chan, Z. Tu, Recent Development of Anion Exchange Membrane Fuel Cells and Performance Optimization Strategies: A Review, Chem. Rec. (2023) e202300067.
[68] L. Liu, C. Wang, Z. He, R. Das, B. Dong, X. Xie, Z. Guo, An overview of amphoteric ion exchange membranes for vanadium redox flow batteries, J. Mater. Sci. Technol. 69 (2021) 212–227, https://doi.org/10.1016/j.jmst.2020.08.032.
[69] H. Matsumoto, Y. Koyama, A. Tanioka, Interaction of proteins with weak amphoteric charged membrane surfaces: effect of pH, J. Colloid Interface Sci. 264 (2003) 82–88, https://doi.org/10.1016/s0021-9797(03)00417-x.
[70] K. Friess Mosaic Membranes E. Drioli L. Giorno E. Drioli L. Giorno Encyclopedia of Membranes 2020 Springer Berlin Heidelberg, Berlin, Heidelberg pp. 1–2, ISBN: 978-3-642-40872-4. 10.1007/978-3-642-40872-4_395-1.
[71] D.S. Peterson Ion Exchange Membranes D. Li Encyclopedia of Microfluidics and Nanofluidics 2008 Springer Boston, MA, Cham pp. 873–876, ISBN: 978-0-387-48998-8. 10.1007/978-0-387-48998-8_739.
[72] B. Bolto, M. Hoang, T. Tran, Review of piezodialysis — salt removal with charge mosaic membranes, Desalination 254 (2010) 1–5, https://doi.org/10.1016/j.desal.2009.12.013.
[73] J. Wang, Y. Zhang, J. Zhu, J. Hou, J. Liu, B. van der Bruggen, Zwitterionic functionalized layered double hydroxides nanosheets for a novel charged mosaic membrane with high salt permeability, J. Membr. Sci. 510 (2016) 27–37, https://doi.org/10.1016/j.memsci.2016.03.016.
[74] Y. Avni, R.M. Adar, D. Andelman, H. Orland, Conductivity of Concentrated Electrolytes, Phys. Rev. Lett. 128 (2022) 98002, https://doi.org/10.1103/PhysRevLett.128.098002.
[75] P. Aydogan Gokturk, R. Sujanani, J. Qian, Y. Wang, L.E. Katz, B.D. Freeman, E. J. Crumlin, The Donnan potential revealed, Nat. Commun. 13 (2022) 5880, https://doi.org/10.1038/s41467-022-33592-3.
[76] A.H. Galama, J.W. Post, M.A. Cohen Stuart, P.M. Biesheuvel, Validity of the Boltzmann equation to describe Donnan equilibrium at the membrane–solution interface, Journal of Membrane Science 442 (2013) 131–139, https://doi.org/10.1016/j.memsci.2013.04.022.
[77] H. Strathmann, J. Krol, H.-J. Rapp, G. Eigenberger, Limiting current density and water dissociation in bipolar membranes, J. Membr. Sci. 125 (1997) 123–142, https://doi.org/10.1016/S0376-7388(96)00185-8.
[78] L. Chen, Q. Xu, S.Z. Oener, K. Fabrizio, S.W. Boettcher, Design principles for water dissociation catalysts in high-performance bipolar membranes, Nat. Commun. 13 (2022) 3846, https://doi.org/10.1038/s41467-022-31429-7.
[79] H.-B. Song, M.-S. Kang, Bipolar Membranes Containing Iron-Based Catalysts for Efficient Water-Splitting Electrodialysis, Membranes (basel) 12 (2022), https://doi.org/10.3390/membranes12121201.

[80] H. Fan, Y. Huang, N.Y. Yip, Advancing ion-exchange membranes to ion-selective membranes: principles, status, and opportunities, Front. Environ. Sci. Eng. 17 (2023), https://doi.org/10.1007/s11783-023-1625-0.
[81] H. Strathmann Chapter 6 Ion-Exchange Membrane Processes in Water Treatment A.I. Schäfer I.C. Escobar Sustainable Water for the Future: Water Recycling versus Desalination 2010 Elsevier Science Amsterdam, Boston, Paris pp. 141–199, ISBN: 9780444531155. 10.1016/S1871-2711(09)00206-2.
[82] T. Sata, Ion exchange membranes: Preparation, characterization, modification and application, Royal Society of Chemistry, Cambridge, 2004.
[83] J.S. Mackie, P. Meares, The diffusion of electrolytes in a cation-exchange resin membrane I. Theoretical, Proc. r. Soc. Lond. A 232 (1955) 498–509, https://doi.org/10.1098/rspa.1955.0234.
[84] T.M. Mubita, S. Porada, P.M. Biesheuvel, A. van der Wal, J.E. Dykstra, Strategies to increase ion selectivity in electrodialysis, Sep. Purif. Technol. 292 (2022) 120944, https://doi.org/10.1016/j.seppur.2022.120944.
[85] T. Luo, S. Abdu, M. Wessling, Selectivity of ion exchange membranes: A review, J. Membr. Sci. 555 (2018) 429–454, https://doi.org/10.1016/j.memsci.2018.03.051.
[86] M. Ahmad, M. Ahmed, Characterization and applications of ion-exchange membranes and selective ion transport through them: a review, J Appl Electrochem 53 (2023) 1537–1562, https://doi.org/10.1007/s10800-023-01882-3.
[87] A. Elattar, A. Elmidaoui, N. Pismenskaia, C. Gavach, G. Pourcelly, Comparison of transport properties of monovalent anions through anion-exchange membranes, J. Membr. Sci. 143 (1998) 249–261, https://doi.org/10.1016/S0376-7388(98)00013-1.
[88] S. Moshtarikhah, N.A.W. Oppers, M.T. de Groot, J.T.F. Keurentjes, J.C. Schouten, J. van der Schaaf, Nernst-Planck modeling of multicomponent ion transport in a Nafion membrane at high current density, J Appl Electrochem 47 (2017) 51–62, https://doi.org/10.1007/s10800-016-1017-2.
[89] A.V. Kovalenko, V.V. Nikonenko, N.O. Chubyr, M. Urtenov, Mathematical modeling of electrodialysis of a dilute solution with accounting for water dissociation-recombination reactions, Desalination 550 (2023) 116398, https://doi.org/10.1016/j.desal.2023.116398.
[90] L. Xing, H. Jiang, X. Tian, H. Yin, W. Shi, E. Yu, V.J. Pinfield, J. Xuan, Combining machine learning with multi-physics modelling for multi-objective optimisation and techno-economic analysis of electrochemical CO2 reduction process, Carbon Capture Science & Technology 9 (2023) 100138, https://doi.org/10.1016/j.ccst.2023.100138.
[91] A.K. Thakur, M. Malmali, Advances in polymeric cation exchange membranes for electrodialysis: An overview, J. Environ. Chem. Eng. 10 (2022) 108295, https://doi.org/10.1016/j.jece.2022.108295.
[92] J. Huang, Z. Yu, J. Tang, P. Wang, Q. Tan, J. Wang, X. Lei, A review on anion exchange membranes for fuel cells: Anion-exchange polyelectrolytes and synthesis strategies, Int. J. Hydrogen Energy 47 (2022) 27800–27820, https://doi.org/10.1016/j.ijhydene.2022.06.140.
[93] M.M. Generous, N.A. Qasem, U.A. Akbar, S.M. Zubair, Techno-economic assessment of electrodialysis and reverse osmosis desalination plants, Sep. Purif. Technol. 272 (2021) 118875, https://doi.org/10.1016/j.seppur.2021.118875.
[94] D.A. Cowan, J.H. Brown, Effect of Turbulence on Limiting Current in Electrodialysis Cells, Ind. Eng. Chem. 51 (1959) 1445–1448, https://doi.org/10.1021/ie50600a026.
[95] K. Li, Q. Fan, H. Chuai, H. Liu, S. Zhang, X. Ma, Revisiting Chlor-Alkali Electrolyzers: from Materials to Devices, Trans. Tianjin Univ. 27 (2021) 202–216, https://doi.org/10.1007/s12209-021-00285-9.
[96] Y. Zhang, L. Wang, W. Sun, Y. Hu, H. Tang, Membrane technologies for Li+/Mg2 + separation from salt-lake brines and seawater: A comprehensive review, J. Ind. Eng. Chem. 81 (2020) 7–23, https://doi.org/10.1016/j.jiec.2019.09.002.
[97] K.H. Chan, M. Malik, G. Azimi, Separation of lithium, nickel, manganese, and cobalt from waste lithium-ion batteries using electrodialysis, Resour. Conserv. Recycl. 178 (2022) 106076, https://doi.org/10.1016/j.resconrec.2021.106076.
[98] S. Ozkul, J.J. van Daal, N.J. Kuipers, R.J. Bisselink, H. Bruning, J.E. Dykstra, H. H. Rijnaarts, Transport mechanisms in electrodialysis: The effect on selective ion transport in multi-ionic solutions, J. Membr. Sci. 665 (2023) 121114, https://doi.org/10.1016/j.memsci.2022.121114.
[99] A. Martin, P. Trinke, B. Bensmann, R. Hanke-Rauschenbach, Hydrogen Crossover in PEM Water Electrolysis at Current Densities up to 10 A cm −2, J. Electrochem. Soc. 169 (2022) 94507, https://doi.org/10.1149/1945-7111/ac908c.
[100] M. Cecchetti, F. Toja, A. Casalegno, M. Zago, A comprehensive experimental and modelling approach for the evaluation of cross-over fluxes in Vanadium Redox Flow Battery, J. Energy Storage 68 (2023) 107846, https://doi.org/10.1016/j.est.2023.107846.
[101] S. Mareev, A. Gorobchenko, D. Ivanov, D. Anokhin, V. Nikonenko, Ion and Water Transport in Ion-Exchange Membranes for Power Generation Systems: Guidelines for Modeling, Int. J. Mol. Sci. 24 (2022), https://doi.org/10.3390/ijms24010034.
[102] Y. Huang, H. Fan, N.Y. Yip, Influence of electrolyte on concentration-induced conductivity-permselectivity tradeoff of ion-exchange membranes, J. Membr. Sci. 668 (2023) 121184, https://doi.org/10.1016/j.memsci.2022.121184.
[103] H. Strathmann, A. Grabowski, G. Eigenberger, Ion-Exchange Membranes in the Chemical Process Industry, Ind. Eng. Chem. Res. 52 (2013) 10364–10379, https://doi.org/10.1021/ie4002102.
[104] H. Fan, N.Y. Yip, Elucidating conductivity-permselectivity tradeoffs in electrodialysis and reverse electrodialysis by structure-property analysis of ion-exchange membranes, J. Membr. Sci. 573 (2019) 668–681, https://doi.org/10.1016/j.memsci.2018.11.045.
[105] G.M. Geise, M.A. Hickner, B.E. Logan, Ionic resistance and permselectivity tradeoffs in anion exchange membranes, ACS Appl. Mater. Interfaces 5 (2013) 10294–10301, https://doi.org/10.1021/am403207w.
[106] B. Jiang, L. Wu, L. Yu, X. Qiu, J. Xi, A comparative study of Nafion series membranes for vanadium redox flow batteries, J. Membr. Sci. 510 (2016) 18–26, https://doi.org/10.1016/j.memsci.2016.03.007.
[107] C. Zhang, Gauging membrane thinness, Nat. Energy 4 (2019) 89, https://doi.org/10.1038/s41560-019-0340-3.
[108] C.S. Gittleman, A. Kongkanand, D. Masten, W. Gu, Materials research and development focus areas for low cost automotive proton-exchange membrane fuel cells, Curr. Opin. Electrochem. 18 (2019) 81–89, https://doi.org/10.1016/j.coelec.2019.10.009.
[109] J. Kamcev, Reformulating the permselectivity-conductivity tradeoff relation in ion-exchange membranes, J. Polym. Sci. 59 (2021) 2510–2520, https://doi.org/10.1002/pol.20210304.
[110] S. Adhikari, M.K. Pagels, J.Y. Jeon, C. Bae, Ionomers for electrochemical energy conversion & storage technologies, Polymer 211 (2020) 123080, https://doi.org/10.1016/j.polymer.2020.123080.
[111] ANIONE (2020), https://doi.org/10.3030/875024.
[112] CHANNEL (2020), https://doi.org/10.3030/875088.
[113] NEWELY (2020), https://doi.org/10.3030/875118.
[114] Horizon, Framework Programme, New Anion Exchange Membrane Electrolysers: FCH-02-4-2019, 2019, accessed 22 February 2024, https://ec.europa.eu/info/funding-tenders/opportunities/portal/screen/opportunities/topic-details/fch-02-4-2019, 2020.
[115] M.D. Guiver, Y.M. Lee, Materials science, Polymer Rigidity Improves Microporous Membranes, Science 339 (2013) 284–285, https://doi.org/10.1126/science.1232714.
[116] S. Holdcroft, J. Fan, Sterically-encumbered ionenes as hydroxide ion-conducting polymer membranes, Curr. Opin. Electrochem. 18 (2019) 99–105, https://doi.org/10.1016/j.coelec.2019.10.014.
[117] A.D. Mohanty, S.E. Tignor, J.A. Krause, Y.-K. Choe, C. Bae, Systematic Alkaline Stability Study of Polymer Backbones for Anion Exchange Membrane Applications, Macromolecules 49 (2016) 3361–3372, https://doi.org/10.1021/acs.macromol.5b02550.
[118] S.A. Nuñez, C. Capparelli, M.A. Hickner, N -Alkyl Interstitial Spacers and Terminal Pendants Influence the Alkaline Stability of Tetraalkylammonium Cations for Anion Exchange Membrane Fuel Cells, Chem. Mater. 28 (2016) 2589–2598, https://doi.org/10.1021/acs.chemmater.5b04767.
[119] N. Chen, C. Long, Y. Li, C. Lu, H. Zhu, Ultrastable and High Ion-Conducting Polyelectrolyte Based on Six-Membered N-Spirocyclic Ammonium for Hydroxide Exchange Membrane Fuel Cell Applications, ACS Appl. Mater. Interfaces 10 (2018) 15720–15732, https://doi.org/10.1021/acsami.8b02884.
[120] T.H. Pham, J.S. Olsson, P. Jannasch, N-Spirocyclic Quaternary Ammonium Ionenes for Anion-Exchange Membranes, J. Am. Chem. Soc. 139 (2017) 2888–2891, https://doi.org/10.1021/jacs.6b12944.
[121] Z. Tao, C. Wang, X. Zhao, J. Li, M.D. Guiver, Progress in High-Performance Anion Exchange Membranes Based on the Design of Stable Cations for Alkaline Fuel Cells, Adv Materials Technologies 6 (2021) 2001220, https://doi.org/10.1002/admt.202001220.
[122] K.M. Hugar, H.A. Kostalik, G.W. Coates, Imidazolium Cations with Exceptional Alkaline Stability: A Systematic Study of Structure-Stability Relationships, J. Am. Chem. Soc. 137 (2015) 8730–8737, https://doi.org/10.1021/jacs.5b02879.
[123] B. Xue, F. Wang, J. Zheng, S. Li, S. Zhang, Highly stable polysulfone anion exchange membranes incorporated with bulky alkyl substituted guanidinium cations, Mol. Syst. Des. Eng. 4 (2019) 1039–1047, https://doi.org/10.1039/C9ME00064J.
[124] B. Zhang, R.B. Kaspar, S. Gu, J. Wang, Z. Zhuang, Y. Yan, A New Alkali-Stable Phosphonium Cation Based on Fundamental Understanding of Degradation Mechanisms, ChemSusChem 9 (2016) 2374–2379, https://doi.org/10.1002/cssc.201600468.
[125] K.M. Hugar, W. You, G.W. Coates, Protocol for the Quantitative Assessment of Organic Cation Stability for Polymer Electrolytes, ACS Energy Lett. 4 (2019) 1681–1686, https://doi.org/10.1021/acsenergylett.9b00908.
[126] C.T. Womble, J. Kang, K.M. Hugar, G.W. Coates, S. Bernhard, K.J.T. Noonan, Rapid Analysis of Tetrakis(dialkylamino)phosphonium Stability in Alkaline Media, Organometallics 36 (2017) 4038–4046, https://doi.org/10.1021/acs.organomet.7b00663.
[127] S. Gu, R. Cai, T. Luo, Z. Chen, M. Sun, Y. Liu, G. He, Y. Yan, A Soluble and Highly Conductive Ionomer for High-Performance Hydroxide Exchange Membrane Fuel Cells, Angew. Chem. Weinheim. Bergstr. Ger. 121 (2009) 6621–6624, https://doi.org/10.1002/ange.200806299.
[128] S. Gu, J. Wang, R.B. Kaspar, Q. Fang, B. Zhang, E. Bryan Coughlin, Y. Yan, Permethyl Cobaltocenium (Cp*2Co+) as an Ultra-Stable Cation for Polymer Hydroxide-Exchange Membranes, Sci. Rep. 5 (2015) 11668, https://doi.org/10.1038/srep11668.
[129] T. Zhu, Y. Sha, H.A. Firouzjaie, X. Peng, Y. Cha, D.M.M.M. Dissanayake, M. D. Smith, A.K. Vannucci, W.E. Mustain, C. Tang, Rational Synthesis of Metallo-Cations Toward Redox- and Alkaline-Stable Metallo-Polyelectrolytes, J. Am. Chem. Soc. 142 (2020) 1083–1089, https://doi.org/10.1021/jacs.9b12051.
[130] N. Chen, Y.M. Lee, Anion exchange polyelectrolytes for membranes and ionomers, Prog. Polym. Sci. 113 (2021) 101345, https://doi.org/10.1016/j.progpolymsci.2020.101345.
[131] E.J. Park, Y.S. Kim, Quaternized aryl ether-free polyaromatics for alkaline membrane fuel cells: synthesis, properties, and performance – a topical review,

J. Mater. Chem. A 6 (2018) 15456–15477, https://doi.org/10.1039/C8TA05428B.
[132] A.M.A. Mahmoud, A.M.M. Elsaghier, K. Otsuji, K. Miyatake, High Hydroxide Ion Conductivity with Enhanced Alkaline Stability of Partially Fluorinated and Quaternized Aromatic Copolymers as Anion Exchange Membranes, Macromolecules 50 (2017) 4256–4266, https://doi.org/10.1021/acs.macromol.7b00401.
[133] J.S. Olsson, T.H. Pham, P. Jannasch, Poly(arylene piperidinium) Hydroxide Ion Exchange Membranes: Synthesis, Alkaline Stability, and Conductivity, Adv. Funct. Mater. 28 (2018) 1702758, https://doi.org/10.1002/adfm.201702758.
[134] R. Souzy, B. Ameduri, Functional fluoropolymers for fuel cell membranes, Prog. Polym. Sci. 30 (2005) 644–687, https://doi.org/10.1016/j.progpolymsci.2005.03.004.
[135] R. Amen, A. Ibrahim, W. Shafqat, E.B. Hassan, A Critical Review on PFAS Removal from Water: Removal Mechanism and Future Challenges, Sustainability 15 (2023) 16173, https://doi.org/10.3390/su152316173.
[136] L.-Y. Zhu, Y.-C. Li, J. Liu, J. He, L.-Y. Wang, J.-D. Lei, Recent developments in high-performance Nafion membranes for hydrogen fuel cells applications, Pet. Sci. 19 (2022) 1371–1381, https://doi.org/10.1016/j.petsci.2021.11.004.
[137] M.B. Karimi, F. Mohammadi, K. Hooshyari, Recent approaches to improve Nafion performance for fuel cell applications: A review, Int. J. Hydrogen Energy 44 (2019) 28919–28938, https://doi.org/10.1016/j.ijhydene.2019.09.096.
[138] C. Yin, Z. Wang, Y. Luo, J. Li, Y. Zhou, X. Zhang, H. Zhang, P. Fang, C. He, Thermal annealing on free volumes, crystallinity and proton conductivity of Nafion membranes, J. Phys. Chem. Solids 120 (2018) 71–78, https://doi.org/10.1016/j.jpcs.2018.04.028.
[139] J.E. Hensley, J.D. Way, S.F. Dec, K.D. Abney, The effects of thermal annealing on commercial Nafion® membranes, J. Membr. Sci. 298 (2007) 190–201, https://doi.org/10.1016/j.memsci.2007.04.019.
[140] D. DeBonis, M. Mayer, A. Omosebi, R.S. Besser, Analysis of mechanism of Nafion® conductivity change due to hot pressing treatment, Renew. Energy 89 (2016) 200–206, https://doi.org/10.1016/j.renene.2015.11.081.
[141] B. Jiang, L. Yu, L. Wu, Mu. Di, J. Le Liu, X.Q. Xi, Insights into the Impact of the Nafion Membrane Pretreatment Process on Vanadium Flow Battery Performance, ACS Appl, Mater. Interfaces 8 (2016) 12228–12238, https://doi.org/10.1021/acsami.6b03529.
[142] R. Kuwertz, C. Kirstein, T. Turek, U. Kunz, Influence of acid pretreatment on ionic conductivity of Nafion® membranes, J. Membr. Sci. 500 (2016) 225–235, https://doi.org/10.1016/j.memsci.2015.11.022.
[143] L. Li, L. Su, Y. Zhang, Enhanced performance of supercritical CO2 treated Nafion 212 membranes for direct methanol fuel cells, Int. J. Hydrogen Energy 37 (2012) 4439–4447, https://doi.org/10.1016/j.ijhydene.2011.11.110.
[144] H.-L. Lin, T.L. Yu, F.-H. Han, A Method for Improving Ionic Conductivity of Nafion Membranes and its Application to PEMFC, J. Polym. Res. 13 (2006) 379–385, https://doi.org/10.1007/s10965-006-9055-9.
[145] C. Yin, J. Li, Y. Zhou, H. Zhang, P. Fang, C. He, Phase Separation and Development of Proton Transport Pathways in Metal Oxide Nanoparticle/Nafion Composite Membranes during Water Uptake, J. Phys. Chem. C Nanomater. Interfaces 122 (2018) 9710–9717, https://doi.org/10.1021/acs.jpcc.8b02535.
[146] L.G. Boutsika, A. Enotiadis, I. Nicotera, C. Simari, G. Charalambopoulou, E. P. Giannelis, T. Steriotis, Nafion® nanocomposite membranes with enhanced properties at high temperature and low humidity environments, Int. J. Hydrogen Energy 41 (2016) 22406–22414, https://doi.org/10.1016/j.ijhydene.2016.08.142.
[147] Y. Li, H. Wu, Y. Yin, L. Cao, X. He, B. Shi, J. Li, M. Xu, Z. Jiang, Fabrication of Nafion/zwitterion-functionalized covalent organic framework composite membranes with improved proton conductivity, J. Membr. Sci. 568 (2018) 1–9, https://doi.org/10.1016/j.memsci.2018.09.050.
[148] P. Trogadas, J. Parrondo, V. Ramani, CeO_2 surface oxygen vacancy concentration governs in situ free radical scavenging efficacy in polymer electrolytes, ACS Appl. Mater. Interfaces 4 (2012) 5098–5102, https://doi.org/10.1021/am3016069.
[149] C.I. Morfopoulou, A.K. Andreopoulou, M.K. Daletou, S.G. Neophytides, J. K. Kallitsis, Cross-linked high temperature polymer electrolytes through oxadiazole bond formation and their applications in HT PEMfuel cells, J. Mater. Chem. A 1 (2013) 1613–1622, https://doi.org/10.1039/C2TA00610C.
[150] B. Liu, W. Hu, G.P. Robertson, M.D. Guiver, Poly(aryl ether ketone)s with carboxylic acid groups: synthesis, sulfonation and crosslinking, J. Mater. Chem. 18 (2008) 4675, https://doi.org/10.1039/b806690f.
[151] C. Wang, S. Young Lee, D. Won Shin, N. Rae Kang, Y.M. Lee, M.D. Guiver, Proton-conducting membranes from poly(ether sulfone)s grafted with sulfoalkylamine, J. Membr. Sci. 427 (2013) 443–450, https://doi.org/10.1016/j.memsci.2012.09.040.
[152] D.W. Shin, S.Y. Lee, C.H. Lee, K.-S. Lee, C.H. Park, J.E. McGrath, M. Zhang, R. B. Moore, M.D. Lingwood, L.A. Madsen, Y.T. Kim, I. Hwang, Y.M. Lee, Sulfonated Poly(arylene sulfide sulfone nitrile) Multiblock Copolymers with Ordered Morphology for Proton Exchange Membranes, Macromolecules 46 (2013) 7797–7804, https://doi.org/10.1021/ma400889t.
[153] M. Adamski, T.J. Skalski, E.M. Schibli, M. Killer, Y. Wu, N. Peressin, B.J. Frisken, S. Holdcroft, Molecular branching as a simple approach to improving polymer electrolyte membranes, J. Membr. Sci. 595 (2020) 117539, https://doi.org/10.1016/j.memsci.2019.117539.
[154] N. Li, D.S. Hwang, S.Y. Lee, Y.-L. Liu, Y.M. Lee, M.D. Guiver, Densely Sulfophenylated Segmented Copoly(arylene ether sulfone) Proton Exchange Membranes, Macromolecules 44 (2011) 4901–4910, https://doi.org/10.1021/ma200937w.
[155] E.B. Trigg, T.W. Gaines, M. Maréchal, D.E. Moed, P. Rannou, K.B. Wagener, M. J. Stevens, K.I. Winey, Self-assembled highly ordered acid layers in precisely sulfonated polyethylene produce efficient proton transport, Nat. Mater. 17 (2018) 725–731, https://doi.org/10.1038/s41563-018-0097-2.
[156] K. Umezawa, T. Oshima, M. Yoshizawa-Fujita, Y. Takeoka, M. Rikukawa, Synthesis of Hydrophilic-Hydrophobic Block Copolymer Ionomers Based on Polyphenylenes, ACS Macro Lett. 1 (2012) 969–972, https://doi.org/10.1021/mz300290x.
[157] B. Motealleh, F. Huang, T.D. Largier, W. Khan, C.J. Cornelius, Solution-blended sulfonated polyphenylene and branched poly(arylene ether sulfone): Synthesis, state of water, surface energy, proton transport, and fuel cell performance, Polymer 160 (2019) 148–161, https://doi.org/10.1016/j.polymer.2018.11.045.
[158] V.P. Greben, N.Y. Pivovarov, N.Y. Kovarskii, G.V. Nefedova, Russ. J. Phys. Chem. A (1978) 2641–2645.
[159] R. Simons, Strong electric field effects on proton transfer between membrane-bound amines and water, Nature 280 (1979) 824–826, https://doi.org/10.1038/280824a0.
[160] J.X. Di Zhao, Y. Sun, M. Li, G. Zhong, X. Hu, J. Sun, X. Li, H. Su, M. Li, Z. Zhang, Y. Zhang, L. Zhao, C. Zheng, X. Sun, Composition and Structure Progress of the Catalytic Interface Layer for Bipolar Membrane, Nanomaterials (basel) 12 (2022), https://doi.org/10.3390/nano12162874.
[161] Y. Xue, T. Xu, R. Fu, Y. Cheng, W. Yang, Catalytic water dissociation using hyperbranched aliphatic polyester (Boltorn series) as the interface of a bipolar membrane, J. Colloid Interface Sci. 316 (2007) 604–611, https://doi.org/10.1016/j.jcis.2007.08.052.
[162] N.H. Rathod, S. Mishra, S. Mishra, P. Upadhyay, L. Fan, V. Jegatheesan, V. Kulshrestha, Fabrication of efficient bipolar membranes with functionalized MOF interfacial layer for generation of various carboxylic acids via electrodialysis, Chem. Eng. J. 477 (2023) 146765, https://doi.org/10.1016/j.cej.2023.146765.
[163] R.J. Martínez, J. Farrell, Water splitting activity of oxygen-containing groups in graphene oxide catalyst in bipolar membranes, Comput. Theor. Chem. 1164 (2019) 112556, https://doi.org/10.1016/j.comptc.2019.112556.
[164] J. Ran, L. Wu, Y. He, Z. Yang, Y. Wang, C. Jiang, L. Ge, E. Bakangura, T. Xu, Ion exchange membranes: New developments and applications, J. Membr. Sci. 522 (2017) 267–291, https://doi.org/10.1016/j.memsci.2016.09.033.
[165] D. Henkensmeier, M. Najibah, C. Harms, J. Žitka, J. Hnát, K. Bouzek, Overview: State-of-the Art Commercial Membranes for Anion Exchange Membrane Water Electrolysis, J. Electrochem. Energy Convers. Storage 18 (2021) 024001, https://doi.org/10.1115/1.4047963.
[166] S. Favero, I.E.L. Stephens, M.-M. Titirci, Anion Exchange Ionomers: Design Considerations and Recent Advances - An Electrochemical Perspective, Adv. Mater. 36 (2024) e2308238.
[167] W. Ng, W. Wong, N. Rosli, K. Loh, Commercial Anion Exchange Membranes (AEMs) for Fuel Cell and Water Electrolyzer Applications: Performance, Durability, and Materials Advancement, Separations 10 (2023) 424, https://doi.org/10.3390/separations10080424.
[168] J.-M. Arana Juve, F.M.S. Christensen, Y. Wang, Z. Wei, Electrodialysis for metal removal and recovery: A review, Chem. Eng. J. 435 (2022) 134857, https://doi.org/10.1016/j.cej.2022.134857.
[169] M. Irfan, T. Xu, L. Ge, Y. Wang, T. Xu, Zwitterion structure membrane provides high monovalent/divalent cation electrodialysis selectivity: Investigating the effect of functional groups and operating parameters, J. Membr. Sci. 588 (2019) 117211, https://doi.org/10.1016/j.memsci.2019.117211.
[170] T. Mubita, S. Porada, P. Aerts, A. van der Wal, Heterogeneous anion exchange membranes with nitrate selectivity and low electrical resistance, J. Membr. Sci. 607 (2020) 118000, https://doi.org/10.1016/j.memsci.2020.118000.
[171] R. Cui, Z. Zhang, Y. Wang, F. Liu, H. Wang, C. Bi, C. Yu, Y. Zhou, Effect of cations (Na+, Co2+, Fe3+) contamination in Nafion membrane: A molecular simulations study, Int. J. Hydrogen Energy 50 (2024) 635–649, https://doi.org/10.1016/j.ijhydene.2023.09.295.
[172] M.C. Martí-Calatayud, D.C. Buzzi, M. García-Gabaldón, A.M. Bernardes, J. Tenório, V. Pérez-Herranz, Ion transport through homogeneous and heterogeneous ion-exchange membranes in single salt and multicomponent electrolyte solutions, J. Membr. Sci. 466 (2014) 45–57, https://doi.org/10.1016/j.memsci.2014.04.033.
[173] E.D. Belashova, N.A. Melnik, N.D. Pismenskaya, K.A. Shevtsova, A.V. Nebavsky, K.A. Lebedev, V.V. Nikonenko, Overlimiting mass transfer through cation-exchange membranes modified by Nafion film and carbon nanotubes, Electrochim. Acta 59 (2012) 412–423, https://doi.org/10.1016/j.electacta.2011.10.077.
[174] E. Volodina, N. Pismenskaya, V. Nikonenko, C. Larchet, G. Pourcelly, Ion transfer across ion-exchange membranes with homogeneous and heterogeneous surfaces, J. Colloid Interface Sci. 285 (2005) 247–258, https://doi.org/10.1016/j.jcis.2004.11.017.
[175] X. Zhou, Z. Wang, R. Epsztein, C. Zhan, W. Li, J.D. Fortner, T.A. Pham, J.-H. Kim, M. Elimelech, Intrapore energy barriers govern ion transport and selectivity of desalination membranes, Sci. Adv. 6 (2020), https://doi.org/10.1126/sciadv.abd9045.
[176] T. Belloň, Z. Slouka, Overlimiting behavior of surface-modified heterogeneous anion-exchange membranes, J. Membr. Sci. 610 (2020) 118291, https://doi.org/10.1016/j.memsci.2020.118291.
[177] A.A. Elozeiri, R.G. Lammertink, H.H. Rijnaarts, J.E. Dykstra, Water content of ion-exchange membranes: Measurement technique and influence on the ion mobility, J. Membr. Sci. 698 (2024) 122538, https://doi.org/10.1016/j.memsci.2024.122538.

[178] Z.-Q. Wu, C.-Y. Li, X.-L. Ding, Z.-Q. Li, X.-H. Xia, Synergistic Effect of Electrostatic Interaction and Ionic Dehydration on Asymmetric Ion Transport in Nanochannel/Ion Channel Composite Membrane, J. Phys. Chem. Lett. (2022) 5267–5274, https://doi.org/10.1021/acs.jpclett.2c01166.
[179] K.-D. Kreuer, A. Münchinger, Fast and Selective Ionic Transport: From Ion-Conducting Channels to Ion Exchange Membranes for Flow Batteries, Annu. Rev. Mater. Res. 51 (2021) 21–46, https://doi.org/10.1146/annurev-matsci-080619-010139.
[180] S.-Y. Sun, X.-Y. Nie, J. Huang, J.-G. Yu, Molecular simulation of diffusion behavior of counterions within polyelectrolyte membranes used in electrodialysis, J. Membr. Sci. 595 (2020) 117528, https://doi.org/10.1016/j.memsci.2019.117528.
[181] W. Wang, Y. Zhang, M. Tan, C. Xue, W. Zhou, H. Bao, C. Hon Lau, X. Yang, J. Ma, L. Shao, Recent advances in monovalent ion selective membranes towards environmental remediation and energy harvesting, Sep. Purif. Technol. 297 (2022) 121520, https://doi.org/10.1016/j.seppur.2022.121520.
[182] S.M. Hosseini, M.M.B. Usefi, M. Habibi, F. Parvizian, B. van der Bruggen, A. Ahmadi, M. Nemati, Fabrication of mixed matrix anion exchange membrane decorated with polyaniline nanoparticles to chloride and sulfate ions removal from water, Ionics 25 (2019) 6135–6145, https://doi.org/10.1007/s11581-019-03151-w.
[183] R.K. Nagarale, G.S. Gohil, V.K. Shahi, Recent developments on ion-exchange membranes and electro-membrane processes, Adv. Colloid Interface Sci. 119 (2006) 97–130, https://doi.org/10.1016/j.cis.2005.09.005.
[184] J.A. Kerres, Blended and Cross-Linked Ionomer Membranes for Application in Membrane Fuel Cells, Fuel Cells 5 (2005) 230–247, https://doi.org/10.1002/fuce.200400079.
[185] A.R. Khodabakhshi, S.S. Madaeni, T.W. Xu, L. Wu, C. Wu, C. Li, W. Na, S. A. Zolanvari, A. Babayi, J. Ghasemi, S.M. Hosseini, A. Khaledi, Preparation, optimization and characterization of novel ion exchange membranes by blending of chemically modified PVDF and SPPO, Sep. Purif. Technol. 90 (2012) 10–21, https://doi.org/10.1016/j.seppur.2012.02.006.
[186] S.H. Kim, K.H. Lee, J.Y. Chu, A.R. Kim, D.J. Yoo, Enhanced Hydroxide Conductivity and Dimensional Stability with Blended Membranes Containing Hyperbranched PAES/Linear PPO as Anion Exchange Membranes, Polymers (basel) 12 (2020), https://doi.org/10.3390/polym12123011.
[187] M.-S. Kang, J.H. Kim, J. Won, S.-H. Moon, Y.S. Kang, Highly charged proton exchange membranes prepared by using water soluble polymer blends for fuel cells, J. Membr. Sci. 247 (2005) 127–135, https://doi.org/10.1016/j.memsci.2004.09.017.
[188] Z. Li, B. Zhang, L. Qu, J. Ren, Y. Li, A novel atmospheric dielectric barrier discharge (DBD) plasma graft-filling technique to fabricate the composite membranes for pervaporation of aromatic/aliphatic hydrocarbons, J. Membr. Sci. 371 (2011) 163–170, https://doi.org/10.1016/j.memsci.2011.01.035.
[189] D.S. Hwang, T.A. Sherazi, J.Y. Sohn, Y.C. Noh, C.H. Park, M.D. Guiver, Y.M. Lee, Anisotropic radio-chemically pore-filled anion exchange membranes for solid alkaline fuel cell (SAFC), J. Membr. Sci. 495 (2015) 206–215, https://doi.org/10.1016/j.memsci.2015.07.067.
[190] C. Agarwal, R.W. Cattrall, S.D. Kolev, Donnan dialysis based separation of gold (III) from electronic waste solutions using an anion exchange pore-filled membrane, J. Membr. Sci. 514 (2016) 210–216, https://doi.org/10.1016/j.memsci.2016.04.033.
[191] K. Kim, S.-K. Kim, J.O. Park, S.-W. Choi, K.-H. Kim, T. Ko, C. Pak, J.-C. Lee, Highly reinforced pore-filling membranes based on sulfonated poly(arylene ether sulfone)s for high-temperature/low-humidity polymer electrolyte membrane fuel cells, J. Membr. Sci. 537 (2017) 11–21, https://doi.org/10.1016/j.memsci.2017.05.014.
[192] R. Gloukhovski, V. Freger, Y. Tsur, Understanding methods of preparation and characterization of pore-filling polymer composites for proton exchange membranes: a beginner's guide, Rev. Chem. Eng. 34 (2018) 455–479, https://doi.org/10.1515/revce-2016-0065.
[193] J. Choi, S. Yang, N.-J. Jeong, H. Kim, W.-S. Kim, Fabrication of an Anion-Exchange Membrane by Pore-Filling Using Catechol-1,4-Diazabicyclo-2,2,2octane Coating and Its Application to Reverse Electrodialysis, Langmuir 34 (2018) 10837–10846, https://doi.org/10.1021/acs.langmuir.8b01666.
[194] R. Guan, H. Dai, C. Li, J. Liu, J. Xu, Effect of casting solvent on the morphology and performance of sulfonated polyethersulfone membranes, J. Membr. Sci. 277 (2006) 148–156, https://doi.org/10.1016/j.memsci.2005.10.025.
[195] T. Xu, J.-J. Woo, S.-J. Seo, S.-H. Moon, In situ polymerization: A novel route for thermally stable proton-conductive membranes, J. Membr. Sci. 325 (2008) 209–216, https://doi.org/10.1016/j.memsci.2008.07.036.
[196] J.B. Arul Joseph Helen Therese, K. Selvakumar, R. Gayathri, M. Ramesh Prabhu, P. Sivakumar, In situ polymerization of poly aniline—SPEEK-PMA-based proton exchange membrane for DMFC application, J. Thermoplast. Compos. Mater. 34 (2021) 221–237, https://doi.org/10.1177/0892705719835293.
[197] G. Zheng, J. Jiang, X. Wang, W. Li, J. Liu, G. Fu, L. Lin, Nanofiber membranes by multi-jet electrospinning arranged as arc-array with sheath gas for electrodialysis applications, Mater. Des. 189 (2020) 108504, https://doi.org/10.1016/j.matdes.2020.108504.
[198] B. Swanckaert, J. Geltmeyer, K. Rabaey, K. de Buysser, L. Bonin, K. de Clerck, A review on ion-exchange nanofiber membranes: properties, structure and application in electrochemical (waste)water treatment, Sep. Purif. Technol. 287 (2022) 120529, https://doi.org/10.1016/j.seppur.2022.120529.
[199] Z. Shang, R. Wycisk, P. Pintauro, Electrospun Composite Proton-Exchange and Anion-Exchange Membranes for Fuel Cells, Energies 14 (2021) 6709, https://doi.org/10.3390/en14206709.
[200] B. Dong, L. Gwee, D. La Salas-de Cruz, K.I. Winey, Y.A. Elabd, Super proton conductive high-purity nafion nanofibers, Nano Lett. 10 (2010) 3785–3790, https://doi.org/10.1021/nl102581w.
[201] J.A. Reyes-Aguilera, L. Villafaña-López, E.C. Rentería-Martínez, S.M. Anderson, J. S. Jaime-Ferrer, Electrospinning of Polyepychlorhydrin and Polyacrylonitrile Anionic Exchange Membranes for Reverse Electrodialysis, Membranes (basel) 11 (2021), https://doi.org/10.3390/membranes11090717.
[202] A.M. Samsudin, M. Roschger, S. Wolf, V. Hacker, Preparation and Characterization of QPVA/PDDA Electrospun Nanofiber Anion Exchange Membranes for Alkaline Fuel Cells, Nanomaterials (basel) 12 (2022), https://doi.org/10.3390/nano12223965.
[203] M. Najibah, E. Tsoy, H. Khalid, Y. Chen, Q. Li, C. Bae, J. Hnát, M. Plevová, K. Bouzek, J.H. Jang, H.S. Park, D. Henkensmeier, PBI nanofiber mat-reinforced anion exchange membranes with covalently linked interfaces for use in water electrolysers, J. Membr. Sci. 640 (2021) 119832, https://doi.org/10.1016/j.memsci.2021.119832.
[204] C. Li, H. Wang, X. Zhao, K. Yang, Q. Meng, L. Zhang, Fabrication of Unidirectional Water Permeable PS/PET Composite Nanofibers Modified with Silver Nanoparticles via Electrospinning, Membranes (basel) 13 (2023), https://doi.org/10.3390/membranes13030257.
[205] P. Kumar, R.P. Bharti, V. Kumar, P.P. Kundu, Chapter 4 - Polymer Electrolyte Membranes for Microbial Fuel Cells: Part A. Nafion-Based Membranes, https://doi.org/10.1016/B978-0-444-64017-8.00004-X, in: P.P. Kundu, K. Dutta (Eds.), Progress and recent trends in microbial fuel cells, Elsevier, Amsterdam Netherlands, Cambridge MA, 2018, ISBN: 978-0-444-64017-8, pp. 47–72.
[206] T.M. Lim, M. Ulaganathan, Q. Yan, Chapter 14 - Advances in membrane and stack design of redox flow batteries (RFBs) for medium- and large-scale energy storage, in: C. Menictas, M. Skyllas-Kazacos, T.M. Lim (Eds.), Advances in Batteries for Medium- and Large-Scale Energy Storage, Elsevier Woodhead Publishing, Cambridge, UK, Waltham, MA, USA, 2015, pp. 477–507, https://doi.org/10.1016/B978-1-78242-013-2.00014-5. ISBN: 978-1-78242-013-2.
[207] N. Kononenko, V. Nikonenko, D. Grande, C. Larchet, L. Dammak, M. Fomenko, Y. Volfkovich, Porous structure of ion exchange membranes investigated by various techniques, Adv. Colloid Interface Sci. 246 (2017) 196–216, https://doi.org/10.1016/j.cis.2017.05.007.
[208] N. Pismenskaya, V. Sarapulova, E. Nevakshenova, N. Kononenko, M. Fomenko, V. Nikonenko, Concentration Dependencies of Diffusion Permeability of Anion-Exchange Membranes in Sodium Hydrogen Carbonate, Monosodium Phosphate, and Potassium Hydrogen Tartrate Solutions, Membranes (basel) 9 (2019), https://doi.org/10.3390/membranes9120170.
[209] A.E. Kozmai, V.V. Nikonenko, S. Zyryanova, N.D. Pismenskaya, L. Dammak, L. Baklouti, Modelling of anion-exchange membrane transport properties with taking into account the change in exchange capacity and swelling when varying bathing solution concentration and pH, J. Membr. Sci. 590 (2019) 117291, https://doi.org/10.1016/j.memsci.2019.117291.
[210] A. Lehmani, P. Turq, M. Périé, J. Périé, J.-P. Simonin, Ion transport in Nafion® 117 membrane, J. Electroanal. Chem. 428 (1997) 81–89, https://doi.org/10.1016/S0022-0728(96)05060-7.
[211] L. Giorno, E. Drioli, H. Strathmann, Ion-Exchange Membrane Characterization, in: L.G. Enrico Drioli (Ed.), Encyclopedia of Membranes, Springer, Berlin Heidelberg, Heidelberg, 2016, pp. 1052–1056, https://doi.org/10.1007/978-3-662-44324-8_994. ISBN: 978-3-662-44323-1.
[212] A. Kozmai, V. Sarapulova, M. Sharafan, K. Melkonian, T. Rusinova, Y. Kozmai, N. Pismenskaya, L. Dammak, V. Nikonenko, Electrochemical Impedance Spectroscopy of Anion-Exchange Membrane AMX-Sb Fouled by Red Wine Components, Membranes (basel) 11 (2020), https://doi.org/10.3390/membranes11010002.
[213] Y. Zhao, L. Duan, Research on Measuring Pure Membrane Electrical Resistance under the Effects of Salinity Gradients and Diffusion Boundary Layer and Double Layer Resistances, Membranes (basel) 12 (2022), https://doi.org/10.3390/membranes12080816.
[214] A.H. Galama, N.A. Hoog, D.R. Yntema, Method for determining ion exchange membrane resistance for electrodialysis systems, Desalination 380 (2016) 1–11, https://doi.org/10.1016/j.desal.2015.11.018.
[215] H. Strathmann, Introduction to membrane science and technology, Wiley-VCH, Weinheim, 2011.
[216] X. Chen, B. Rajendran, Q.-M. Liu, X.-Q. Feng, K.B. Goh, Divalent ion partitioning through dense ion exchange membranes, J. Membr. Sci. 687 (2023) 122077, https://doi.org/10.1016/j.memsci.2023.122077.
[217] K. Solonchenko, A. Kirichenko, K. Kirichenko, Stability of Ion Exchange Membranes in Electrodialysis, Membranes (basel) 13 (2022), https://doi.org/10.3390/membranes13010052.
[218] N. Pismenskaya, M. Bdiri, V. Sarapulova, A. Kozmai, J. Fouilloux, L. Baklouti, C. Larchet, E. Renard, L. Dammak, A Review on Ion-Exchange Membranes Fouling during Electrodialysis Process in Food Industry, Part 2: Influence on Transport Properties and Electrochemical Characteristics, Cleaning and Its Consequences, Membranes (basel) 11 (2021), https://doi.org/10.3390/membranes11110811.
[219] M. Akter, J.-S. Park, Fouling and Mitigation Behavior of Foulants on Ion Exchange Membranes with Surface Property in Reverse Electrodialysis, Membranes (basel) 13 (2023), https://doi.org/10.3390/membranes13010106.
[220] B. de Jaegher, E. Larumbe, W. de Schepper, A. Verliefde, I. Nopens, Colloidal fouling in electrodialysis: A neural differential equations model, Sep. Purif. Technol. 249 (2020) 116939, https://doi.org/10.1016/j.seppur.2020.116939.
[221] G. Grossman, A.A. Sonin, Membrane fouling in electrodialysis: a model and experiments, Desalination 12 (1973) 107–125, https://doi.org/10.1016/S0011-9164(00)80178-2.

[222] D.Y. Butylskii, V.A. Troitskiy, M.A. Ponomar, I.A. Moroz, K.G. Sabbatovskiy, M. V. Sharafan, Efficient Anion-Exchange Membranes with Anti-Scaling Properties Obtained by Surface Modification of Commercial Membranes Using a Polyquaternium-22, Membranes (basel) 12 (2022), https://doi.org/10.3390/membranes12111065.
[223] D.Y. Butylskii, V.A. Troitskiy, M.V. Sharafan, N.D. Pismenskaya, V.V. Nikonenko, Scaling-resistant anion-exchange membrane prepared by in situ modification with a bifunctional polymer containing quaternary amino groups, Desalination 537 (2022) 115821, https://doi.org/10.1016/j.desal.2022.115821.
[224] W. Xiang, J. Yao, S. Velizarov, Le Han, Unravelling the fouling behavior of anion-exchange membrane (AEM) by organic solute of varying characteristics, J. Membr. Sci. 662 (2022) 120986, https://doi.org/10.1016/j.memsci.2022.120986.
[225] Y.W. Berkessa, Q. Lang, B. Yan, S. Kuang, D. Mao, L. Shu, Y. Zhang, Anion exchange membrane organic fouling and mitigation in salt valorization process from high salinity textile wastewater by bipolar membrane electrodialysis, Desalination 465 (2019) 94–103, https://doi.org/10.1016/j.desal.2019.04.027.
[226] M. Persico, S. Mikhaylin, A. Doyen, L. Firdaous, V. Nikonenko, N. Pismenskaya, L. Bazinet, Prevention of peptide fouling on ion-exchange membranes during electrodialysis in overlimiting conditions, J. Membr. Sci. 543 (2017) 212–221, https://doi.org/10.1016/j.memsci.2017.08.039.
[227] E.N. Nielsen, U. Cordin, M. Gøtke, S. Velizarov, C.F. Galinha, L.H. Skibsted, J. G. Crespo, L.M. Ahrné, Fouling of ion-exchange membranes during electrodialytic acid whey processing analysed by 2D fluorescence and FTIR spectroscopy, Sep. Purif. Technol. 316 (2023) 123814, https://doi.org/10.1016/j.seppur.2023.123814.
[228] S. Mikhaylin, L. Bazinet, Fouling on ion-exchange membranes: Classification, characterization and strategies of prevention and control, Adv. Colloid Interface Sci. 229 (2016) 34–56, https://doi.org/10.1016/j.cis.2015.12.006.
[229] J.R. Varcoe, P. Atanassov, D.R. Dekel, A.M. Herring, M.A. Hickner, P.A. Kohl, A. R. Kucernak, W.E. Mustain, K. Nijmeijer, K. Scott, T. Xu, L. Zhuang, Anion-exchange membranes in electrochemical energy systems, Energy Environ. Sci. 7 (2014) 3135–3191, https://doi.org/10.1039/C4EE01303D.
[230] Z. Sun, J. Pan, J. Guo, F. Yan, The Alkaline Stability of Anion Exchange Membrane for Fuel Cell Applications: The Effects of Alkaline Media, Adv. Sci. 5 (2018) 1800065, https://doi.org/10.1002/advs.201800065.
[231] K.F.L. Hagesteijn, S. Jiang, B.P. Ladewig, A review of the synthesis and characterization of anion exchange membranes, J Mater Sci 53 (2018) 11131–11150, https://doi.org/10.1007/s10853-018-2409-y.
[232] Z. Sun, B. Lin, F. Yan, Anion-Exchange Membranes for Alkaline Fuel-Cell Applications: The Effects of Cations, ChemSusChem 11 (2018) 58–70, https://doi.org/10.1002/cssc.201701600.
[233] C.G. Arges, Le Zhang, Anion Exchange Membranes' Evolution toward High Hydroxide Ion Conductivity and Alkaline Resiliency, ACS Appl. Energy Mater. 1 (2018) 2991–3012, https://doi.org/10.1021/acsaem.8b00387.
[234] J.R. Varcoe, R.C.T. Slade, Prospects for Alkaline Anion-Exchange Membranes in Low Temperature Fuel Cells, Fuel Cells 5 (2005) 187–200, https://doi.org/10.1002/fuce.200400045.
[235] J. Ying, Y. Lin, Y. Zhang, Y. Jin, X. Li, Q. She, H. Matsuyama, J. Yu, Mechanistic insights into the degradation of monovalent selective ion exchange membrane towards long-term application of real salt lake brines, J. Membr. Sci. 652 (2022) 120446, https://doi.org/10.1016/j.memsci.2022.120446.
[236] O.A. Rybalkina, K.A. Tsygurina, V.V. Sarapulova, S.A. Mareev, V.V. Nikonenko, N.D. Pismenskaya, Evolution of Current-Voltage Characteristics and Surface Morphology of Homogeneous Anion-Exchange Membranes during the Electrodialysis Desalination of Alkali Metal Salt Solutions, Membr, Membr. Technol. 1 (2019) 107–119, https://doi.org/10.1134/S2517751619020094.
[237] L.B. Railsback, Some Fundamentals of Mineralogy and Geochemistry: Variation in hydrated radius of ions, 2006. https://railsback.org/FundamentalsIndex.html (accessed 14 February 2024).
[238] X. Guo, L. Xiang, M. Sun, S. Wang, Z. Ji, J. Bi, Y. Zhao, Selective electrodialysis process for the recovery of potassium from multicomponent solution systems, Water Sci. Technol. 88 (2023) 1317–1331, https://doi.org/10.2166/wst.2023.269.
[239] Y. Liu, X. Wu, X. Wu, L. Dai, J. Ding, X. Ye, R. Chen, R. Ding, J. Liu, Y. Jin, B. van der Bruggen, Recovery of nickel, phosphorus and nitrogen from electroless nickel-plating wastewater using bipolar membrane electrodialysis, J. Clean. Prod. 382 (2023) 135326, https://doi.org/10.1016/j.jclepro.2022.135326.
[240] Z. Peng, Y. Li, Y. Sun, Treatment of 2-Mercapto-5-methyl-1,3,4-thiadiazole (MMTD) wastewater by bipolar membrane electrodialysis: MMTD migration, process factors and implications, J. Membr. Sci. 664 (2022) 121110, https://doi.org/10.1016/j.memsci.2022.121110.
[241] X. Lin, J. Pan, M. Zhou, Y. Xu, J. Lin, J. Shen, C. Gao, B. van der Bruggen, Extraction of Amphoteric Amino Acid by Bipolar Membrane Electrodialysis: Methionine Acid as a Case Study, Ind. Eng. Chem. Res. 55 (2016) 2813–2820, https://doi.org/10.1021/acs.iecr.6b00116.
[242] G.J. Doornbusch, M. Tedesco, J.W. Post, Z. Borneman, K. Nijmeijer, Experimental investigation of multistage electrodialysis for seawater desalination, Desalination 464 (2019) 105–114, https://doi.org/10.1016/j.desal.2019.04.025.
[243] J.P. Ibáñez, A. Vásquez, Á. Aracena, Valorisation of sulphate rich effluents by electrodialysis, Can. Metall. Q. (2023) 1–10, https://doi.org/10.1080/00084433.2023.2179713.
[244] M. Xu, S. Li, Z. Jin, W. Jiang, Y. Li, Mathematical model and experiment investigation on electrodialysis separation process of LiBr from NH3-H2O-LiBr ternary solution in ammonia absorption refrigeration system, Int. J. Refrig 158 (2024) 9–24, https://doi.org/10.1016/j.ijrefrig.2023.11.003.
[245] H. Wang, Y. Wang, J. Yan, R. Fu, B. Wang, C. Jiang, Y. Wang, T. Xu, Bipolar membrane electrodialysis: A promising paradigm for caustic soda production, AIChE J 70 (2024) e18260.
[246] S. Kırmızı, B. Karabacakoğlu, Performance of electrodialysis for Ni(II) and Cr(VI) removal from effluents: effect of process parameters on removal efficiency, energy consumption and current efficiency, J Appl Electrochem 53 (2023) 2039–2055, https://doi.org/10.1007/s10800-023-01894-z.
[247] A. Voutetaki, K.V. Plakas, A.I. Papadopoulos, D. Bollas, S. Parcharidis, P. Seferlis, Pilot-scale separation of lead and sulfate ions from aqueous solutions using electrodialysis: Application and parameter optimization for the battery industry, J. Clean. Prod. 410 (2023) 137200, https://doi.org/10.1016/j.jclepro.2023.137200.
[248] M. Sadrzadeh, T. Mohammadi, Sea water desalination using electrodialysis, Desalination 221 (2008) 440–447, https://doi.org/10.1016/j.desal.2007.01.103.
[249] V.M. Ortiz-Martínez, L. Gómez-Coma, C. Tristán, G. Pérez, M. Fallanza, A. Ortiz, R. Ibañez, I. Ortiz, A comprehensive study on the effects of operation variables on reverse electrodialysis performance, Desalination 482 (2020) 114389, https://doi.org/10.1016/j.desal.2020.114389.
[250] W. Gao, Q. Fang, H. Yan, X. Wei, K. Wu, Recovery of Acid and Base from Sodium Sulfate Containing Lithium Carbonate Using Bipolar Membrane Electrodialysis, Membranes (basel) 11 (2021), https://doi.org/10.3390/membranes11020152.
[251] Y. Zhou, H. Yan, X. Wang, Y. Wang, T. Xu, A closed loop production of water insoluble organic acid using bipolar membranes electrodialysis (BMED), J. Membr. Sci. 520 (2016) 345–353, https://doi.org/10.1016/j.memsci.2016.08.011.
[252] Y. Zhao, X. Wang, J. Yuan, Z. Ji, J. Liu, S. Wang, X. Guo, F. Li, J. Wang, J. Bi, An efficient electrodialysis metathesis route to recover concentrated NaOH-NH4Cl products from simulated ammonia and saline wastewater in coal chemical industry, Sep. Purif. Technol. 301 (2022) 122042, https://doi.org/10.1016/j.seppur.2022.122042.
[253] Y. Zhang, Y. Chen, M. Yue, L. Wang, Production of l -lysine from l -lysine monohydrochloride by bipolar membrane electrodialysis, Desalin. Water Treat. 41 (2012) 105–113, https://doi.org/10.1080/19443994.2012.664695.
[254] M. Adigüzel, J. Erkmen, M.T. Yilmaz, Application and optimization of bipolar membrane process for drinking water production from Black Sea, J. Clean. Prod. 408 (2023) 136814, https://doi.org/10.1016/j.jclepro.2023.136814.
[255] C.X. Lin, X.L. Huang, D. Guo, Q.G. Zhang, A.M. Zhu, M.L. Ye, Q.L. Liu, Side-chain-type anion exchange membranes bearing pendant quaternary ammonium groups via flexible spacers for fuel cells, J. Mater. Chem. A 4 (2016) 13938–13948, https://doi.org/10.1039/C6TA05090E.
[256] A.N. Filippov, E.M. Akberova, V.I. Vasil'eva, Study of the Thermochemical Effect on the Transport and Structural Characteristics of Heterogeneous Ion-Exchange Membranes by Combining the Cell Model and the Fine-Porous Membrane Model, Polymers (basel) 15 (2023), https://doi.org/10.3390/polym15163390.
[257] G. Das, J.-H. Choi, P.K.T. Nguyen, D.-J. Kim, Y.S. Yoon, Anion Exchange Membranes for Fuel Cell Application: A Review, Polymers (basel) 14 (2022), https://doi.org/10.3390/polym14061197.
[258] J. Surowiec, R. Bogoczek, Studies on the thermal stability of the perfluorinated cation-exchange membrane Nafion-417, J. Therm. Anal. 33 (1988) 1097–1102, https://doi.org/10.1007/bf01912735.
[259] W.D. Kuldeep, P. Badenhorst, H. Kauranen, R. Pajari, P. Ruismäki, L. Mannela, Murtomäki, Bipolar Membrane Electrodialysis for Sulfate Recycling in the Metallurgical Industries, Membranes (basel) 11 (2021) 718, https://doi.org/10.3390/membranes11090718.
[260] C. Li, G. Wang, H. Feng, T. He, Y. Wang, T. Xu, Cleaner production of Niacin using bipolar membranes electrodialysis (BMED), Sep. Purif. Technol. 156 (2015) 391–395, https://doi.org/10.1016/j.seppur.2015.10.027.
[261] H. Lu, L. Wang, R. Wycisk, P.N. Pintauro, S. Lin, Quantifying the kinetics-energetics performance tradeoff in bipolar membrane electrodialysis, J. Membr. Sci. 612 (2020) 118279, https://doi.org/10.1016/j.memsci.2020.118279.
[262] Y. Dong, H. Wei, H. Cui, H. Lu, J. Liao, Y. Qiu, J. Shen, Techno-Economic Analysis of Bipolar Membranes Electrodialysis for the Hexacyanocobalic Acid Green Conversion, Ind. Eng. Chem. Res. 62 (2023) 20996–21006, https://doi.org/10.1021/acs.iecr.3c02954.
[263] Y. Delgado, J. Llanos, F.J. Fernández-Morales, Coupling of electrodialysis and bio-electrochemical systems for metal and energy recovery from acid mine drainage, J of Chemical Tech & Biotech jctb.7317 (2023), https://doi.org/10.1002/jctb.7317.
[264] F.Z. Addar, I. Mohamed, S. Kitanou, M. Tahaikt, A. Elmidaoui, M. Taky, Performance of three anion-exchange membranes in fluoride ions removal by electrodialysis, Water Sci Technol 89 (2024) 132–145, https://doi.org/10.2166/wst.2023.423.
[265] P.-Y. Ji, Z.-Y. Ji, Q.-B. Chen, J. Liu, Y.-Y. Zhao, S.-Z. Wang, F. Li, J.-S. Yuan, Effect of coexisting ions on recovering lithium from high Mg2+/Li+ ratio brines by selective-electrodialysis, Sep. Purif. Technol. 207 (2018) 1–11, https://doi.org/10.1016/j.seppur.2018.06.012.
[266] S. Honarparvar, D. Reible, Modeling multicomponent ion transport to investigate selective ion removal in electrodialysis, Environ. Sci. Ecotechnol. 1 (2020) 100007, https://doi.org/10.1016/j.ese.2019.100007.
[267] D. Pintossi, C. Simões, M. Saakes, Z. Borneman, K. Nijmeijer, Predicting reverse electrodialysis performance in the presence of divalent ions for renewable energy generation, Energy Convers. Manag. 243 (2021) 114369, https://doi.org/10.1016/j.enconman.2021.114369.
[268] D. Jin, Y. Jin, Sustainable power generation from salinity gradients by reverse electrodialysis: Influence of divalent ions, Chem. Eng. Res. Des. 198 (2023) 69–80, https://doi.org/10.1016/j.cherd.2023.08.044.

[269] J. Yoon, M.T. Flavin, J. Han, Current efficiency and selectivity reduction caused by co-ion leakage in electromembrane processes, Water Res. 201 (2021) 117351, https://doi.org/10.1016/j.watres.2021.117351.
[270] J. Yan, H. Wang, H. Yan, R. Li, R. Fu, W. Fu, L. Ge, B. Wang, Y. Wang, T. Xu, Ion transmembrane behaviors in selective electrodialysis for acid recovery: Impact of ion categories, Desalination 554 (2023) 116513, https://doi.org/10.1016/j.desal.2023.116513.
[271] Q.-B. Chen, Y. Xu, P.-F. Li, J. Wang, L. Dong, J. Zhao, J. Wang, An emerging pilot-scale electrodialysis system for desalination of SWNF permeate: Evaluating the role of typical factors, Desalination 542 (2022) 116064, https://doi.org/10.1016/j.desal.2022.116064.
[272] A.T. Cherif, J. Molenat, A. Elmidaoui, Nitric acid and sodium hydroxide generation by electrodialysis using bipolar membranes, J Appl Electrochem 27 (1997) 1069–1074, https://doi.org/10.1023/A:1018438710451.
[273] C. Jiang, Q. Wang, Y. Li, Y. Wang, T. Xu, Water electro-transport with hydrated cations in electrodialysis, Desalination 365 (2015) 204–212, https://doi.org/10.1016/j.desal.2015.03.007.
[274] S. Porada, W.J. van Egmond, J.W. Post, M. Saakes, H. Hamelers, Tailoring ion exchange membranes to enable low osmotic water transport and energy efficient electrodialysis, J. Membr. Sci. 552 (2018) 22–30, https://doi.org/10.1016/j.memsci.2018.01.050.
[275] K. Haerens, P. de Vreese, E. Matthijs, L. Pinoy, K. Binnemans, B. van der Bruggen, Production of ionic liquids by electrodialysis, Sep. Purif. Technol. 97 (2012) 90–95, https://doi.org/10.1016/j.seppur.2012.02.017.
[276] L.-P. Ling, H.-F. Leow, M.R. Sarmidi, Citric acid concentration by electrodialysis: ion and water transport modelling, J. Membr. Sci. 199 (2002) 59–67, https://doi.org/10.1016/S0376-7388(01)00678-0.
[277] H. Liu, Q. She, Influence of membrane structure-dependent water transport on conductivity-permselectivity trade-off and salt/water selectivity in electrodialysis: Implications for osmotic electrodialysis using porous ion exchange membranes, J. Membr. Sci. 650 (2022) 120398, https://doi.org/10.1016/j.memsci.2022.120398.
[278] H. Strathmann (Ed.), Membrane Science and Technology Ion-Exchange Membrane Separation Processes, Elsevier, 2004.
[279] S. Le Han, H. Galier, Roux-de Balmann, Ion hydration number and electro-osmosis during electrodialysis of mixed salt solution, Desalination 373 (2015) 38–46, https://doi.org/10.1016/j.desal.2015.06.023.
[280] H. Jaroszek, A. Lis, P. Dydo, Transport of impurities and water during potassium nitrate synthesis by electrodialysis metathesis, Sep. Purif. Technol. 158 (2016) 87–93, https://doi.org/10.1016/j.seppur.2015.12.009.
[281] V.I. Zabolotskii, A.V. Demin, O.A. Demina, Ion and water transport during lithium chloride concentration from aqueous organic solutions by electrodialysis, Russ. J. Electrochem. 47 (2011) 327–335, https://doi.org/10.1134/S1023193511030153.
[282] H. Jaroszek, P. Dydo, Potassium nitrate synthesis by electrodialysis-metathesis: The effect of membrane type, J. Membr. Sci. 549 (2018) 28–37, https://doi.org/10.1016/j.memsci.2017.11.062.
[283] L. Yu, Q. Guo, J. Hao, W. Jiang, Recovery of acetic acid from dilute wastewater by means of bipolar membrane electrodialysis, Desalination 129 (2000) 283–288, https://doi.org/10.1016/S0011-9164(00)00068-0.
[284] M. Baldea, From process integration to process intensification, Comput. Chem. Eng. 81 (2015) 104–114, https://doi.org/10.1016/j.compchemeng.2015.03.011.
[285] A. Kovalenko, M. Urtenov, V. Chekanov, N. Kandaurova, Theoretical Analysis of the Influence of Spacers on Salt Ion Transport in Electromembrane Systems Considering the Main Coupled Effects, Membranes (basel) 14 (2024), https://doi.org/10.3390/membranes14010020.
[286] J. Choi, M. Cho, J. Shin, R. Kwak, B. Kim, Electroconvective instability at the surface of one-dimensionally patterned ion exchange membranes, J. Membr. Sci. 691 (2024) 122256, https://doi.org/10.1016/j.memsci.2023.122256.
[287] Y. Ibrahim, N. Hilal, A Critical Assessment of Surface-Patterned Membranes and Their Role in Advancing Membrane Technologies, ACS ES T Water 3 (2023) 3807–3834, https://doi.org/10.1021/acsestwater.3c00564.
[288] A. Campione, L. Gurreri, M. Ciofalo, G. Micale, A. Tamburini, A. Cipollina, Electrodialysis for water desalination: A critical assessment of recent developments on process fundamentals, models and applications, Desalination 434 (2018) 121–160, https://doi.org/10.1016/j.desal.2017.12.044.
[289] S.K.A. Al-Amshawee, M.Y. Bin Mohd Yunus, N.A. Binti Ismail, Y. Hafiz Zaki, Electrodialysis with Irregular Membrane Spacers: Which is the Right Choice? Chem. Eng. Technol. 46 (2023) 2453–2468, https://doi.org/10.1002/ceat.202200563.
[290] E. Sandoval-Sánchez, Z. de La Cruz-Barragán, M. Miranda-Hernández, E. Mendoza, Effect of Gaskets Geometry on the Performance of a Reverse Electrodialysis Cell, Energies (basel) 15 (2022) 3361, https://doi.org/10.3390/en15093361.
[291] L. Gurreri, A. Filingeri, M. Ciofalo, A. Cipollina, M. Tedesco, A. Tamburini, G. Micale, Electrodialysis with asymmetrically profiled membranes: Influence of profiles geometry on desalination performance and limiting current phenomena, Desalination 506 (2021) 115001, https://doi.org/10.1016/j.desal.2021.115001.
[292] F. Dong, D. Jin, S. Xu, L. Xu, X. Wu, P. Wang, Q. Leng, R. Xi, Numerical simulation of flow and mass transfer in profiled membrane channels for reverse electrodialysis, Chem. Eng. Res. Des. 157 (2020) 77–91, https://doi.org/10.1016/j.cherd.2020.02.025.
[293] J.G.D. Tadimeti, S. Chattopadhyay, Uninterrupted swirling motion facilitating ion transport in electrodialysis, Desalination 392 (2016) 54–62, https://doi.org/10.1016/j.desal.2016.04.007.
[294] E.P. Rivero, I.J. González-Panzo, A. Zavala-Vázquez, E. Rosado-Tamariz, R. Muñoz-Quezada, M.R. Díaz-Guillen, M.R. Cruz-Díaz, Analyzing the pressure drop in spacer stacks for electrodialytic processes considering the effect of mechanical compression: Experimental vs. free and porous flow model prediction, Chem. Eng. Sci. 282 (2023) 119297, https://doi.org/10.1016/j.ces.2023.119297.
[295] S. Mehdizadeh, M. Yasukawa, T. Abo, Y. Kakihana, M. Higa, Effect of spacer geometry on membrane and solution compartment resistances in reverse electrodialysis, J. Membr. Sci. 572 (2019) 271–280, https://doi.org/10.1016/j.memsci.2018.09.051.
[296] O. Kedem, Reduction of polarization in electrodialysis by ion-conducting spacers, Desalination 16 (1975) 105–118, https://doi.org/10.1016/S0011-9164(00)84095-3.
[297] O. Kedem, Y. Maoz, Ion conducting spacer for improved ed, Desalination 19 (1976) 465–470. https://doi.org/10.1016/S0011-9164(00)88055-8.
[298] P. Długołęcki, J. Dąbrowska, K. Nijmeijer, M. Wessling, Ion conductive spacers for increased power generation in reverse electrodialysis, J. Membr. Sci. 347 (2010) 101–107, https://doi.org/10.1016/j.memsci.2009.10.011.
[299] K. Zhang, M. Wang, C. Gao, Ion conductive spacers for the energy-saving production of the tartaric acid in bipolar membrane electrodialysis, J. Membr. Sci. 387–388 (2012) 48–53, https://doi.org/10.1016/j.memsci.2011.10.012.
[300] W. Lu, H. Dong, J. Xia, Y. Zheng, S. Lu, J.H. Barber, R.J. Macdonald, Ion conductive spacer, preparing process thereof and electrodialysis reversal stack, WO (2018).
[301] A. Chandra, D. Pathiwada, S. Chattopadhyay, COMSOL simulation and experimental validation of promoter geometries facilitating citric acid transport in electrodialysis, Chem. Eng. Res. Des. 142 (2019) 386–411, https://doi.org/10.1016/j.cherd.2018.12.024.
[302] P. Mandal, P. Goel, B.E.S. Chattopadhyay, Ion transport facilitation through template based optimization of corrugation geometry over membrane surface, J. Membr. Sci. 669 (2023) 121279, https://doi.org/10.1016/j.memsci.2022.121279.
[303] J.G.D. Tadimeti, V. Kurian, A. Chandra, S. Chattopadhyay, Corrugated membrane surfaces for effective ion transport in electrodialysis, J. Membr. Sci. 499 (2016) 418–428, https://doi.org/10.1016/j.memsci.2015.11.001.
[304] G. Eigenberger, H. Strathmann, A. Grabowskiy, Membrane assembly, electrodialysis device and method for continuous electrodialytic desalination, WO2005009596A1, 2005.
[305] H. Strathmann, Electrodialysis, a mature technology with a multitude of new applications, Desalination 264 (2010) 268–288, https://doi.org/10.1016/j.desal.2010.04.069.
[306] J. Liu, G.M. Geise, X. Luo, H. Hou, F. Zhang, Y. Feng, M.A. Hickner, B.E. Logan, Patterned ion exchange membranes for improved power production in microbial reverse-electrodialysis cells, J. Power Sources 271 (2014) 437–443, https://doi.org/10.1016/j.jpowsour.2014.08.026.
[307] S. Pawlowski, T. Rijnaarts, M. Saakes, K. Nijmeijer, J.G. Crespo, S. Velizarov, Improved fluid mixing and power density in reverse electrodialysis stacks with chevron-profiled membranes, J. Membr. Sci. 531 (2017) 111–121, https://doi.org/10.1016/j.memsci.2017.03.003.
[308] E. Güler, R. Elizen, M. Saakes, K. Nijmeijer, Micro-structured membranes for electricity generation by reverse electrodialysis, J. Membr. Sci. 458 (2014) 136–148, https://doi.org/10.1016/j.memsci.2014.01.060.
[309] L. Gurreri, A. Tamburini, A. Cipollina, G. Micale, CFD analysis of the fluid flow behavior in a reverse electrodialysis stack, Desalin. Water Treat. 48 (2012) 390–403, https://doi.org/10.1080/19443994.2012.705966.
[310] S.-K. Hong, C.-S. Kim, K.-S. Hwang, J.-H. Han, H.-K. Kim, N.-J. Jeong, K.-S. Choi, Experimental and numerical studies on pressure drop in reverse electrodialysis: Effect of unit cell configuration, J. Mech. Sci. Technol. 30 (2016) 5287–5292, https://doi.org/10.1007/s12206-016-1047-z.
[311] M.R. Cruz-Díaz, A. Laureano, F.A. Rodríguez, L.F. Arenas, J.J.H. Pijpers, E. P. Rivero, Modelling of flow distribution within spacer-filled channels fed by dividing manifolds as found in stacks for membrane-based technologies, Chem. Eng. J. 423 (2021) 130232, https://doi.org/10.1016/j.cej.2021.130232.
[312] D. Aili, M.R. Kraglund, S.C. Rajappan, D. Serhiichuk, Y. Xia, V. Deimede, J. Kallitsis, C. Bae, P. Jannasch, D. Henkensmeier, J.O. Jensen, Electrode Separators for the Next-Generation Alkaline Water Electrolyzers, ACS Energy Lett. 8 (2023) 1900–1910, https://doi.org/10.1021/acsenergylett.3c00185.
[313] A.K. Singh, P. Sharma, K. Singh, V.K. Shahi, Improved performance of vanadium redox flow battery with tuneable alkyl spacer based cross-linked anion exchange membranes, J. Power Sources 520 (2022) 230856, https://doi.org/10.1016/j.jpowsour.2021.230856.
[314] R. Qi, M. Becker, J. Brauns, T. Turek, J. Lin, Y. Song, Channel design optimization of alkaline electrolysis stacks considering the trade-off between current efficiency and pressure drop, J. Power Sources 579 (2023) 233222, https://doi.org/10.1016/j.jpowsour.2023.233222.
[315] M. Tedesco, H. Hamelers, P.M. Biesheuvel, Nernst-Planck transport theory for (reverse) electrodialysis: I, Effect of Co-Ion Transport through the Membranes, Journal of Membrane Science 510 (2016) 370–381, https://doi.org/10.1016/j.memsci.2016.03.012.
[316] J. Kim, K. Park, D.R. Yang, S. Hong, A comprehensive review of energy consumption of seawater reverse osmosis desalination plants, Appl. Energy 254 (2019) 113652, https://doi.org/10.1016/j.apenergy.2019.113652.
[317] R.K. McGovern, A.M. Weiner, L. Sun, C.G. Chambers, S.M. Zubair, J.H. V. Lienhard, On the cost of electrodialysis for the desalination of high salinity feeds, Appl. Energy 136 (2014) 649–661, https://doi.org/10.1016/j.apenergy.2014.09.050.

[318] Q. Leng, S. Xu, X. Wu, S. Wang, D. Wu, F. Dong, D. Jin, P. Wang, Decolorization efficiency of methyl orange simulative wastewater by a reverse electrodialysis reactor: experiments and kinetics models, Desalin. Water Treat. 258 (2022) 72–84, https://doi.org/10.5004/dwt.2022.28392.
[319] T. León, J. López, R. Torres, J. Grau, L. Jofre, J.-L. Cortina, Time-dependent 2-D model for transport of species analysis in electrodialysis: Concentration profiles and fluxes, Desalination 565 (2023) 116819, https://doi.org/10.1016/j.desal.2023.116819.
[320] Z. Zourmand, F. Faridirad, N. Kasiri, T. Mohammadi, Mass transfer modeling of desalination through an electrodialysis cell, Desalination 359 (2015) 41–51, https://doi.org/10.1016/j.desal.2014.12.008.
[321] S. Pawlowski, P. Sistat, J.G. Crespo, S. Velizarov, Mass transfer in reverse electrodialysis: Flow entrance effects and diffusion boundary layer thickness, J. Membr. Sci. 471 (2014) 72–83, https://doi.org/10.1016/j.memsci.2014.07.075.
[322] J. Ledingham, K.L. Sedransk Campbell, B. in 't Veen, L. Keyzer, N.Y. Yip, A. N. Campbell, The development and validation of a novel, parameter-free, modelling strategy for electromembrane processes: Electrodialysis, Desalination 576 (2024) 117386, https://doi.org/10.1016/j.desal.2024.117386.
[323] B. Sun, M. Zhang, S. Huang, J. Wang, X. Zhang, Limiting concentration during batch electrodialysis process for concentrating high salinity solutions: A theoretical and experimental study, Desalination 498 (2021) 114793, https://doi.org/10.1016/j.desal.2020.114793.
[324] H. Zhu, B. Yang, C. Gao, Y. Wu, Ion transfer modeling based on Nernst-Planck theory for saline water desalination during electrodialysis process, Asia Pac. J. Chem. Eng. 15 (2020) e2410.
[325] L. Gurreri, A. Tamburini, A. Cipollina, G. Micale, M. Ciofalo, CFD prediction of concentration polarization phenomena in spacer-filled channels for reverse electrodialysis, J. Membr. Sci. 468 (2014) 133–148, https://doi.org/10.1016/j.memsci.2014.05.058.
[326] A. Campione, A. Cipollina, I.D.L. Bogle, L. Gurreri, A. Tamburini, M. Tedesco, G. Micale, A hierarchical model for novel schemes of electrodialysis desalination, Desalination 465 (2019) 79–93, https://doi.org/10.1016/j.desal.2019.04.020.
[327] V.V. Nikonenko, A.E. Kozmai, Electrical equivalent circuit of an ion-exchange membrane system, Electrochim. Acta 56 (2011) 1262–1269, https://doi.org/10.1016/j.electacta.2010.10.094.
[328] W.S. Ryoo, J. Yoo, Study on Key Parameters of Reverse Electrodialysis (RED) Cell-Stack Performance Based on Equivalent Circuit Model, Meet. Abstr. MA2022-02 (2022) 2550, https://doi.org/10.1149/MA2022-02502550mtgabs.
[329] J. Yan, R. Li, H. Wang, B. Hou, S. Wu, W. Fu, D. He, Z. Wang, Q. Li, B. Wang, Y. Wang, T. Xu, Alcohol splitting with bipolar membranes for the production of metal alkoxides: Alcohol splitting behaviour and ion transport kinetics, Chem. Eng. Sci. 286 (2024) 119657, https://doi.org/10.1016/j.ces.2023.119657.
[330] R. Takagi, M. Vaselbehagh, H. Matsuyama, Theoretical study of the permselectivity of an anion exchange membrane in electrodialysis, J. Membr. Sci. 470 (2014) 486–493, https://doi.org/10.1016/j.memsci.2014.07.053.
[331] B.A. Qureshi, S.M. Zubair, Design of electrodialysis desalination plants by considering dimensionless groups and variable equivalent conductivity, Desalination 430 (2018) 197–207, https://doi.org/10.1016/j.desal.2017.12.030.
[332] H.-J. Lee, F. Sarfert, H. Strathmann, S.-H. Moon, Designing of an electrodialysis desalination plant, Desalination 142 (2002) 267–286, https://doi.org/10.1016/S0011-9164(02)00208-4.
[333] B.A. Qureshi, N.A. Qasem, S.M. Zubair, Normalized sensitivity analysis of electrodialysis desalination plants for mitigating hypersalinity, Sep. Purif. Technol. 257 (2021) 117858, https://doi.org/10.1016/j.seppur.2020.117858.
[334] S. Gmar, A. Chagnes, I. Ben Salah Sayadi, J.-F. Fauvarque, M. Tlili, M. Ben Amor, Semiempirical kinetic modelling of water desalination by electrodialysis processes, Sep. Sci. Technol. 52 (2017) 574–581, https://doi.org/10.1080/01496395.2016.1254661.
[335] P. Zimmermann, Ö. Tekinalp, S.B.B. Solberg, Ø. Wilhelmsen, L. Deng, O. S. Burheim, Limiting current density as a selectivity factor in electrodialysis of multi-ionic mixtures, Desalination 558 (2023) 116613, https://doi.org/10.1016/j.desal.2023.116613.
[336] M. Fidaleo, M. Moresi, Optimal strategy to model the electrodialytic recovery of a strong electrolyte, J. Membr. Sci. 260 (2005) 90–111, https://doi.org/10.1016/j.memsci.2005.01.048.
[337] Z. Liu, T. Chen, G. Liu, Effect of the dielectric membrane channel on salinity gradient energy conversion, Desalination 574 (2024) 117287, https://doi.org/10.1016/j.desal.2023.117287.
[338] D.T. Nguyen, V.-S. Pham, Modeling non-linear ion transport phenomena in ion-selective membranes: Three simplified models, Sep. Purif. Technol. 333 (2024) 125929, https://doi.org/10.1016/j.seppur.2023.125929.
[339] M.M. Generous, N.A. Qasem, S.M. Zubair, The significance of modeling electrodialysis desalination using multi-component saline water, Desalination 496 (2020) 114347, https://doi.org/10.1016/j.desal.2020.114347.
[340] S.K. Patel, B. Lee, P. Westerhoff, M. Elimelech, The potential of electrodialysis as a cost-effective alternative to reverse osmosis for brackish water desalination, Water Res. 250 (2024) 121009, https://doi.org/10.1016/j.watres.2023.121009.
[341] E. Nosova, A. Achoh, V. Zabolotsky, S. Melnikov, Electrodialysis Desalination with Simultaneous pH Adjustment Using Bilayer and Bipolar Membranes, Modeling and Experiment, Membranes (basel) 12 (2022), https://doi.org/10.3390/membranes12111102.
[342] G. Kraaijeveld, V. Sumberova, S. Kuindersma, H. Wesselingh, Modelling electrodialysis using the Maxwell-Stefan description, The Chemical Engineering Journal and the Biochemical Engineering Journal 57 (1995) 163–176, https://doi.org/10.1016/0923-0467(94)02940-7.
[343] D. Wang, X.F. Lu, D. Luan, X.W. Lou, Selective Electrocatalytic Conversion of Nitric Oxide to High Value-Added Chemicals, Adv. Mater. (2024) e2312645.
[344] H. Song, H. Yang, X. Yu, X. Wang, H. Jing, Y. Tan, J. Hu, Research progress of industrial application of membrane electrolysis technology, Ionics (2024), https://doi.org/10.1007/s11581-024-05395-7.
[345] P. Goel, P. Mandal, B.E.V.K. Shahi, S. Chattopadhyay, Sulfonated poly (ether ether ketone) composite cation exchange membrane for NaOH production by electro-electrodialysis using agro-based paper mill green liquor, J. Environ. Chem. Eng. 9 (2021) 106409, https://doi.org/10.1016/j.jece.2021.106409.
[346] C. Jiang, Y. Wang, Q. Wang, H. Feng, T. Xu, Production of Lithium Hydroxide from Lake Brines through Electro-Electrodialysis with Bipolar Membranes (EEDBM), Ind. Eng. Chem. Res. 53 (2014) 6103–6112, https://doi.org/10.1021/ie404334s.
[347] R.F. Alshebli, N. Salsabila, B. Yuzer, Y. Bicer, Boron and lithium recovery from aqueous solutions by ion-exchange resin stuffed electro-electrodialysis process with hydrogen production, J. Environ. Chem. Eng. 11 (2023) 110687, https://doi.org/10.1016/j.jece.2023.110687.
[348] G. Liu, D. Wu, G. Chen, R. Halim, J. Liu, H. Deng, Comparative study on tartaric acid production by two-chamber and three-chamber electro-electrodialysis, Sep. Purif. Technol. 263 (2021) 118403, https://doi.org/10.1016/j.seppur.2021.118403.
[349] F. Chen, J. Wang, Q. Ru, S.H. Aung, T.Z. Oo, B. Chu, Continuous Electrochemical Desalination via a Viologen Redox Flow Reaction, J. Electrochem. Soc. 167 (2020) 83503, https://doi.org/10.1149/1945-7111/ab8c86.
[350] F. Chen, J. Wang, C. Feng, J. Ma, T. David Waite, Low energy consumption and mechanism study of redox flow desalination, Chem. Eng. J. 401 (2020) 126111, https://doi.org/10.1016/j.cej.2020.126111.
[351] N. Kim, J. Jeon, J. Elbert, C. Kim, X. Su, Redox-mediated electrochemical desalination for waste valorization in dairy production, Chem. Eng. J. 428 (2022) 131082, https://doi.org/10.1016/j.cej.2021.131082.
[352] S.A. Maclean, S. Raza, H. Wang, C. Igbomezie, J. Liu, N. Makowski, Y. Ma, Y. Shen, J.A. Röhr, G.-M. Weng, A.D. Taylor, Investigation of flow rate in symmetric four-channel redox flow desalination system, Cell Rep. Phys. Sci. 5 (2024) 101761, https://doi.org/10.1016/j.xcrp.2023.101761.
[353] F.Y. AlJaberi, S.A. Ahmed, H.F. Makki, A.S. Naje, H.M. Zwain, A.D. Salman, T. Juzsakova, S. Viktor, B. Van, P.-C. Le, D.D. La, S.W. Chang, M.-J. Um, H. H. Ngo, D.D. Nguyen, Recent advances and applicable flexibility potential of electrochemical processes for wastewater treatment, Sci. Total Environ. 867 (2023) 161361, https://doi.org/10.1016/j.scitotenv.2022.161361.
[354] J. Lin, W. Ye, M. Xie, D.H. Seo, J. Luo, Y. Wan, B. van der Bruggen, Environmental impacts and remediation of dye-containing wastewater, Nat. Rev. Earth Environ. 4 (2023) 785–803, https://doi.org/10.1038/s43017-023-00489-8.
[355] T. Chen, J. Bi, M. Sun, J. Liu, J. Yuan, Y. Zhao, Z. Ji, Electrodialysis metathesis for high-value resource conversion and recovery: From sustainable applications to future prospects, Chem. Eng. J. 473 (2023) 145299, https://doi.org/10.1016/j.cej.2023.145299.
[356] J. Feng, Q. Wang, N. Li, Y. Sun, Z. Ma, D. Xu, J. Gao, J. Wang, L. Wang, X. Gao, Techno-economic evaluation of preparing high-valued TPAOH from its low-cost bromide via electrodialysis metathesis (EDM), Sep. Purif. Technol. 237 (2020) 116371, https://doi.org/10.1016/j.seppur.2019.116371.
[357] W.-F. Wen, J. Wang, C.-Y. Zhong, Q. Chen, W.-M. Zhang, Direct production of lithium nitrate from the primary lithium salt by electrodialysis metathesis, J. Membr. Sci. 654 (2022) 120555, https://doi.org/10.1016/j.memsci.2022.120555.
[358] W. Gao, H. Zhao, X. Wei, X. Meng, K. Wu, Y. Liu, A Green and Economical Method for Preparing Potassium Glutamate through Electrodialysis Metathesis, Ind. Eng. Chem. Res. 61 (2022) 1486–1493, https://doi.org/10.1021/acs.iecr.1c04556.
[359] S.K.A. Al-Amshawee, M.Y.B.M. Yunus, Electrodialysis membrane with concentration polarization – A review, Chem. Eng. Res. Des. 201 (2024) 645–678, https://doi.org/10.1016/j.cherd.2023.10.060.
[360] F. Liu, R. Zhou, C. Zhang, Z. Wu, H. Ren, H.Y. Ng, Critical review on the pulsed electrochemical technologies for wastewater treatment: Fundamentals, current trends, and future studies, Chem. Eng. J. 479 (2024) 147588, https://doi.org/10.1016/j.cej.2023.147588.
[361] B. de Jaegher, W. de Schepper, A. Verliefde, I. Nopens, A model-based analysis of electrodialysis fouling during pulsed electric field operation, J. Membr. Sci. 642 (2022) 119975, https://doi.org/10.1016/j.memsci.2021.119975.
[362] L. Bazinet, T.R. Geoffroy, Electrodialytic Processes: Market Overview, Membrane Phenomena, Recent Developments and Sustainable Strategies, Membranes (basel) 10 (2020), https://doi.org/10.3390/membranes10090221.
[363] S. Honarparvar, R. Al-Rashed, A.G.V. Winter, Investigation of pulsed electric field operation as a chemical-free anti-scaling approach for electrodialysis desalination of brackish water, Desalination 551 (2023) 116386, https://doi.org/10.1016/j.desal.2023.116386.
[364] D. Butylskii, I. Moroz, K. Tsygurina, S. Mareev, Effect of Surface Inhomogeneity of Ion-Exchange Membranes on the Mass Transfer Efficiency in Pulsed Electric Field Modes, Membranes (basel) 10 (2020), https://doi.org/10.3390/membranes10030040.
[365] A.M. Uzdenova, A.V. Kovalenko, M.K. Urtenov, V.V. Nikonenko, Effect of electroconvection during pulsed electric field electrodialysis, Numerical Experiments, Electrochem. Commun. 51 (2015) 1–5, https://doi.org/10.1016/j.elecom.2014.11.021.
[366] S. Mikhaylin, V. Nikonenko, N. Pismenskaya, G. Pourcelly, S. Choi, H.J. Kwon, J. Han, L. Bazinet, How physico-chemical and surface properties of cation-exchange membrane affect membrane scaling and electroconvective vortices:

Influence on performance of electrodialysis with pulsed electric field, Desalination 393 (2016) 102–114, https://doi.org/10.1016/j.desal.2015.09.011.
[367] Y.V. Karlin, V.N. Kropotov, Electrodialysis separation of Na^+ and Ca^{2+} in a pulsed current mode, Russ. J. Electrochem. 31 (1995) 472–476.
[368] N.A. Mishchuk, L.K. Koopal, F. Gonzalez-Caballero, Intensification of electrodialysis by applying a non-stationary electric field, Colloids Surf A Physicochem Eng Asp 176 (2001) 195–212, https://doi.org/10.1016/S0927-7757(00)00568-9.
[369] G. Dufton, S. Mikhaylin, S. Gaaloul, L. Bazinet, Systematic Study of the Impact of Pulsed Electric Field Parameters (Pulse/Pause Duration and Frequency) on ED Performances during Acid Whey Treatment, Membranes (Basel) 10 (2020). https://doi.org/10.3390/membranes10010014.
[370] H.-J. Lee, S.-H. Moon, S.-P. Tsai, Effects of pulsed electric fields on membrane fouling in electrodialysis of NaCl solution containing humate, Sep. Purif. Technol. 27 (2002) 89–95, https://doi.org/10.1016/S1383-5866(01)00167-8.
[371] A.G. Capodaglio, Pulse Electric Field Technology for Wastewater and Biomass Residues' Improved Valorization, Processes (basel) 9 (2021) 736, https://doi.org/10.3390/pr9050736.
[372] P. Saremirad, H.G. Gomaa, J. Zhu, Effect of flow oscillations on mass transfer in electrodialysis with bipolar membrane, J. Membr. Sci. 405–406 (2012) 158–166, https://doi.org/10.1016/j.memsci.2012.03.006.
[373] R. Bert, C. Manes, A. Tiraferri, New Facility for Membrane Fouling Investigations under Customizable Hydrodynamics: Validation and Preliminary Experiments with Pulsating Cross-Flow, Membranes (basel) 12 (2022), https://doi.org/10.3390/membranes12030334.
[374] S.K.A. Al-Amshawee, M.Y.B.M. Yunus, Electrodialysis desalination: The impact of solution flowrate (or Reynolds number) on fluid dynamics throughout membrane spacers, Environ. Res. 219 (2023) 115115, https://doi.org/10.1016/j.envres.2022.115115.
[375] C. Rodrigues, M. Rodrigues, V. Semiao, V. Geraldes, Enhancement of mass transfer in spacer-filled channels under laminar regime by pulsatile flow, Chem. Eng. Sci. 123 (2015) 536–541, https://doi.org/10.1016/j.ces.2014.11.047.
[376] C. Jiang, H. Chen, Y. Zhang, H. Feng, M.A. Shehzad, Y. Wang, T. Xu, Complexation Electrodialysis as a general method to simultaneously treat wastewaters with metal and organic matter, Chem. Eng. J. 348 (2018) 952–959, https://doi.org/10.1016/j.cej.2018.05.022.
[377] Q. Wang, C. Jiang, Y. Wang, Z. Yang, T. Xu, Reclamation of Aniline Wastewater and CO 2 Capture Using Bipolar Membrane Electrodialysis, ACS Sustain. Chem. Eng. 4 (2016) 5743–5751, https://doi.org/10.1021/acssuschemeng.6b01686.
[378] D. Babilas, J. Muszyński, A. Milewski, K. Leśniak-Ziółkowska, P. Dydo, Electrodialysis enhanced with disodium EDTA as an innovative method for separating Cu(II) ions from zinc salts in wastewater, Chem. Eng. J. 408 (2021) 127908, https://doi.org/10.1016/j.cej.2020.127908.
[379] K.N. Han, R. Kim, J. Kim, Recent Advancements in Hydrometallurgy: Solubility and Separation, Trans. Indian Inst. Met. (2023), https://doi.org/10.1007/s12666-023-02956-8.
[380] H.C. Hershey, R.D. Mitchell, W.H. Webb, Separation of cesium and strontium by electrodialysis, J. Inorg. Nucl. Chem. 28 (1966) 645–649, https://doi.org/10.1016/0022-1902(66)80346-9.
[381] S. Frioui, R. Oumeddour, S. Lacour, Highly selective extraction of metal ions from dilute solutions by hybrid electrodialysis technology, Sep. Purif. Technol. 174 (2017) 264–274, https://doi.org/10.1016/j.seppur.2016.10.028.
[382] T. Huang, J.-K. Wang, Preferential transport of nickel and cupric ions through cation exchange membrane in electrodialysis with a complex agent, Desalination 86 (1992) 257–271, https://doi.org/10.1016/0011-9164(92)80037-A.
[383] L. Karimi, A. Ghassemi, An empirical/theoretical model with dimensionless numbers to predict the performance of electrodialysis systems on the basis of operating conditions, Water Res. 98 (2016) 270–279, https://doi.org/10.1016/j.watres.2016.04.014.
[384] F. Aubras, M. Rhandi, J. Deseure, A.-J.-J. Kadjo, M. Bessafi, J. Majasan, B. Grondin-Perez, F. Druart, J.-P. Chabriat, Dimensionless approach of a polymer electrolyte membrane water electrolysis: Advanced analytical modelling, J. Power Sources 481 (2021) 228858, https://doi.org/10.1016/j.jpowsour.2020.228858.
[385] J.-Y. Nam, K.-S. Hwang, H.-C. Kim, H. Jeong, H. Kim, E. Jwa, S. Yang, J. Choi, C.-S. Kim, J.-H. Han, N. Jeong, Assessing the behavior of the feed-water constituents of a pilot-scale 1000-cell-pair reverse electrodialysis with seawater and municipal wastewater effluent, Water Res. 148 (2019) 261–271, https://doi.org/10.1016/j.watres.2018.10.054.
[386] A.J. Ward, K. Arola, E. Thompson Brewster, C.M. Mehta, D.J. Batstone, Nutrient recovery from wastewater through pilot scale electrodialysis, Water Res. 135 (2018) 57–65, https://doi.org/10.1016/j.watres.2018.02.021.
[387] V. Giovanni, C. Calogero, T. Alessandro, C. Andrea, M. Giorgio, Performance Evaluation of an Electrodialysis with Bipolar Membranes Pilot Plant Operated in Feed Bleed Mode, Chem. Eng. Trans. 105 (2023) 73–78, https://doi.org/10.3303/CET23105013.
[388] Z. Peng, Y. Sun, Leakage circuit characteristics of a bipolar membrane electrodialyzer with 5 BP-A-C units, J. Membr. Sci. 597 (2020) 117762, https://doi.org/10.1016/j.memsci.2019.117762.
[389] J. Veerman, J.W. Post, M. Saakes, S.J. Metz, G.J. Harmsen, Reducing power losses caused by ionic shortcut currents in reverse electrodialysis stacks by a validated model, J. Membr. Sci. 310 (2008) 418–430, https://doi.org/10.1016/j.memsci.2007.11.032.
[390] M. Doležel, K. Keslerová, Measurement of Non-Effective Electric Current in Electrodialysis Stacks, J. Electrochem. Soc. 164 (2017) E276–E282, https://doi.org/10.1149/2.1481709jes.
[391] J. Xia, G. Eigenberger, H. Strathmann, U. Nieken, Acid-Base Flow Battery, Based on Reverse Electrodialysis with Bi-Polar Membranes: Stack Experiments, Processes (basel) 8 (2020) 99, https://doi.org/10.3390/pr8010099.
[392] A. Culcasi, L. Gurreri, A. Zaffora, A. Cosenza, A. Tamburini, A. Cipollina, G. Micale, Ionic shortcut currents via manifolds in reverse electrodialysis stacks, Desalination 485 (2020) 114450, https://doi.org/10.1016/j.desal.2020.114450.
[393] J.-H. Han, Experimental visualization of leakage current in reverse electrodialysis and its effect on inorganic scaling, Desalination 527 (2022) 115584, https://doi.org/10.1016/j.desal.2022.115584.
[394] B.R. Bligh, Reverse Electrodialysis (1988).
[395] T. Wen, G.S. Solt, Y.F. Sun, Modelling the cross flow spirally wound electrodualysis (SpED) process, Desalination 103 (1995) 165–176, https://doi.org/10.1016/0011-9164(95)00070-4.
[396] P. Mardle, B. Chen, S. Holdcroft, Opportunities of Ionomer Development for Anion-Exchange Membrane Water Electrolysis, ACS Energy Lett. 8 (2023) 3330–3342, https://doi.org/10.1021/acsenergylett.3c01040.
[397] G. Campisi, A. Cosenza, S. Randazzo, A. Tamburini, G. Micale, Economic Analysis of an Innovative Scheme for the Treatment of Produced Waters, Chem. Eng. Trans. 105 (2023) 367–372, https://doi.org/10.3303/CET23105062.
[398] S. Lahnid, M. Tahaikt, K. Elaroui, I. Idrissi, M. Hafsi, I. Laaziz, Z. Amor, F. Tiyal, A. Elmidaoui, Economic evaluation of fluoride removal by electrodialysis, Desalination 230 (2008) 213–219, https://doi.org/10.1016/j.desal.2007.11.027.
[399] C.-W. Lin, H.N. Tran, R.-S. Juang, Reclamation and reuse of wastewater by membrane-based processes in a typical midstream petrochemical factory: a techno-economic analysis, Environ. Dev. Sustain. 26 (2024) 5419–5430, https://doi.org/10.1007/s10668-022-02880-9.
[400] D. Ankoliya, A. Mudgal, M.K. Sinha, P. Davies, K. Park, R.R. Alegre, V. Patel, J. Patel, Techno-economic analysis of integrated bipolar membrane electrodialysis and batch reverse osmosis for water and chemical recovery from dairy wastewater, J. Clean. Prod. 420 (2023) 138264, https://doi.org/10.1016/j.jclepro.2023.138264.
[401] F. Sabatino, M. Mehta, A. Grimm, M. Gazzani, F. Gallucci, G.J. Kramer, M. van Sint Annaland, Evaluation of a Direct Air Capture Process Combining Wet Scrubbing and Bipolar Membrane Electrodialysis, Ind. Eng. Chem. Res. 59 (2020) 7007–7020, https://doi.org/10.1021/acs.iecr.9b05641.
[402] M. Herrero-Gonzalez, A. Culcasi, A. Tamburini, R. Ibañez, A. Cipollina, G. Micale, Techno-economic feasibility of photovoltaic solar electrodialysis with bipolar membranes, Desalination 582 (2024) 117624, https://doi.org/10.1016/j.desal.2024.117624.
[403] D. Vineyard, A. Hicks, K.G. Karthikeyan, C. Davidson, P. Barak, Life cycle assessment of electrodialysis for sidestream nitrogen recovery in municipal wastewater treatment, Cleaner Environ. Syst. 2 (2021) 100026, https://doi.org/10.1016/j.cesys.2021.100026.
[404] J. Lu, S. Kumagai, Y. Fukushima, H. Ohno, T. Kameda, Y. Saito, T. Yoshioka, Combined Experiment, Simulation, and Ex-ante LCA Approach for Sustainable Cl Recovery from NaCl/Ethylene Glycol by Electrodialysis, Ind. Eng. Chem. Res. 59 (2020) 20112–20122, https://doi.org/10.1021/acs.iecr.0c03565.
[405] A. Alrashidi, E. Aleisa, K. Alshayji, Life cycle assessment of hybrid electrodialysis and reverse osmosis seawater desalination systems, Desalination 578 (2024) 117448, https://doi.org/10.1016/j.desal.2024.117448.
[406] V.V. Akula, G. Ramalingam, A.K. Verma, Z. Ronen, Y. Oren, J. Gilron, L. Philip, Performance evaluation of pilot scale ion exchange membrane bioreactor for nitrate removal from secondary effluent, J. Clean. Prod. 442 (2024) 141087, https://doi.org/10.1016/j.jclepro.2024.141087.
[407] P.K. Cornejo, M.V.E. Santana, D.R. Hokanson, J.R. Mihelcic, Q. Zhang, Carbon footprint of water reuse and desalination: a review of greenhouse gas emissions and estimation tools, J. Water Reuse Desalin. 4 (2014) 238–252, https://doi.org/10.2166/wrd.2014.058.
[408] M. Herrero-Gonzalez, N. Admon, A. Dominguez-Ramos, R. Ibañez, A. Wolfson, A. Irabien, Environmental sustainability assessment of seawater reverse osmosis brine valorization by means of electrodialysis with bipolar membranes, Environ. Sci. Pollut. Res. Int. 27 (2020) 1256–1266, https://doi.org/10.1007/s11356-019-04788-w.
[409] S.K.A. Al-Amshawee, M.Y.B.M. Yunus, Electrodialysis membrane desalination with diagonal membrane spacers: a review, Environ. Sci. Pollut. Res. Int. (2023), https://doi.org/10.1007/s11356-023-28727-y.
[410] P.P. Gohil, H. Desai, A. Kumar, R. Kumar, Current Status and Advancement in Thermal and Membrane-Based Hybrid Seawater Desalination Technologies, Water (basel) 15 (2023) 2274, https://doi.org/10.3390/w15122274.
[411] O. Scialdone, Electrochemical synthesis of chemicals and treatment of wastewater promoted by salinity gradients using reverse electrodialysis and assisted reverse electrodialysis, Curr. Opin. Electrochem. 43 (2024) 101421, https://doi.org/10.1016/j.coelec.2023.101421.
[412] R. Mejía-Marchena, A. Maturana-Córdoba, S. Fernández-Rojano, Unveiling the enhancing potential of water pretreatment on energy efficiency in reverse electrodialysis systems - A comprehensive review, J. Water Process Eng. 56 (2023) 104548, https://doi.org/10.1016/j.jwpe.2023.104548.
[413] S. Pandit, C. Pandit, A. Singh Mathuriya, D.A. Jadhav, Blue energy meets green energy in microbial reverse electrodialysis cells: Recent advancements and prospective, Sustainable Energy Technol. Assess. 57 (2023) 103260, https://doi.org/10.1016/j.seta.2023.103260.
[414] A. Cassano, E. Drioli, Membrane Systems in the Food Production, De Gruyter, 2021.
[415] M. Wang, S. Kuang, X. Wang, D. Kang, D. Mao, G. Qian, X. Cai, M. Tan, F. Liu, Y. Zhang, Transport of Amino Acids in Soy Sauce Desalination Process by

Electrodialysis, Membranes (basel) 11 (2021), https://doi.org/10.3390/membranes11060408.
[416] M. Faucher, L. Henaux, C. Chaudron, S. Mikhaylin, M. Margni, L. Bazinet, Electromembrane approach to substantially improve the ecoefficiency of deacidified cranberry juice production: Physicochemical properties, life cycle assessment and ecoefficiency score, J. Food Eng. 273 (2020) 109802, https://doi.org/10.1016/j.jfoodeng.2019.109802.
[417] E.E. Nevakshenova, V.V. Sarapulova, V.V. Nikonenko, N.D. Pismenskaya, Application of Sodium Chloride Solutions to Regeneration of Anion-Exchange Membranes Used for Improving Grape Juices and Wines, Membr, Membr. Technol. 1 (2019) 14–22, https://doi.org/10.1134/S2517751619010062.
[418] S. Valluri, S.K. Kawatra, Reduced reagent regeneration energy for CO2 capture with bipolar membrane electrodialysis, Fuel Process. Technol. 213 (2021) 106691, https://doi.org/10.1016/j.fuproc.2020.106691.
[419] M. Mahmoudkhani, D.W. Keith, Low-energy sodium hydroxide recovery for CO2 capture from atmospheric air—Thermodynamic analysis, Int. J. Greenhouse Gas Control 3 (2009) 376–384, https://doi.org/10.1016/j.ijggc.2009.02.003.
[420] S.Y.W. Chai, L.H. Ngu, B.S. How, Review of carbon capture absorbents for CO 2 utilization, Greenhouse Gases, Sci. Technol. 12 (2022) 394–427, https://doi.org/10.1002/ghg.2151.
[421] M.D. Eisaman, K. Parajuly, A. Tuganov, C. Eldershaw, N. Chang, K.A. Littau, CO2 extraction from seawater using bipolar membrane electrodialysis, Energy Environ. Sci. 5 (2012) 7346, https://doi.org/10.1039/c2ee03393c.
[422] W. Jiang, W. Liu, Y. Wang, Z. Zhao, Q. Li, Y. Wu, T. Liu, H. Xie, Electrochemically Regenerated Amine for CO 2 Capture Driven by a Proton-Coupled Electron Transfer Reaction, Ind. Eng. Chem. Res. 61 (2022) 13578–13588, https://doi.org/10.1021/acs.iecr.2c01047.
[423] C. Huang, T. Xu, X. Yang, Regenerating fuel-gas desulfurizing agents by using bipolar membrane electrodialysis (BMED): effect of molecular structure of alkanolamines on the regeneration performance, Environ. Sci. Technol. 41 (2007) 984–989, https://doi.org/10.1021/es061918e.
[424] C. Li, C. Jiang, L. Qu, H.-H. Yu, X. Qi, W. De-xin, J. Du, Calculation and Analysis of Energy Consumption Index of Environmental Protection Facilities in Coal-fired Power Plant, IOP Conf. Ser. Earth Environ. Sci. 295 (2019) 52053, https://doi.org/10.1088/1755-1315/295/5/052053.
[425] R. Anttonen Life cycle assessment for lithium hydroxide production preoperational study of carbon footprint for Keliber's lithium hydroxide production in 2021 Central Ostrobothnia.
[426] P. Zimmermann, K. Wahl, Ö. Tekinalp, S.B.B. Solberg, L. Deng, Ø. Wilhelmsen, O. S. Burheim, Selective recovery of silver ions from copper-contaminated effluents using electrodialysis, Desalination 572 (2024) 117108, https://doi.org/10.1016/j.desal.2023.117108.
[427] S. Syed, Silver recovery aqueous techniques from diverse sources: Hydrometallurgy in recycling, Waste Manag. 50 (2016) 234–256, https://doi.org/10.1016/j.wasman.2016.02.006.
[428] Y. Liu, M. Lv, X. Wu, J. Ding, L. Dai, H. Xue, X. Ye, R. Chen, R. Ding, J. Liu, B. van der Bruggen, Recovery of copper from electroplating sludge using integrated bipolar membrane electrodialysis and electrodeposition, J. Colloid Interface Sci. 642 (2023) 29–40, https://doi.org/10.1016/j.jcis.2023.03.154.
[429] M. Gómez, S. Grimes, G. Fowler, Novel hydrometallurgical process for the recovery of copper from end-of-life mobile phone printed circuit boards using ionic liquids, J. Clean. Prod. 420 (2023) 138379, https://doi.org/10.1016/j.jclepro.2023.138379.
[430] I. Frenzel, H. Holdik, D. Stamatialis, G. Pourcelly, M. Wessling, Chromic acid recovery by electro-electrodialysisI, Evaluation of Anion-Exchange Membrane, Journal of Membrane Science 261 (2005) 49–57, https://doi.org/10.1016/j.memsci.2005.03.031.
[431] E. Kokkinos, V. Proskynitopoulou, A. Zouboulis, Chromium and energy recovery from tannery wastewater treatment waste: Investigation of major mechanisms in the framework of circular economy, J. Environ. Chem. Eng. 7 (2019) 103307, https://doi.org/10.1016/j.jece.2019.103307.
[432] O. Bruinsma, D.J. Branken, T.N. Lemmer, L. van der Westhuizen, S. Rossouw, Sodium sulfate splitting as zero brine process in a base metal refinery: Screening and optimization in batch mode, Desalination 511 (2021) 115096, https://doi.org/10.1016/j.desal.2021.115096.
[433] A. Kumar, F. Du, J.H. Lienhard, Caustic Soda Production, Energy Efficiency, and Electrolyzers, ACS Energy Lett. 6 (2021) 3563–3566, https://doi.org/10.1021/acsenergylett.1c01827.
[434] M. Marwa, A. Soumaya, N. Hajjaji, M.R. Jeday, An environmental life cycle assessment of an industrial system: case of industrial sulfuric acid, International Journal of Energy, Environment and Economics 25 (2017) 255–268.
[435] B. Yuzer, M.I. Aydin, B. Hasançebi, H. Selcuk, Application of an electrodialysis process to recover nitric acid from aluminum finishing industry waste, Desalin. Water Treat. 172 (2019) 199–205, https://doi.org/10.5004/dwt.2019.24914.
[436] R.M. Altarawneh, P.G. Pickup, Product Distributions and Efficiencies for Ethanol Oxidation in a Proton Exchange Membrane Electrolysis Cell, J. Electrochem. Soc. 164 (2017) F861–F865, https://doi.org/10.1149/2.0051709jes.
[437] S. Loza, N. Loza, A. Korzhov, N. Romanyuk, N. Kovalchuk, S. Melnikov, Hybrid Membrane Technology for Acid Recovery from Wastewater in Coated Steel Wire Production: A Pilot Scale Study, Membranes (basel) 12 (2022), https://doi.org/10.3390/membranes12121196.
[438] V. Boor, J.E.B.M. Frijns, E. Perez-Gallent, E. Giling, A.T. Laitinen, E.L.V. Goetheer, L.J.P. van den Broeke, R. Kortlever, W. de Jong, O.A. Moultos, T.J.H. Vlugt, M. Ramdin, Electrochemical Reduction of CO2 to Oxalic Acid: Experiments, Process Modeling, and Economics, Ind. Eng. Chem. Res. 61 (2022) 14837–14846, https://doi.org/10.1021/acs.iecr.2c02647.
[439] Y. Wang, N. Zhang, C. Huang, T. Xu, Production of monoprotic, diprotic, and triprotic organic acids by using electrodialysis with bipolar membranes: Effect of cell configurations, J. Membr. Sci. 385–386 (2011) 226–233, https://doi.org/10.1016/J.MEMSCI.2011.09.044.
[440] J. Wang, Z. Cui, Y. Li, L. Cao, Z. Lu, Techno-economic analysis and environmental impact assessment of citric acid production through different recovery methods, J. Clean. Prod. 249 (2020) 119315, https://doi.org/10.1016/j.jclepro.2019.119315.
[441] M.I. González, S. Álvarez, F. Riera, R. Álvarez, Economic evaluation of an integrated process for lactic acid production from ultrafiltered whey, J. Food Eng. 80 (2007) 553–561, https://doi.org/10.1016/j.jfoodeng.2006.06.021.
[442] S.S. Yi, Y.C. Lu, G.S. Luo, Separation and concentration of lactic acid by electro-electrodialysis, Sep. Purif. Technol. 60 (2008) 308–314, https://doi.org/10.1016/j.seppur.2007.09.004.
[443] K. Zhang, M. Wang, C. Gao, Tartaric acid production by ion exchange resin-filling electrometathesis and its process economics, J. Membr. Sci. 366 (2011) 266–271, https://doi.org/10.1016/j.memsci.2010.10.013.
[444] E.S. Koivisto, T. Reuter, R. Zevenhoven, Performance Optimization of Bipolar Membrane Electrodialysis of Ammonium Sulfate/Bisulfate Reagents for CO 2 Mineralization, ACS ES T Water 3 (2023) 1953–1962, https://doi.org/10.1021/acsestwater.3c00028.
[445] X. Zhang, W. Lu, P. Yang, W. Cong, Application of response surface methodology to optimize the operation process for regeneration of acid and base using bipolar membrane electrodialysis, J of Chemical Tech & Biotech 83 (2008) 12–19, https://doi.org/10.1002/jctb.1732.
[446] T. Spietz, S. Dobras, T. Chwoła, A. Wilk, A. Krótki, L. Więcław-Solny, Experimental results of amine emission from the CO2 capture process using 2-amino-2-methyl-1-propanol (AMP) with piperazine (PZ), Int. J. Greenhouse Gas Control 102 (2020) 103155, https://doi.org/10.1016/j.ijggc.2020.103155.
[447] E. Grushevenko, S. Bazhenov, V. Vasilevsky, E. Novitsky, M. Shalygin, A. Volkov, Effect of Carbon Dioxide Loading on Removal of Heat Stable Salts from Amine Solvent by Electrodialysis, Membranes (basel) 9 (2019), https://doi.org/10.3390/membranes9110152.
[448] B. Lv, B. Guo, Z. Zhou, G. Jing, Mechanisms of CO2 Capture into Monoethanolamine Solution with Different CO2 Loading during the Absorption/Desorption Processes, Environ. Sci. Technol. 49 (2015) 10728–10735, https://doi.org/10.1021/acs.est.5b02356.
[449] H. Ruan, S. Wu, X. Chen, J. Zou, J. Liao, H. Cui, Y. Dong, Y. Qiu, J. Shen, Capturing CO2 with NaOH solution from reject brine via an integrated technology based on bipolar membrane electrodialysis and hollow fiber membrane contactor, Chem. Eng. J. 450 (2022) 138095, https://doi.org/10.1016/j.cej.2022.138095.
[450] M. Rahimi, A. Khurram, T.A. Hatton, B. Gallant, Electrochemical carbon capture processes for mitigation of CO2 emissions, Chem. Soc. Rev. 51 (2022) 8676–8695, https://doi.org/10.1039/D2CS00443G.
[451] T.-N.-D. Cao, S.W. Snyder, Y.-I. Lin, Y.J. Lin, S. Negi, S.-Y. Pan, Unraveling the Potential of Electrochemical pH-Swing Processes for Carbon Dioxide Capture and Utilization, Ind. Eng. Chem. Res. 62 (2023) 20979–20995, https://doi.org/10.1021/acs.iecr.3c02183.
[452] Y. Liu, É. Lucas, I. Sullivan, X. Li, C. Xiang, Challenges and opportunities in continuous flow processes for electrochemically mediated carbon capture, iScience 25 (2022) 105153. https://doi.org/10.1016/j.isci.2022.105153.
[453] H. Yan, K. Peng, J. Yan, C. Jiang, Y. Wang, H. Feng, Z. Yang, L. Wu, T. Xu, Bipolar membrane-assisted reverse electrodialysis for high power density energy conversion via acid-base neutralization, J. Membr. Sci. 647 (2022) 120288, https://doi.org/10.1016/j.memsci.2022.120288.
[454] M. Wang, M. Rahimi, A. Kumar, S. Hariharan, W. Choi, T.A. Hatton, Flue gas CO2 capture via electrochemically mediated amine regeneration: System design and performance, Appl. Energy 255 (2019) 113879, https://doi.org/10.1016/j.apenergy.2019.113879.
[455] Q. Shu, C.S. Sin, M. Tedesco, H.V. Hamelers, P. Kuntke, Optimization of an electrochemical direct air capture process with decreased CO2 desorption pressure and addition of background electrolyte, Chem. Eng. J. 470 (2023) 144251, https://doi.org/10.1016/j.cej.2023.144251.
[456] I.A. Digdaya, I. Sullivan, M. Lin, L. Han, W.-H. Cheng, H.A. Atwater, C. Xiang, A direct coupled electrochemical system for capture and conversion of CO2 from oceanwater, Nat. Commun. 11 (2020) 4412, https://doi.org/10.1038/s41467-020-18232-y.
[457] I. Taniguchi, T. Yamada, Low Energy CO2 Capture by Electrodialysis, Energy Procedia 114 (2017) 1615–1620, https://doi.org/10.1016/j.egypro.2017.03.1902.
[458] E.G. Novitsky, E.A. Grushevenko, I.L. Borisov, T.S. Anokhina, S.D. Bazhenov, Monoethanolamine (MEA) Degradation: Influence on the Electrodialysis Treatment of MEA-Absorbent, Membranes (basel) 13 (2023), https://doi.org/10.3390/membranes13050491.
[459] E.G. Novitskii, V.P. Vasilevskii, E.A. Grushevenko, A.V. Volkov, V.I. Vasil'eva, The effect of monoethanolamine on conductivity and efficiency of electrodialysis of acid and salt solutions, Russ. J. Electrochem. 53 (2017) 391–397, https://doi.org/10.1134/S1023193517040103.
[460] S. Bazhenov, V. Vasilevsky, A. Rieder, S. Unterberger, E. Grushevenko, V. Volkov, B. Schallert, A. Volkov, Heat Stable Salts (HSS) Removal by Electrodialysis: Reclaiming of MEA Used in Post-combustion CO2-Capture, Energy Procedia 63 (2014) 6349–6356, https://doi.org/10.1016/j.egypro.2014.11.668.
[461] E.G. Novitsky, V.P. Vasilevsky, S.D. Bazhenov, E.A. Grushevenko, V.I. Vasilyeva, A.V. Volkov, Influence of the composition of concentrate solutions on the efficiency of carbon dioxide removal from monoethanolamine aqueous solution

by electrodialysis, Pet. Chem. 54 (2014) 680–685, https://doi.org/10.1134/S0965544114080118.
[462] K.-J. Liu, F.P. Chlanda, K. Nagasubramanian, Application of bipolar membrane technology: A novel process for control of sulfur dioxide from flue gases, J. Membr. Sci. 3 (1978) 57–70, https://doi.org/10.1016/S0376-7388(00)80412-3.
[463] Y. Yongtao, Q. NingPing, L. Guangfei, Z. Junyan, Qian, Remove Sulfur Dioxide from Flue Gases to Obtain Sulfuric Acid through Electrodialysis Enrichment, J. Electrochem. Soc. 162 (2015) E141–E147, https://doi.org/10.1149/2.0591509jes.
[464] M.M. Del Cerrillo-Gonzalez, M. Villen-Guzman, J.M. Rodriguez-Maroto, J.M. Paz-Garcia, Metal Recovery from Wastewater Using Electrodialysis Separation, Metals (basel) 14 (2024) 38, https://doi.org/10.3390/met14010038.
[465] P. Zimmermann, Ö. Tekinalp, L. Deng, K. Forsberg, Ø. Wilhelmsen, O. Burheim, Electrodialysis in Hydrometallurgical Processes, https://doi.org/10.1007/978-3-030-36758-9_15, in: G. Azimi, K. Forsberg, T. Ouchi, H. Kim, S. Alam, A.A. Baba (Eds.), Rare Metal Technology 2020, Springer International Publishing, Cham, 2020, ISBN: 978-3-030-36757-2, pp. 159–167.
[466] S. Gmar, A. Chagnes, F. Lutin, L. Muhr, Application of Electrodialysis for the Selective Lithium Extraction Towards Cobalt, Nickel and Manganese from Leach Solutions Containing High Divalent Cations/li Ratio, Recycling 7 (2022) 14, https://doi.org/10.3390/recycling7020014.
[467] I.R. Rodrigues, C. Deferm, K. Binnemans, S. Riaño, Separation of cobalt and nickel via solvent extraction with Cyanex-272: Batch experiments and comparison of mixer-settlers and an agitated column as contactors for continuous counter-current extraction, Sep. Purif. Technol. 296 (2022) 121326, https://doi.org/10.1016/j.seppur.2022.121326.
[468] A. Asadi, D. Kang, H. Bazargan Harandi, J. Chung-Yen Jung, P.-C. Sui, Utilization of lithium sulphate electrodialysis for closed-loop LIB recycling: Experimental study and process simulation, Sep. Purif. Technol. 343 (2024) 126989, https://doi.org/10.1016/j.seppur.2024.126989.
[469] S. Gmar, A. Chagnes, Recent advances on electrodialysis for the recovery of lithium from primary and secondary resources, Hydrometall. 189 (2019) 105124, https://doi.org/10.1016/j.hydromet.2019.105124.
[470] R. Kumar, S. Chakrabortty, P. Chakrabortty, J. Nayak, C. Liu, M. Ali Khan, G.-S. Ha, K. Ho Kim, M. Son, H.-S. Roh, S.K. Tripathy, B.-H. Jeon, Sustainable recovery of high-valued resources from spent lithium-ion batteries: A review of the membrane-integrated hybrid approach, Chem. Eng. J. 470 (2023) 144169, https://doi.org/10.1016/j.cej.2023.144169.
[471] G. Liu, Z. Zhao, L. He, Highly selective lithium recovery from high Mg/Li ratio brines, Desalination 474 (2020) 114185, https://doi.org/10.1016/j.desal.2019.114185.
[472] Y. Song, Z. Zhao, Recovery of lithium from spent lithium-ion batteries using precipitation and electrodialysis techniques, Sep. Purif. Technol. 206 (2018) 335–342, https://doi.org/10.1016/j.seppur.2018.06.022.
[473] K.V. Shestakov, S.I. Lazarev, K.K. Polyanskii, N.N. Ignatov, Recovery of Iron, Nickel, and Copper in Waste Water from Printed Circuit Board Manufacture by Electrodialysis Method, Russ. J. Appl. Chem. 94 (2021) 555–559, https://doi.org/10.1134/S1070427221050013.
[474] P. Zimmermann, Ö. Tekinalp, L. Deng, Ø. Wilhelmsen, O.S. Burheim, Electrodialysis for Removal of Impurities in Silver Electrowinning, Meet. Abstr. MA2023-01 (2023) 1608, https://doi.org/10.1149/ma2023-01241608mtgabs.
[475] H.I. Gomes, V. Funari, E. Dinelli, F. Soavi, Enhanced electrodialytic bioleaching of fly ashes of municipal solid waste incineration for metal recovery, Electrochim. Acta 345 (2020) 136188, https://doi.org/10.1016/j.electacta.2020.136188.
[476] X. Pan, H. Wu, Z. Lv, H. Yu, G. Tu, Recovery of valuable metals from red mud: A comprehensive review, Sci. Total Environ. 904 (2023) 166686, https://doi.org/10.1016/j.scitotenv.2023.166686.
[477] B. Wang, Y. Wang, T. Xu, Recent Advances in the Selective Transport and Recovery of Metal Ions using Polymer Inclusion Membranes, Adv Materials Technologies 8 (2023) 2300829, https://doi.org/10.1002/admt.202300829.
[478] A.B. Botelho Junior, J.A.S. Tenório, D.C.R. Espinosa, Separation of Critical Metals by Membrane Technology under a Circular Economy Framework: A Review of the State-of-the-Art, Processes (basel) 11 (2023) 1256, https://doi.org/10.3390/pr11041256.
[479] K.J. Min, S.Y. Choi, D. Jang, J. Lee, K.Y. Park, Separation of metals from electroplating wastewater using electrodialysis, Energy Sources Part A 41 (2019) 2471–2480, https://doi.org/10.1080/15567036.2019.1568629.
[480] H.K. Hansen, C. Gutiérrez, J. Leiva Gonzalez, A. Lazo, M.E. Hansen, P. Lazo, L. M. Ottosen, R. Ortiz, Combined Electrodialysis and Electrocoagulation as Treatment for Industrial Wastewater Containing Arsenic and Copper, Membranes (basel) 13 (2023), https://doi.org/10.3390/membranes13030264.
[481] C. Wang, T. Li, G. Yu, S. Deng, Removal of low concentrations of nickel ions in electroplating wastewater by combination of electrodialysis and electrodeposition, Chemosphere 263 (2021) 128208, https://doi.org/10.1016/j.chemosphere.2020.128208.
[482] J. Liu, F. Xu, J. Yuan, Z. Ji, Y. Zhao, F. Li, X. Guo, High-value conversion of Na2SO4 wastewater by a continuous electrodialytic metathesis process: Effects of coexisting ions, J. Membr. Sci. 615 (2020) 118584, https://doi.org/10.1016/j.memsci.2020.118584.
[483] M. Rakib, P. Moçotéguy, P. Viers, E. Petit, G. Durand, Behaviour of Nafion® 350 membrane in sodium sulfate electrochemical splitting: continuous process modelling and pilot scale tests, J Appl Electrochem 29 (1999) 1439–1448, https://doi.org/10.1023/A:1003861413943.
[484] Y. He, A. Gong, A. Osabutey, T. Gao, N. Haleem, X. Yang, P. Liang, Emerging electro-driven technologies for phosphorus enrichment and recovery from wastewater: A review, Water Res. 246 (2023) 120699, https://doi.org/10.1016/j.watres.2023.120699.
[485] P. Devos, A. Filali, P. Grau, S. Gillot, Sidestream characteristics in water resource recovery facilities: A critical review, Water Res. 232 (2023) 119620, https://doi.org/10.1016/j.watres.2023.119620.
[486] S.L. Aung, J. Choi, H. Cha, G. Woo, K.G. Song, Ammonia-selective recovery from anaerobic digestate using electrochemical ammonia stripping combined with electrodialysis, Chem. Eng. J. 479 (2024) 147949, https://doi.org/10.1016/j.cej.2023.147949.
[487] J. de Paepe, L. de Pryck, A.R.D. Verliefde, K. Rabaey, P. Clauwaert, Electrochemically Induced Precipitation Enables Fresh Urine Stabilization and Facilitates Source Separation, Environ. Sci. Technol. 54 (2020) 3618–3627, https://doi.org/10.1021/acs.est.9b06804.
[488] J. Yao, Y. Sun, P. Shi, Y. Liu, Phosphorous acid separation and recovery from glyphosate mother liquor by two-stage bipolar membrane electrodialysis, Sep. Purif. Technol. 341 (2024) 126700, https://doi.org/10.1016/j.seppur.2024.126700.
[489] A.F.R. Silva, L.A. Ribeiro, M.C.S. Amaral, Efficiency of nutrients recovery from sugarcane vinasse treatment by different electrodialysis configurations and in sequential-batch operation, Sep. Purif. Technol. 311 (2023) 123295, https://doi.org/10.1016/j.seppur.2023.123295.
[490] Y. Li, Z.-L. Ye, R. Yang, S. Chen, Synchronously recovering different nutrient ions from wastewater by using selective electrodialysis, Water Sci Technol 86 (2022) 2627–2641, https://doi.org/10.2166/wst.2022.352.
[491] H. Zhou, P. Ju, S. Hu, L. Shi, W. Yuan, D. Chen, Y. Wang, S. Shi, Separation of Hydrochloric Acid and Oxalic Acid from Rare Earth Oxalic Acid Precipitation Mother Liquor by Electrodialysis, Membranes (basel) 13 (2023), https://doi.org/10.3390/membranes13020162.
[492] M. Ali, M. Rakib, S. Laborie, P. Viers, G. Durand, Coupling of bipolar membrane electrodialysis and ammonia stripping for direct treatment of wastewaters containing ammonium nitrate, J. Membr. Sci. 244 (2004) 89–96, https://doi.org/10.1016/j.memsci.2004.07.007.
[493] B. Yuzer, M.I. Aydin, H. Yildiz, B. Hasançebi, H. Selcuk, Y. Kadmi, Optimal performance of electrodialysis process for the recovery of acid wastes in wastewater: Practicing circular economy in aluminum finishing industry, Chem. Eng. J. 434 (2022) 134755, https://doi.org/10.1016/j.cej.2022.134755.
[494] N.V. Kovalev, T.V. Karpenko, N.V. Sheldeshov, V.I. Zabolotskii, Ion Transport through a Modified Heterogeneous Bipolar Membrane and Electromembrane Recovery of Sulfuric Acid and Sodium Hydroxide from a Sodium Sulfate Solution, Membr, Membr. Technol. 2 (2020) 391–398, https://doi.org/10.1134/S2517751620060050.
[495] C. Xue, Q. Chen, Y.-Y. Liu, Y.-L. Yang, D. Xu, L. Xue, W.-M. Zhang, Acid blue 9 desalting using electrodialysis, J. Membr. Sci. 493 (2015) 28–36, https://doi.org/10.1016/j.memsci.2015.06.027.
[496] J. Lin, Q. Chen, X. Huang, Z. Yan, X. Lin, W. Ye, S. Arcadio, P. Luis, J. Bi, B. van der Bruggen, S. Zhao, Integrated loose nanofiltration-electrodialysis process for sustainable resource extraction from high-salinity textile wastewater, J. Hazard. Mater. 419 (2021) 126505, https://doi.org/10.1016/j.jhazmat.2021.126505.
[497] B.M. An, S.L. Aung, J. Choi, H. Cha, J. Cho, B. Byambaa, K.G. Song, Behavior of solutes and membrane fouling in an electrodialysis to treat a side-stream: Migration of ions, dissolved organics and micropollutants, Desalination 549 (2023) 116361, https://doi.org/10.1016/j.desal.2022.116361.
[498] K. Arola, A. Ward, M. Mänttäri, M. Kallioinen, D. Batstone, Transport of pharmaceuticals during electrodialysis treatment of wastewater, Water Res. 161 (2019) 496–504, https://doi.org/10.1016/j.watres.2019.06.031.
[499] R. Guedes-Alonso, S. Montesdeoca-Esponda, J. Pacheco-Juárez, Z. Sosa-Ferrera, J. J. Santana-Rodríguez, A Survey of the Presence of Pharmaceutical Residues in Wastewaters. Evaluation of Their Removal using Conventional and Natural Treatment Procedures, Molecules 25 (2020). https://doi.org/10.3390/molecules25071639.
[500] E.Y. Bulychev, N.Y. Rubanyak, Commercial Synthesis of 2-Aminoethanesulfonic Acid (Taurine), Pharm. Chem. J. 46 (2013) 740–741, https://doi.org/10.1007/s11094-013-0882-9.
[501] S. Song, Y. Tao, H. Shen, B. Chen, P. Qin, T. Tan, Use of bipolar membrane electrodialysis (BME) in purification of l-ascorbyl-2-monophosphate, Sep. Purif. Technol. 98 (2012) 158–164, https://doi.org/10.1016/j.seppur.2012.06.023.
[502] L. Yu, A. Lin, L. Zhang, C. Chen, W. Jiang, Application of electrodialysis to the production of Vitamin C, Chem. Eng. J. 78 (2000) 153–157, https://doi.org/10.1016/S1385-8947(00)00136-4.
[503] L. Yu, A. Lin, L. Zhang, W. Jiang, Large scale experiment on the preparation of vitamin C from sodium ascorbate using bipolar membrane electrodialysis, Chem. Eng. Commun. 189 (2002) 237–246, https://doi.org/10.1080/00986440211835.
[504] R.A. Gross, B. Kalra, Biodegradable polymers for the environment, Science 297 (2002) 803–807, https://doi.org/10.1126/SCIENCE.297.5582.803.
[505] S.A. Rafiqah, A. Khalina, A.S. Harmaen, I.A. Tawakkal, K. Zaman, M. Asim, M. N. Nurrazi, C.H. Lee, A Review on Properties and Application of Bio-Based Poly (Butylene Succinate), Polymers (basel) 13 (2021), https://doi.org/10.3390/polym13091436.
[506] K. Kirimura I. Yoshioka Citric Acid 2019 Comprehensive Biotechnology, Elsevier in 10.1016/B978-0-444-64046-8.00157-9 158 165 ISBN: 9780444640475.
[507] J. Liesivuori Formic Acid 2014 Encyclopedia of Toxicology, Elsevier in 10.1016/B978-0-12-386454-3.00989-1 659 661 ISBN: 9780123864550.
[508] Q. Wang, G.Q. Chen, L. Lin, X. Li, S.E. Kentish, Purification of organic acids using electrodialysis with bipolar membranes (EDBM) combined with monovalent anion selective membranes, Sep. Purif. Technol. 279 (2021) 119739, https://doi.org/10.1016/j.seppur.2021.119739.

[509] E. Papadopoulou, M.C. González, D. Reif, A. Ahmed, P. Tsapekos, I. Angelidaki, M. Harasek, Separation of lactic acid from fermented residual resources using membrane technology, J. Environ. Chem. Eng. 11 (2023) 110881, https://doi.org/10.1016/j.jece.2023.110881.
[510] G. Caputo, I. Balog, A. Giaconia, S. Sau, A. Pozio, Experimental Study for HIx Concentration by Electro-Electrodialysis (EED) Cells in the Water Splitting Sulfur-Iodine Thermochemical Cycle, ChemEngineering 3 (2019) 50, https://doi.org/10.3390/chemengineering3020050.
[511] B. Ghorbani, S. Zendehboudi, Y. Zhang, H. Zarrin, I. Chatzis, Thermochemical water-splitting structures for hydrogen production: Thermodynamic, economic, and environmental impacts, Energy Convers. Manag. 297 (2023) 117599, https://doi.org/10.1016/j.enconman.2023.117599.
[512] P. Mandal, R. Mondal, P. Goel, B.E.U. Chatterjee, S. Chattopadhyay, Selective recovery of carboxylic acid through PVDF blended anion exchange membranes using electrodialysis, Sep. Purif. Technol. 292 (2022) 121069, https://doi.org/10.1016/j.seppur.2022.121069.
[513] B. Igliński, U. Kiełkowska, G. Piechota, Proecological aspects of citric acid technology, Clean Technol. Environ, Policy 24 (2022) 2061–2079, https://doi.org/10.1007/s10098-022-02316-y.
[514] A.J. Weier, B.A. Glatz, C.E. Glatz, Recovery of Propionic and Acetic Acids from Fermentation Broth by Electrodialysis, Biotechnol. Prog. 8 (1992) 479–485, https://doi.org/10.1021/bp00018a002.
[515] R. Caveriviere, S. Galier, H. Roux-de Balmann, On the Use of Permselectivity to Describe the Selective Transfer of Organic Acids in Electrodialysis, Membranes (basel) 13 (2023), https://doi.org/10.3390/membranes13060545.
[516] K. Zhang, M. Wang, D. Wang, C. Gao, The energy-saving production of tartaric acid using ion exchange resin-filling bipolar membrane electrodialysis, J. Membr. Sci. 341 (2009) 246–251, https://doi.org/10.1016/J.MEMSCI.2009.06.010.
[517] C. Lei, Z. Li, Q. Gao, R. Fu, W. Wang, Q. Li, Z. Liu, Comparative study on the production of gluconic acid by electrodialysis and bipolar membrane electrodialysis: Effects of cell configurations, J. Membr. Sci. 608 (2020) 118192, https://doi.org/10.1016/j.memsci.2020.118192.
[518] J. Pan, M. Miao, X. Lin, J. Shen, B. van der Bruggen, C. Gao, Production of Aldonic Acids by Bipolar Membrane Electrodialysis, Ind. Eng. Chem. Res. 56 (2017) 7824–7829, https://doi.org/10.1021/ACS.IECR.7B01529.
[519] L. Sun, Q. Chen, H. Lu, J. Wang, J. Zhao, P. Li, Electrodialysis with porous membrane for bioproduct separation: Technology, features, and progress, Food Res. Int. 137 (2020) 109343, https://doi.org/10.1016/j.foodres.2020.109343.
[520] Z. Lazarova, V. Beschkov, S. Velizarov, Electro-membrane separations in biotechnology, Phys. Sci. Rev. 5 (2020) 20180063, https://doi.org/10.1515/psr-2018-0063.
[521] O. Dlask, N. Václavíková, Electrodialysis with ultrafiltration membranes for peptide separation, Chem. Pap. 72 (2018) 261–271, https://doi.org/10.1007/s11696-017-0293-6.
[522] Desalination technology for the water challenge of the 21st century, https://doi.org/10.3030/969116.
[523] Next Generation Lithium Extraction & Battery Technology (2024) accessed 10 June 2024, https://energyx.com/.
[524] Euroserum ingrédients laitiers, 2024. https://www.euroserum.com/ (accessed 4 June 2024).
[525] Juclas - A guarantee to the tartaric stabilisation process, 2024. https://www.juclas.it/index.cfm/en/products/electrodialysis/ (accessed 4 June 2024).
[526] Bruce T. Batchelder, Electrodialysis method for demineralization of liquid, whey-based material, US5223107A, 1993.
[527] S. Al-Amshawee, M.Y.B.M. Yunus, A.A.M. Azoddein, D.G. Hassell, I.H. Dakhil, H. A. Hasan, Electrodialysis desalination for water and wastewater: A review, Chem. Eng. J. 380 (2020) 122231, https://doi.org/10.1016/j.cej.2019.122231.
[528] GE introduces microfiltration products and EDR technology, Membr. Technol. 2007 (2007) 2, https://doi.org/10.1016/S0958-2118(07)70253-7.
[529] D.H. Snydacker, N. Grosso Giordano, A. indranada, A. Lukito, S. Mock, T. Sawant, M.P. Cooke, M.J. Bootwala, E.B. Packer, D.J. Alt, LITHIUM EXTRACTION FROM BRINES WITH MODULATED ION CONCENTRATIONS, WO2024112604A2.
[530] A. Patwardhan, T. Egan, Systems and methods for direct lithium hydroxide production, WO2022/173852A1, 2022.
[531] K.J. Min, J.H. Kim, K.Y. Park, Characteristics of heavy metal separation and determination of limiting current density in a pilot-scale electrodialysis process for plating wastewater treatment, Sci. Total Environ. 757 (2021) 143762, https://doi.org/10.1016/j.scitotenv.2020.143762.
[532] Andreas Fischer, Christoph Martin, Jürgen Müller, Method for purification of amino acid containing solutions by electrodialysis, US6551803B1, 2000.
[533] PCCell GmbH, Electrodialysis Systems and Ion Exchange Membranes - PCCell GmbH, 2024. https://www.pccell.de/en/P160-Industrial-scale-system_18_content3_Acid-Recovery_34_Produktdetail.html (accessed 4 June 2024).
[534] Laboratory and pilot units – MemBrain - Industrial research and innovations, 2024. https://www.membrain.cz/en/laboratory-and-pilot-units.html (accessed 4 June 2024).
[535] Bipolar Electrodialysis (BPED) - Ionics - Veolia, 2024. https://www.watertechnologies.com/products/bipolar-electrodialysis-bped (accessed 4 June 2024).
[536] ASTOM, 2024. https://www.astom-corp.jp/en/index.html (accessed 4 June 2024).
[537] Eurodia – The optimal process solutions, 2024. https://eurodia.com/ (accessed 5 June 2024).
[538] W.-T. Gao, Q. Chen, M.-G. Du, W.-M. Zhang, C.-Y. Cao, W.-G. Song, Enabling an atom-economic production of chiral amino alcohols by electrodialysis with bipolar membranes, Green Chem. 22 (2020) 2213–2224, https://doi.org/10.1039/C9GC02460C.
[539] Q. Chen, C. Xue, W.-M. Zhang, W.-G. Song, L.-J. Wan, K.-S. Ma, Green Production of Ultrahigh-Basicity Polyaluminum Salts with Maximum Atomic Economy by Ultrafiltration and Electrodialysis with Bipolar Membranes, Ind. Eng. Chem. Res. 53 (2014) 13467–13474, https://doi.org/10.1021/ie5023546.
[540] REvivED water project, 2021. https://www.revivedwater.eu/ (accessed 4 June 2024).
[541] Eurodia – The optimal process solutions, 2024. https://eurodia.com/en/?avia_forced_reroute=1 (accessed 4 June 2024).
[542] AQUABATTERY - revolutionising long duration energy storage, 2024. https://aquabattery.nl/ (accessed 4 June 2024).